8-31-1991

Implementation of an integrated high energy beam workcell

Varadaraj Souda
New Jersey Institute of Technology

Copyright Warning & Restrictions

The copyright law of the United States (Title 17, United States Code) governs the making of photocopies or other reproductions of copyrighted material.

Under certain conditions specified in the law, libraries and archives are authorized to furnish a photocopy or other reproduction. One of these specified conditions is that the photocopy or reproduction is not to be "used for any purpose other than private study, scholarship, or research." If a, user makes a request for, or later uses, a photocopy or reproduction for purposes in excess of "fair use" that user may be liable for copyright infringement,

This institution reserves the right to refuse to accept a copying order if, in its judgment, fulfillment of the order would involve violation of copyright law.

Please Note: The author retains the copyright while the New Jersey Institute of Technology reserves the right to distribute this thesis or dissertation

Printing note: If you do not wish to print this page, then select "Pages from: first page # to: last page #" on the print dialog screen

Implementation of an Integrated High Energy Beam Workcell

Varadaraj V. Souda,
M.S. in Manufacturing Engineering, 1991

ABSTRACT

This study is an effort to advance the technology of machining by High energy beams. Investigation of the Waterjet, Plasma and the Oxyfuel beams was carried out to explore novel machining techniques. The study was focussed on three major objectives.

One of the major objectives was to set up an Integrated beam workcell consisting of the three beams. A hydroabrasive waterjet workcell was modified to install the three cutting tools to be along the same line of traverse. An integrated beam consisting of the thermal and the waterjet beams was produced because of this arrangement. The feasibility of using the integrated beam for machining of steel samples was investigated by various methods.

The thermal beams were used for heating a focussed spot on the metal. Piercing experiments by impinging the high pressure waterjet on the heated steel samples resulted in a 3-4 fold increase in the material removal volume when compared to the impingement on the non-heated surface of steel. Results indicate that the depth of beam penetration increases significantly when the metal surface is heated, when compared to the impingement of the waterjet without any heating. The results also suggest the feasibility of practical implementation of the integration of the thermal and the waterjet beams.

Linear cutting experiments were carried out by moving the heat beam and the high pressure waterjet beam simultaneously along the metal surface. The results indicate that the process parameters concerned with the heating process such as temperature of beam and intensity of heat need to be optimized during the cutting process.

The improvement of the surface finish by Abrasive-Waterjet (AWJ) machining was another major objective of this study. The AWJ beam was used as a finishing tool for machining of Stainless steel SS 304 metal. The machining was performed by using the beam to strike the surface at a 90^{o} tangent. The experimental results obtained clearly demonstrate that AWJ can be used as a finishing tool for producing precision surfaces with Roughness Average (Ra) value of less than 1 micron. The particle size was an important factor affecting the Roughness of the surface.

The third major objective of this study was to investigate the cutting of fiber-composites by AWJ. The feasibility of using AWJ to prevent the composite delamination during the cutting of various types of composites is demonstrated as a result of this work.

IMPLEMENTATION OF AN INTEGRATED HIGH ENERGY BEAM WORKCELL

By

Varadaraj V. Souda

Thesis Submitted to the Faculty of the Graduate School of The New Jersey Institute of Technology in Partial Fulfillment of the Requirements for the Degree of Master of Science in Manufacturing Engineering

1991

APPROVAL SHEET

Title of Thesis: **Implementation of An Integrated High Energy Beam Workcell**

By

Varadaraj V. Souda
Master of Sceince in Manufacturing Engineering, 1991.

Thesis and Abstract Approved by:

Dr. E. S. Geskin Date
Professor
Department of Mechanical and Industrial Engineering

Dr. N. Levy Date
Associate Professor
Department of Mechanical and Industrial Engineering

Dr. A. Harnoy Date
Associate Professor
Department of Mechanical and Industrial Engineering

VITA

Name: Varadaraj V. Souda

Address:

Degree to be conferred and date: M. S. Mn. E., 1991.

Date of birth:

Place of birth:

Collegiate Institutions attended:

Sri Jayachamarajendra College of Engineering
Sept 1978 - Dec 1983
B.S. in Mechanical Engineering

New Jersey Institute of Technology
Sept 1989 - Aug 1991
M.S. in Manufacturing Engineering

Positions held:

Research Assistant Sept 1989 - Present
Waterjet Machining Laboratory, M.E. Dept., NJIT

Graduate Assistant Jan 1991 - May 1991
Computer Aided Engineering Laboratory, NJIT

Engineer - Production and Development
Sept 1986 - Aug 1989
M/s. Widia (India) Ltd., India.

Engineer - Quality Assurance
Dec 1983 - Sept 1986
M/s Karnataka Ball Bearing Co., India.

To,

My parents,

for all you have done to me.

ACKNOWLEDGEMENT

I take this opportunity to express my deepest gratitude to my thesis advisor, Dr. E.S. Geskin, Professor, Department of Mechanical and Industrial Engineering of the New Jersey Institute of Technology for his valuable guidance and advise throughout the course of this work. It was a honor to work under my esteemed teacher.

I also take this opportunity to thank Dr. N. Levy, Associate Professor, Department of Mechanical and Industrial Engineering, NJIT and Dr. A. Harnoy, Associate Professor, Department of Mechanical and Industrial Engineering, NJIT for their valuable suggestions during the preparation of this Thesis report. I also thank Dr. M. Shimanovich for his valuable advise during the course of my work.

Finally, my thanks to the technical staff of the Mechanical Engineering Department (Don Rosander, Joe Glaz and David Singh) for their help to set up the Integrated Workcell.

CONTENTS

List of Figures

Figures (contd) *Page*

List of Tables

I. INTRODUCTION

This study is an effort to advance the technology of machining by high energy beams. The Waterjet, Plasma and the Oxyfuel beams, included into this category constitute the main focus of this study. The investigations to improve the machining technologies is conducted in three major avenues. These are desribed briefly in the following paragraphs.

A major objective identified for this study was to set up an Integrated beam workcell consisting of the three beams mentioned above. A hydroabrasive CNC Waterjet workcell was modified to install the three cutting tools. The three tools were arranged so as to be along the same line of traverse along one axis of traverse and one behind the other (Fig 1). Experiments were carried out on steel samples by separately integrating the high pressure (50 ksi) waterjet beam with the plasma and the Oxyfuel beams. The schematic is illustrated in Fig 1. Various experimental studies were carried out to investigate the cutting by the integrated beams under such an arrangement as shown in Fig 3 and Fig 1. A brief summary of the experiments carried out follows:

1.1 Summary of Experiments to improve high energy beam machining :

1.1.1 Experiment I

The effect of heating the metal close to melting point and simultaneous cutting with pure water jet was studied. The two beams were focussed at the same point. The surface was heated initially for a fixed time period and then subjected to impingement by the waterjet. Linear cutting experiments with steel used as test material was also investigated under different conditions of heating and traverse speeds. The effects of various process parameters on the cutting results was investigated.

1.1.2 Experiment II

Another major objective of the study is concerned with the improvement of the surface finish by Abrasive-Waterjet (AWJ). The AWJ beam was used solely for the purpose of finish machining rather than actual cutting. Stainless steel was used as the sample material. The machining process was performed by using the AWJ beam to strike the surface at a 90^{o} tangent (Fig 2). The lateral depth of cut was kept very low and AWJ was used as a surface finishing tool rather than a cutting tool. Multiple passes were performed to study the improvement in surface finish. At certain conditions AWJ

cutting produces surface finish with an Ra value of 1 micron or less. The results are tabulated elsewhere in this report. The principal parameters affecting surface finish were found to be grit size, traverse speed, and the number of passes.

1.1.3 Experiment III

The third major objective of this study was to investigate the AWJ cutting of fiber-composites. The objective was to determine the conditions under which the delamination of the different types of fiber composites is avoided during the AWJ machining. Experimental results show that the operational conditions for cutting the composites without delamination depend upon the property of the composite and needs to be studied experimentally for each type of composite. In this study we have described two instances wherein AWJ cutting was used successfully for cutting two different types of composite materials. One was a type G-10 composite material 1.25 mm. thick and the other a kevlar composite 1/2" thick. The details of machining of both materials are provided in later chapter. The major objective of this study was to avoid delamination of the composites entirely. The results demonstrate the feasibility of AWJ machining of composites without de-lamination.

1.2 Background

High energy beam machining processes have been in focus since the last decade for a variety of reasons. The important ones being that they offer a scope for high material removal rates in the machining of hard to machine materials such as stainless steel [1], glass [2], composites [3], etc., where other methods have failed. Also high energy beam machining processes have proved to be cost effective and can be easily automated [4]. All high energy beam machining techniques operate more or less in the same mode although the mechanism of material removal varies. The cutting medium is expelled through a small orifice of a fraction of an inch diameter and impinges upon the workpiece material. This results in removal of material by heating (as in the case of laser or plasma cutting) [1], by heating and oxidation (as in flame cutting) [1], or by particle erosion (as in abrasive waterjet cutting) [6]. The most usable high energy beam machining techniques are Water jet and Abrasive waterjet cutting, Plasma cutting, Laser beam cutting and Oxyfuel cutting. Water jet cutting was introduced in the early seventies and AWJ cutting was put into practise in the last decade. Plasma cutting was invented in 1955 whereas flame cutting has been known since the World War I.

The present study is concerned with the development of an integrated technology comprising different types of high energy beams. Although water jet cutting and AWJ cutting offer great flexibility and advantages in some instances the material removal rates are substantially lower than desired for certain types of material. For example for machining of titanium above 12.5 mm thick , cutting speeds for Plasma arc cutting are generally 3-4 times higher than for AWJ cutting, (Table IV). A 12.5 mm. thick stainless steel can be cut using waterjet at a maximum speed of 2 ipm whereas Plasma arc cutting can machine the material at well above 20 ipm. It was therefore a major objective of the study to investigate the possibility of increasing the material removal rate by integration.

1.3 Advantages due to Beam Integration:

1. Material removal rate can be improved since the shear stress of the material is reduced.

2. Heating the material reduces its shear stress. Hence less jet energy is needed to deform the material.

3. The objective is to use pure waterjet instead of AWJ for cutting the metals. Abrasive particles in the waterjet

stream are eliminated and the surface finish can be improved.

1.4 Motivation behind the present study:

It is by now well established that High energy beams offer many advantages over conventional machining techniques in terms of productivity and flexibility of machining[2-7]. The present research was conducted with the objective of increasing our knowledge base with regard to the capabilities of material removal of integrated beams. The theories behind the cutting mechanism of individual beams are sufficiently known and documented [1-10] but much needs to be done experimentally to attain a full knowledge of practical limitations of beam machining. This study attempts to make such knowledge available.

It is to be noted that a theoretical model for a integrated beam machining process is not very easy to establish because of the large number of parameters involved in the individual as well as the integrated process. It was felt necessary at this stage to focus the study upon the practical limitations in the process and the practical effects of various parameters on actual cutting process. It is sincerely hoped that the results from this study will be useful to construct a realistic theoretical model of the integrated beam cutting process.

1.5 The equipment:

Although the nature of this study is experimental the equipments used were all of industrial scale so as to simulate the production environment of the industry. The conditions and the parameters used for cutting experiments were chosen with a practical point of view.

In this study the main equipment used is a CNC controlled 2 and 1/2 axis hydro-abrasive workcell equipped with ALLEN BRADLEY series 8400 CNC controller. This machine is manufactured by the Ingersoll Rand Co. and uses a abrasive water jet nozzle for performing the cutting operations. A Plasma Arc cutting machine manufactured by Linde Co. and equipped with a mechanized torch was used to integrate the two modes of cutting. Also a Oxyfuel cutting torch was used as a third cutting tool. Both the Plasma arc torch and the Oxyfuel cutting torch were mounted using a special fixture (Fig. 3) so as to be in line with the AWJ nozzle. The operation of the workcell was modified electrically so as to be able to operate the Plasma arc cutting torch and the Oxyfuel cutting torch by the CNC controller. Thus it was possible to program the operation of the plasma and the Oxyfuel cutting beams. A detailed description of the workcell operation is provided in the Appendix.

II. Review of Previous Work

A number of detailed studies both on Waterjet as well as Abrasive waterjet machining was carried out by various researchers. These studies have focussed upon varying topics such as application, modeling of jet cutting phenomena for various materials and jet characteristics, etc.

Plasma arc cutting and Oxyfuel cutting has been the subject of a number of studies. The main issues studied were the properties of the heat beams, the temperature zone and the nozzle characteristics, etc.

2.1 Previous work on Waterjet and Abrasive-Waterjet:

2.1.1 Theories of jet dynamics and jet cutting:

The parameters involved in waterjet cutting are listed in Table I. The principal characteristics of a continuous waterjet are pressure, diameter and velocity.

In [5], Hashish and duPlessis have attempted to model penetration of solid material by a continuous waterjet. The control volume technique was used in this study. The momentum balance of the control volume was constructed to derive an equation for the depth of penetration by the continuous waterjet.

The factors considered in the model are the characteristics of the jet itself, the material properties, and the feed rate. This model however is concerned with jet penetration for soft materials since hard materials like glass, metals, etc cannot be destroyed by the pressure exerted by a water jet at existing velocities.

Hashish [7], describes the visualization of the jet cutting process. The actual mechanism of jet penetration was studied by taking high speed movies of the cutting process in transparent materials. The effect of the nozzle geometry on the erosion process of metallic materials was studied by Kobayashi, et al [8]. Geskin, et al, [9] have investigated the forces exerted by a WJ on the workpiece at different stand-off distances and with varying sapphire nozzle diameters. Experimental studies by Chen [10] has showed that the velocity of a waterjet is above 750 m/sec. at water pressure of 345 Mpa.

A number of investigations on the use of high pressure waterjets for surface processing, for example, for cleaning applications has been carried out by a number of researchers [11] [12].

A large number of studies concerned with material machining by the use of specific high energy beams has been reported up to date. The list is too exhaustive to be

mentioned in full. In all these studies however integration of different types of high energy beams has not been investigated. In the present study it is proposed to construct an Integrated workcell comprising the Waterjet, Plasma and the Oxyfuel cutting beams and carry out machining experiments by integrating two or more beams.

2.1.2 Study of Surface Finish improvement by AWJ:

The study of the finish of surfaces generated by high energy beam cutting was carried out by different researchers. It was found that the factors influencing the surface finish in AWJ cutting include the particles' size, cutting speed, material properties, the water pressure, etc.

A statistical characterization of surface finish for ceramic composites was given by Kim and Burnham [13]. Matsui, et al, [14] have discussed the application of AWJ for precision cutting performance. It is pointed out that surface finish in AWJ cutting is superior at the upper 2mm. area of the kerf and then tends to deteriorate dramatically with depth. Hashish [15] discusses the feasibility of milling with Abrasive Waterjets. Blickwedel, et al, [16] have derived an equation for predicting the kerf depth. This equation is given as

$$h = Cs*(p - po)/V^{(0.86+2.09/V)}$$

A method to correlate the depth of cut with the surface finish is also proposed .

Hashish [17,18] discusses the performance optimization of the AWJ cutting process. The effects of various parameters on AWJ cutting performance was studied. The surface finish obtained during the AWJ machining is found to be strongly affected by the particle size and the cutting speed.

None of the available studies suggests the use of AWJ as a surface finishing tool. Such use was one of the principal objectives of this study. The main experimental results of the previous studies is that surface finish is affected strongly by particle size and cutting speed. This conclusion is also investigated in our experimental study.

2.2 Plasma Arc cutting

A. Process parameters:

Plasma arc cutting is not a new process and its operating principles and parameters are well known. The main parameters affecting the cutting performance are the type of ionizing gas, the cooling gas, the material thickness and the type of material, the standoff, the traverse speed, and the output current of the machine.

Applications of plasma arc cutting have been discussed in [1], [26], [28] [32]. Various types of Plasma Arc cutting exists in the industry today [35]. Air Plasma cutting has a special edge over other processes due to the use of compressed air as ionizing gas which is cheaper than other gases.

The effect of the nozzle wear and its geometry and the condition of the electrode also strongly affect the quality of the cut [30], [33].

B. Heat affected zone:

One of the principal features of the Plasma arc cutting process is the formation of the Heat Affected Zone (HAZ). A detailed study of the HAZ and its effect on material properties has been investigated [27], [30]. The HAZ depends upon the material thickness and the cutting speed Particularly a high cutting speed results in low heat input to the bulk metal and therefore the HAZ is very narrow. One of the negative features of HAZ for some kinds of steels is the increase in the micro-hardness and thereby increases the brittleness and susceptibility to crack development [30].

Studies have been also carried out on other factors related to the machine performance such as the noise

generation, the cutting torch performance [29], electrode and the cutting tip wear [26], etc.

Due to the small thickness of the heat affected zone, secondary finishing of the PAC can be conveniently carried out with AWJ which was one of the objectives of this study. The feasibility of finishing the Plasma cut surfaces by the AWJ is successfully demonstrated by the performed experiments.

2.3 Oxyacetylene Cutting

The technology and the principles of the process are described in [1]. It is observed that the HAZ in case of the OFC is maximum compared to PAC. The microstructure study of the metal surface of steel near the cutting edge [within 2mm] shows that the carburization of the material is substantial [2]. This is known to affect the fatigue strength of the oxyfuel cut specimen [1]. Cutting speeds are less than plasma arc upto 2.0" thickness and exceed the plasma arc cutting speeds beyond these thicknesses for steel. Oxyfuel beam cannot cut metals like Copper, aluminium etc, since the oxides formed by these metals have a higher melting point than the base metal. These oxides form a film on the base metal and prevent further oxidation of the base metal. The main advantage of OFC is that it can cut steel upto 20 thickness and the equipment cost is relatively low when compared to other processes.

III. Objectives

The main objectives of this study are

- Installation and operation of an integrated workcell incorporating the Waterjet, Plasma and the Oxyfuel cutting beams. The Plasma arc and the Oxyfuel cutting torches and the AWJ nozzle were mounted on a single cutting head. It was the objective of this study to determine the feasibility of cutting with individual beams or integrate the Waterjet with the Plasma or the Oxyfuel beam.

- To investigate the use of AWJ for application as a precision surface finishing tool. The conditions necessary to generate precision surfaces by AWJ were sought to be determined experimentally. Roughness average (Ra) value of the surfaces generated was less than 1 micron.

IV. Principles of Different High Energy Beam Cutting Methods

4.1 Principle of Waterjet Cutting:

Water at high pressure is forced through a tiny sapphire orifice to form a coherent fluid jet of stable laminar flow. The jet exits the sapphire nozzle at more than twice the speed of sound and cuts as it passes through the workpiece.

The technology involves pumping a 0.08mm to 0.46mm (0.003in - 0.018in) diameter water stream at 207 to 414 Mpa. (30 - 60ksi). The waterjet is used to cut or slit nonwoven materials, corrugated box materials, plastics, paper, fish, meat, vegetables, etc.

For a pure water jet the ideal relationship between static water pressure and the resultant jet velocity is characterized by the following relationship.

$$P = 1/2*p*V^2$$

The velocity values over a typical range of pressures are given below:

Static pressure (psi)	Jet velocity (fps.)
25,000	1800
35,000	2100
45,000	2400
55,000	2700

4.2 Principles of Abrasive Waterjet Cutting:

The Abrasive waterjets are formed in hydroabrasive jet nozzles. These comprise of a sapphire nozzle and a focussing tube made of tungsten carbide (Fig 7a and 7b).

The high pressure water is forced through the sapphire orifice to form a stable coherent high velocity waterjet [10]. The waterjet immediately passes through the mixing chamber in the focussing tube. Abrasive particles are introduced into the hydroabrasive nozzle body and are drawn into the high pressure water stream. In the mixing chamber, part of the waterjet's momentum is transferred to the abrasive particles whose velocities rapidly increase. Typical particle velocities are 300-600 m/sec and mass flow rate is about 150-280 g/min. [15].

A focussed high velocity abrasive-waterjet exits the focussing tube nozzle and performs the cutting action. Cutting of the material occurs as a result of complex erosion phenomena and is controlled by a several parameters listed in Table I [8].

4.3 Principle of Plasma arc cutting:

Unlike waterjet cutting Plasma arc cutting is a thermal process in which energy for the melting or vaporization of the metal is obtained from a stabilized electric arc. After ignition of the arc between the cutting electrode and the metal a pressurized gas is supplied through the orifice (Fig 10b). The voltage between the electrode and the metal ionizes the gas. Now the gas is called plasma and is electrically conductive. Due to the constriction in flow at the orifice the resistivity of the gas increases and its temperature rises. The extreme heat of the jet melts the metal. The kinetic energy of the pressurized gas blows the molten material out of the cutting area.

PAC can be used to cut all types of conducting material. The cutting speed with plasma arc cutting exceeds any other high beam cutting processes. The major disadvantage of the plasma arc cutting is the quality of the plasma cut surface as the thickness increases. The edges of the generated surfaces are rounded off in many instances. It becomes necessary to use a secondary process to improve the surface finish. The use of AWJ as an effective tool for this purpose was one of the objectives of this study.

4.4 Principle of Oxyacetylene cutting:

In Oxyfuel cutting (OFC) a fuel gas/oxygen flame heats the surface to ignition temperature, and a stream of pure oxygen feeds the cutting action. In practise, OFC begins by heating a small area on the surface of the metal to the ignition temperature of 760-870^{o}C. (1400-1600^{o}F.) with an oxyfuel gas flame. Upon reaching this temperature the metal surface appears bright red. A cutting oxygen stream is then directed at the preheated spot, causing rapid oxidation of the heated metal and generating large amounts of heated metal. The heat supports continued oxidation of the metal as the cut progresses. This causes the metal in the path of the jet to burn, exposing fresh surfaces for further oxidation (Fig 13). The cut progresses making a narrow slot or kerf through the metal.

The surface generated by the Oxyfuel beam has the maximum roughness compared to the Plasma arc cutting and the Abrasive Waterjet Cutting. Also OFC can be used to cut only plain and medium carbon steels only. The main advantage of AWJ is that it can cut steel more than 6.0" thick. Upto 20" thick steel is known to be cut with Oxyfuel Cutting [1].

4.5 Principle of Integrated cutting:

Integrated cutting refers to the process of cutting any material using two or more different types of cutting beams at the same time, or it could also refer to the availability of several different cutting processes in a single workcell. As mentioned earlier AWJ cutting is the ideal tool for cutting materials such as composites, ceramics, glass, etc., whereas Plasma arc cutting is more efficient for cutting tough metals like titanium, stainless steel, etc., if surface finish is not very critical. It is therefore expedient to develop an integrated workcell equipped with several types of cutting beams which are suited for different purposes.

The principle advantage of the AWJ is that it can be used for cutting any known material. But the material removal in AWJ is due to particle erosion [6]. Abrasive particles impinge the surface at velocity of 400-500 m/sec which results in material erosion. Surface finish can be improved by reducing the cutting speed as well as the particle size, this improvement is however limited. Pure water jet on the other hand does not possess the strength necessary for cutting. However, if the material surface can be heated by a heat source focussed in a small area the shear strength of the material is reduced and cutting can be carried out by pure waterjet.

The heating of the material at the focussed area can be accomplished by either the plasma arc cutting beam or the Oxyfuel beam. The feasibility of using both the plasma as well as the Oxyfuel cutting for heating the metal surface was carried out experimentally. Several factors need to be considered. The prominent ones being the jet turbulence, the stability of the flame, the heating time involved, etc. The effects of these factors are studied in the experiments that were carried out.

V. The Equipment Set-up

5.1 The Equipment Set-up

One of the main objectives of this study was to integrate the various modes of cutting and to perform cutting tests with the integrated beam. This could be possible only if all the three cutting tools namely the Plasma torch, the Oxyfuel torch and the Waterjet nozzle were accommodated on the same cutting head. The following steps were taken to ensure that this objective was fulfilled:

1. The water jet nozzle was mounted directly on the cutting head as supplied by the manufacturer.

2. A special L-shaped fixture (Fig 3) was manufactured and fixed to the cutting head. The plasma arc cutting torch and the oxyfuel cutting torch are mounted on this fixture to be **in-line** with the abrasive water jet nozzle.

Due to this arrangement of the torches it was possible to investigate different types of cutting techniques.

1. It was possible to investigate the simultaneous operation of the water jet beam with either plasma arc or the Oxyfuel cutting beam. The two beams were focussed at a common point in this type of cutting operation (Fig 1).

2. The heat beam was focussed at a fixed distance in front of the waterjet beam. This raised the surface temperature of the material before impingement by the waterjet. (Fig. 1)

3. The heat beam was used for cutting the material in one pass and in the second pass the surface was finished using the AWJ (Fig 2).

The operation of the three cutting beam processes is described in the Appendix so as to give the reader an idea regarding the technique of integration.

VI. SYSTEM DESCRIPTION

The main objective of this research is to construct an integrated workcell comprising the hydroabrasive jet, the plasma arc cutting and the oxyfuel cutting torch. The basic HS-3000 CNC hydroabrasive workcell is modified in order to incorporate the PAC and the OFC torches. The workcell was supplied by Ingersoll Rand Co. (Fig 4).

The equipment for the entire workcell can be classified into three component systems.

1. Waterjet system components.
2. Plasma arc cutting system components
3. Oxyfuel cutting system components.

6.1 Waterjet System Components

Any basic waterjet system consists of the following parts (Fig 5a.):

a. A water treatment system
b. A water intensifier system
c. A polymer mixer
d. A water delivery system
e. A cutting head (either pure water or hydroabrasive)
f. A abrasive delivery system
g. A catcher system
h. Settlement tank

i. Motion equipment for moving the cutting head.

6.1.1 Water Treatment System:

The water treatment system involves the process of softening of the water prior to feeding it to the intensifier. The water must be softened to remove the iron and calcium dissolved solids since they tend damage the orifice if not eliminated. To treat the water mechanically and chemically, low pressure filters (1-10 microns) and softener is used.

6.1.2 Water Intensifier System (Fig 5b):

The system uses a hydraulically driven, double acting reciprocating plunger type intensifier made by the Streamline water jet cutting division (Fig 5b). The pressure ratio is 40:1. The primary circuit is provided with oil up to 1500 psi from a hydraulic pump. The secondary circuit provides water at up to 60000 psi to the nozzle. For reasons of safety, the maximum operating pressure of the intensifier is maintained at 50,000 psi. Most materials can be cut satisfactorily at the pressure of 25-50 ksi.

The intensifier system also contains a water accumulator which is used to store the high pressure water. This large pressure vessel contains no moving parts and acts

as a storage chamber for the high pressure water in the same manner as the storage chamber of a air compressor functions. It is also used to house a filter element to protect the cutting nozzle from dirt particles.

6.1.3 Polymer Mixer

A reciprocating polymer mixer pump is available in the system. This pump delivers the polymer into the supply water. Addition of polymer into the water in quantities of 0.3-0.5% by volume increases the viscosity of the water and improves the jet coherence expelled through the orifice. The addition of polymer into the system is optional.

6.1.4 Water Delivery System

Water is carried from the pumping unit to the cutting station through high pressure tubing. The connections to the tubing are made with high pressure fittings. The end of each tubing is coned, threaded and forced into a conical seat with jamb nuts.

6.1.5 The Cutting Head.

The cutting head can be a simple nozzle made of sapphire and positioned in a special nut threaded to the end of the high pressure pipe. A pure water jet is formed which

can be used to cut soft materials like plastic, wood, Styrofoam, non woven polythene etc.,

Abrasive-Waterjet cutting can be enhanced by the an alignable nozzle assembly. The main parts of the nozzle assembly are shown in Fig 7a and 7b. The nozzle comprises of a ball type sapphire orifice and a tungsten carbide focussing tube. The longitudinal axis of the sapphire can be adjusted by four set screws so as to be coaxial with the focussing tube. The life of the sapphire orifice varies between 10 - 100 hrs. and that of the focussing tube is about 2-6 hrs. The main cause of failure of the sapphire orifice is presence of entrained dirt particles in the high pressure water supply.

6.1.6 Abrasive Transfer System

The abrasive supply to the nozzle is carried out by a bulk abrasive supply system (Fig 6b). The bulk abrasive supply system consists of a container for storing the abrasive and can handle up to 500 lbs of 80 mesh abrasive. The abrasive particles are supplied to the hopper by means of compressed air through a hose. The bulk abrasive transfer supply system requires minimum operator attention and can run continuously for 16 hrs without a refill. The system needs compressed air at 60 psig. The outlet pressure maintained with a pressure regulator at approx 30 psig.

carries the abrasive to a temporary hopper attached to the machine head through a flexible hose. An electronically controlled vibrating tray meters the flow of abrasive to a catch hopper. It is then aspirated through a short section of a flexible tube into the mixing chamber of the nozzle assembly. Here it mixes with the high pressure water stream which accelerates the abrasive through the focussing tube to the workpiece.

The abrasive transfer system poses some difficulty if it is necessary to change the type of abrasive. Removal of the abrasive from the storage tank consumes considerable time. The system operates at maximum efficiency when only type of abrasive is used for a long period of time.

6.1.7 Catcher System

The catcher tank installed below the cutting table collects the spent abrasive, the water and the cutting debris, which settle to the bottom of the tank. The size of the tank enables us to contain the noise of the high pressure jet. The base of the catcher tank is provided with a slope to facilitate easy flow of water. The water and the abrasive flow into a settlement tank where the water drains out and the abrasive grit settles down. The grit is disposed off periodically from the tank. The greater depth of the catcher tank reduces the noise from the high pressure jet.

6.1.8 Settlement Tank

The water and the abrasive from the catcher tank flows into the settlement tank which is usually placed behind the machine. The water in the settlement tank is drained or recycled after passing through a filter unit.

6.1.9 Motion Equipment.

Schematic of the waterjet cutting workcell with the arrangement of the torches on the z axis slide is shown in Fig 3. The basic workcell consists of a 60 cm. X 120 cm cutting area. The nozzle is mounted on a gantry. The cutting head motion is controlled entirely by the Allen Bradley series 8400 CNC controller. The controller provides the programmable and the manual motion to the nozzle along the X and Y axis whereas the position of the nozzle along the Z axis can be controlled independently. Along the Y axis the motion is achieved by means of ball screw and along the X axis a rack and pinion system provides the motion.

The principal features of the workcell can be summarized below:

a. Workcell Enclosure

The workcell is fully enclosed and thus the noise outside the workcell area is considerably reduced (Fig 4).

A metallic steel enclosure is provided to the workcell. The inside wall of the enclosure is lined with a noise insulating material to absorb the noise.

b. The Allen Bradley Series 8400 controller (Fig 8)

The CNC control of the workcell is achieved by a series 8400 Allen Bradley controller. The control has provisions of intensifier start up and shut off, booster on and off, nozzle on and off, manual control for the slides, and abrasive feeder on and off. An alphanumeric keyboard allows the operator to key in the task program for execution. A set of soft keys guide the operator through different menu as the user makes his choice. The control is also used for the operation of the Plasma cutting torch and Oxy fuel cutting torch. Another important feature of the control is that the graphical simulation of the nozzle motion can be viewed on the monitor for program verification.

6.2 Plasma Cutting Equipment:

The plasma cutting equipment is manufactured by Linde Co.. The main parts of the plasma cutting equipment are shown in the Fig 9 and Fig 10.

The different parts of the Plasma arc cutting equipment are:

1. The transformer housing unit.
2. The gas supply cylinders.
3. The cutting torch.

6.2.1 The Transformer Housing unit: (Fig 9)

This houses the main transformer and contains the output current controlling unit. The output current can be controlled from 0-250 amps. and depends on the material properties and the thickness to be cut. The input power is 460V at 95amps. It also contains a gas flow control unit. This helps to precisely control the gas flow to the torches. The transformer ON/OFF switch is located on the transformer housing unit.

6.2.2 The Gas Supply Cylinders:

Plasma arc cutting utilizes argon as the chief ionizing gas and either nitrogen or hydrogen as a shielding gas. Both the gases have excellent thermal conductivity properties. The mixture supplied is usually 65% argon and 35 % nitrogen. The supply of gas is done through solenoids which are operated automatically.

6.2.3 The Cutting Torch

The unit uses a PT 251M mechanized cutting torch. The torch is mounted upon a special fixture attached to the cutting head of the HS-3000 hydroabrasive workcell. A control panel fixed on the front side of the machine operates the torch. The construction of the torch is also shown in Fig 10b. The unit uses a tungsten electrode at the center of the torch and is held by a brass collet. A copper nozzle is provided for gas flow. In practise the mixture of argon and nitrogen or argon and hydrogen flows through the nozzle at a predetermined rate. The unit uses a transferred mode of plasma arc cutting in which the current passes from the positive tungsten electrode to the negative workpiece.

6.3 Oxy-fuel cutting equipment

The fuel gas used is acetylene. The equipment consists of an oxy-fuel cutting torch (Fig 13). The torch has inlet ports for preheat oxygen, cutting oxygen and the fuel gas (in our case the acetylene). The gas supply is through electrically operated solenoids. Stainless steel nozzles are used for regulating gas flow. Depending upon the thickness of the material to be cut the nozzle size varies as well as the gas flow rate.

6.3.1 The Cutting Torch

The unit uses a type C-58 torch (Fig 13) manufactured by the Linde Gas Co. The torch is provided with inlet ports for fuel gas, preheat oxygen and cutting oxygen. A rack and pinion mechanism allows for adjusting the stand-off of the nozzle. The torch can be used for cutting material upto 4.0" thick.

VII. The Experimental procedure

7.1 Machining Tools Used For the Study:

The following tools were used for the experiments:

1. Waterjet nozzle, for producing pure waterjet.
2. Abrasive-waterjet nozzle, for producing Abrasive-water jets.
3. The plasma arc cutting torch.
4. The oxyfuel cutting torch.

The major equipments used in the study are the HS-3000 workcell, the streamline intensifier unit, the Plasma arc cutting unit PCM-250, and the Oxy-acetylene cutting unit. All these equipment are available at the Waterjet machining laboratory at NJIT.

7.1.1 Tools for WJ and AWJ :-

Different sizes of sapphire nozzles ranging from 0.004"- 0.014" were used for the formation of the Waterjet and the AWJ. Also the focussing tubes made of tungsten Carbide were used for obtaining the AWJ. The sizes of focussing tubes used in our experiments are 0.030" and 0.043".

The abrasive particles used for the AWJ beam is garnet supplied by the Barton Mine Co. Available grit sizes range from 50 mesh to up to 1400 mesh. In our experiments the mesh sizes #80, #220, #280 and #1000W are used.

7.1.2 Tools for Plasma arc cutting -

The main tools used are the tungsten electrode and the copper nozzle. For steel, upto 12.5 mm thickness a 1.6mm dia electrode is used, above 12.5 mm thickness 2.0mm diameter electrode is used (Table IV).

Copper nozzles for gas flow are available in 3 sizes, 1.4mm, 1.6mm., 2.0mm.. Selection of nozzle depends upon the material thickness (Table IV).

7.1.3 Tools for Oxyfuel Cutting :-

The Oxyfuel cutting torch uses a nozzle for gas flow. The nozzle design is shown in Fig 13. The hole at the center, allows for the flow of the mixture of cutting oxygen and the fuel gas (Acetylene). The smaller holes on the periphery of the nozzle allow for the flow of the preheat oxygen.

7.2 Description of Experiments:

The experiments performed in this study can be broadly classified into three categories.

I. Experiments with individual cutting beams.
II. Experiments related to integration of the beams
III. Experiments to improve quality of surface finish using AWJ.

7.2.1 Experiments with individual cutting beams.

Experiments were carried out with the individual modes of cutting with following objectives :-

1. Determine the feasibility of performing cutting operations with the Plasma beam and the Oxyacetylene beam on the HS-3000 workcell.

2. To determine the surface finish obtained by the three processes.

Cutting experiments were carried out on following materials:

Plain carbon steel, stainless steel, Aluminium and titanium.

The material thickness used in the experiments were 6.35mm, 12.5mm, 25.4mm.

The parameters were chosen such that the test material was always cut through. Cutting speed was used as a variable parameter. All other parameters were used as recommended by the manufacturers (Tables IV,V).

7.2.2. Experiments related to integrated cutting:

The heating of the material at the focussed area can be accomplished by either the plasma arc cutting beam or the Oxyfuel beam. Plasma arc was rejected as a source of heat for several reasons.

1. The temperature of the plasma arc beam is too high, of the order of 20,000 deg [28, Fig. 10c] Celsius. Impingement of this beam results in instantaneous melting of the material.

2. The cutting speeds of PAC and the waterjet beam are incompatible. At low material thickness (below 12.5mm) the rate of PAC cutting is at least 10 times higher than the WJ.

The Oxyfuel cutting beam is an useful tool for integration with the waterjet for the following reasons:

1. The maximum temperature obtained from the OFC is about 3000 deg celsius. The beam needs to be focussed for at least 30 sec before it melts the metal surface.

2. The cutting speed with OFC is considerably low and is only slightly higher than the AWJ.

Following experiments were carried out in relation to the study of Integrated cutting:

7.2.2.1 Experiments with pure Waterjet :

The objective of these experiments was to determine the pierce capability of the pure water jet and the variation in the depth of penetration for different jet diameters. Pure water jet formed with different sapphire nozzles was used for piercing of the aluminium plate. The plate thickness was chosen as 6.25 mm. The nozzle diameter was varied from 0.004"-0.014".

Piercing experiments on steel specimen were not successful. The capability of pure waterjet to pierce through hard materials is limited.

The time taken for piercing through the thickness of the material was measured. It is seen (Table - X) that with the reduction of diameter of the sapphire nozzle the time taken for through piercing increases exponentially for the same thickness of the material. Also the time required for through penetration as the thickness of the material is increased is considerably higher than at smaller thickness.

7.2.2.2 Experiments with Oxyfuel cutting beam.

The time taken for the oxy-acetylene beam to pierce through the metal was measured. The oxy-acetylene beam was focussed at one point on a plain carbon steel specimen. Material thickness of 6.35 and 3.25mm was chosen for the experiment. The focus time was gradually increased keeping the gas flow rate and the other parameters affecting the beam temperature constant. The beam was maintained at the same point until the material on the surface started to melt.

This experiment made it possible to determine the time of heating of the material surface before impingement of the high pressure waterjet.

7.2.2.3 Experiments for integration of Oxyfuel-Waterjet beam for cutting.

The Oxyfuel torch was fixed to the L - fixture attached to the machine head. The torch was rotated through an angle of 50 -60^0 to focus the beam and the waterjet at the same focal point (Fig 14).

Test samples were sized to 50 mm. X 50 mm. Two different thickness 3.125mm and 6.25mm were chosen for the experiment.

The following experimental procedure was adopted to study the effect of heating the material on water jet cutting.

(i) Piercing using the integrated beam:

The objective of the study was to determine the effect of the heating and subsequent impingement by pure waterjet on the volume of material removal.

The parameters varied included

1. Heating time of the material, 0-25 sec gradual variation.
2. The time of piercing of the jet, 0.5s, 1.0s, 1.5s 2.0s..

3. The sapphire diameter for waterjet, 0.1016-0.3556mm.
4. The standoff distance for the thermal beam, 25-50mm.
5. The water jet standoff distance was varied between 2-25mm.

The following procedure was carried out to conduct the experiment.

1. The thermal beam was initially focussed on the metal surface for a time t sec.

2. At the end of time t sec. the waterjet was impinged upon the heated spot for a time period t1 sec.

It was observed from the heating experiment carried out with the oxy-acetylene beam that when the heating time for carbon steel was varied keeping all other factors constant the minimum heating time (t) necessary for the waterjet to pierce through a sample of thickness 3.125mm was about 25 sec. The piercing time of the waterjet (t1) was kept fixed at 0.5 sec.

(ii) Linear cutting experiments:

The Oxyfuel beam nozzle was located approximately 1" in front of the waterjet beam nozzle (Fig 1). The region immediately in front of the waterjet nozzle was heated and the waterjet beam and the Oxyfuel beam were moved

simultaneously such that the Oxyfuel beam is constantly heating the metal surface in front of the waterjet nozzle. Even at speeds as low as 0.3-0.5 ipm. cutting was not possible since the heat on the surface could not be sustained for more than 1-2 seconds.

Following observations were noted during the experiments:

1. The highly turbulent flow generated during waterjet impingement prevented focussing of the Oxyfuel beam at one point for more than 5 seconds time period. In attempts of at least 20 cases of linear cutting, the turbulence due to the Waterjet shut off the Oxyfuel beam in less than 5 seconds at least 10 times.

2. Initial heating of the material to a certain level (red hot) over a length of 1"-2" and subsequent cutting by waterjet also failed. It was observed that as soon as the waterjet impinged upon the heated surface the surface lost all the heat and returned to the original temperature within 2-3 sec making further impingement of the waterjet ineffective.

7.2.3 Experiments to improve Quality of surface finish using AWJ :

AWJ machining gives the best roughness on the surface for any material compared to PAC and OFC. Experiments were conducted to study and determine the conditions to achieve the best roughness due to AWJ cutting. The experimental matrix is given in Tables VIII -A,B,C.

Stainless steel material was chosen as the test material. Due to its high toughness stainless steel cannot be finish machined easily by conventional grinding process [1]. Material removal by grinding becomes difficult due to the "loading" of the grinding wheel. As a result precision grinding of a stainless steel surface is very difficult.

AWJ cuts stainless steel material relatively faster. In our experiment the main objective was the use of AWJ as a surface finishing tool for generating precision surfaces. 5" wide flats of stainless steel of grade SS 403 was chosen for the experiment. Two different thickness 0.5 inch and 1.0 inch were chosen for the experiment. The flats were cut approximately into 1.5 inch long pieces by plasma arc cutting (Fig 22). These pieces were then used for further finishing by AWJ.

The specimen was held securely in a vise. The AWJ was moved tangential to the plasma cut surface (Fig 15).

Minimum material was removed from the surface in each pass. The lateral depth of cut was less than 0.03 in.

The parameters varied were the cutting speed, sapphire diameter, carbide diameter, abrasive grit size, water pressure, the number of passes and the material thickness. Results are tabulated in Tables XIX -XXIII.

Limitations of the experiment:

It is not possible to measure the actual depth of cut for the first pass while finishing a workpiece. This is due to the fact that the nozzle was positioned visually with reference to the workpiece surface. Hence the depth of cut during the first pass was varying upto a maximum of 0.03". The depth of cut for subsequent passes could be set accurately with reference to the first pass position of the nozzle.

7.2.4 The measurement procedure for Surface Roughness:

A Hommelwerke make surface analyzer (Fig 24) was used for the purpose of measuring the Roughness Average (R_a) of the waterjet machined surfaces. This is a stylus probe instrument and has features to measure the R_a, R_z and R_m [37]. Three tracing lengths (sampling lengths) of 1.5mm, 4.8mm and 15mm are possible for measurement purposes. In our

experiments 4.8mm tracing length was used for measuring the Roughness Average. The Roughness Average can be measured in either micrometers or microinches. The measurements in our experiments was done in micrometers.

VIII. Results and Discussion

8.1 Results of Individual Cutting:

Out of the three high energy beams Oxyfuel cutting produces the surface with the maximum roughness at thicknesses upto 2.0", and the AWJ cutting gives the best roughness. Above 2.0" thickness Plasma cut surfaces have the roughest surface finish. The cutting speeds for the PAC and the OFC are given in Tables IV and V. Tables I-III list the parameters affecting each of the three processes. It is seen that Plasma arc cuts the fastest for a given thickness and AWJ cuts the slowest, below a thickness of 2". Table VIII compares the two thermal cutting processes. The Heat affected zone (HAZ) thickness is less in case of PAC than in OFC.

8.2 Results of Integrated beam Cutting:

8.2.1 Piercing tests:

Summary of results:

The impingement of waterjet on the heated steel sample of 3.125mm thickness resulted in a through pierce. The samples indicate that the material removal occurs as a result of instantaneous displacement due to the impact force of the high pressure jet. The impingement results in the

formation of a large dimple about 8mm. in diameter and 4mm. deep (Fig 18). The diameter of the pierce hole varies between 2-3mm diameter.

The following factors influence the formation of the dimple.

1. The heating time of the surface.
2. Material thickness.
3. The piercing time of the jet.
4. The accuracy of focus of the jets.

8.2.1.1 Effect of heating time on the material removal:

A low heating time reduces the effect of impingement of the waterjet. The material removal volume and the depth of pierce of the integrated beam is directly proportional to the heating time (Fig 27-30, Tables XIII-XVI).

Excessive heating time results in the melting of the surface of the impingement zone. For the plain carbon steel workpiece of thickness 3.125mm, the optimum heating time of the material is 25 sec. The jet was able to pierce the material after a heating time of 25sec. The jet pressure was maintained at 50ksi.

For a steel plate of 6.25mm. thickness the heating time could not be increased beyond 30 sec., since the surface of

the material started to melt at this stage. Impingement of the jet on the surface prior to this period resulted in the formation of a dimple similar to that with material of thickness 3.25mm. The maximum depth of the jet penetration at these conditions was 2.0mm.

8.2.1.2 Effect of material thickness on impingement:

As the material thickness increases the heat input to the workpiece needs to be increased to maintain the intensity of the heat. At the same time excess heat input results in melting of the material surface. For 3.25mm thickness heating for 25 sec. was sufficient. For 6.35mm thickness the maximum heating time was 30 sec. above which the material surface was melted.

8.2.1.3 Pierce time of the jet:

In the experiments carried out the time of piercing of the waterjet was 0.5 sec. and 1.0 sec. Increasing the piercing time above 1 sec. duration practically did not effect an increase in the material removal due to intensive heat dissipation in the impingement zone.

8.2.2 Surface finishing tests:

It was shown that the AWJ finishing enables us to reduce surface roughness. The effect of the specific operational conditions on the topography is discussed below:

8.2.2.1 Effect of Sapphire and Carbide tube Diameter on Roughness Average (Ra): (Tables XX and XXIII)

Results of experiments show that the sapphire nozzle and the focussing tube nozzle diameters do not effect significantly the surface finish. Sapphire/ Carbide nozzle combinations of (0.007/0/03), (0.009/0.030), (0.009/0.043) in. show almost no deviation in the Roughness Average value.

8.2.2.2 Effect of Particle Size: (Tables XIX - A,B and Figures 35-38)

Particle size has a very decisive effect on the surface Roughness. The use of the finest available grit size of 220 mesh resulted in a (R_a) value of 0.92 microns (36 micro-inch) at a nozzle traverse speed of 12.5 mmpm. The corresponding R_z value obtained was 4.35 microns, (172 micro-inch).

The use of abrasive particles of mesh size 280 in Garnet and Silicon carbide was tested. It was observed that abrasive flow rate of 225 gm/min. is not sufficient to effect finishing beyond a depth of 7mm. from the top of the surface. Higher mass flow rates are desirable for consistent Roughness at depths greater than 100mm for these grit sizes.

The use of 1000W and finer grit were not successful for the machining operation because the dry abrasive feeding of these sizes was not feasible with the existing suction type abrasive feeding.

8.2.2.3 Effect of Number of Machining passes :

The Roughness average value will become more uniform as the number of passes are increased. Also the uniformity of the Roughness value with Depth is improved as the number of passes are increased (Figures 34 and 39).

In this experiment the depth of cut for the second and successive passes was kept minimum (<0.005").

8.2.2.4 Effect of lateral Depth of Cut:

Lateral Depth of cut refers to the lateral feed of the AWJ beam per pass. The best results with regard to Roughness are achieved with a depth of cut of 0.1-0.4 mm. depending upon the uniformity of the original surface. As the depth of

cut is increased the Roughness value increases with increasing depth from the top surface.

Garnet when used as abrasive material with mesh size of 280 results in an increase in the surface waviness although the Roughness is improved. Experimental results using Silicon Carbide of 240 mesh, show that the surface finish is improved when compared to the samples using garnet abrasive.

IX. Conclusions and Recommendations

1. The experiments with the individual modes of cutting demonstrate that an Integrated High energy beam workcell can greatly increase the productivity and the flexibility of the manufacturing processes. Depending upon the surface finish and tolerance requirements the suitable cutting process can be adopted. The accuracies of machine cutting are applicable for Plasma Arc cutting and Oxyfuel cutting as a result of integration.

2. Integrated beam cutting with thermal and Waterjet beams was investigated in stages. The following conclusions are drawn from these investigations:

(i) The results demonstrate that the integration of the thermal and the Waterjet beams can be implemented and needs further investigation concerning the cutting parameters.

(ii) For a plain carbon steel plate of 3.125 mm thickness the maximum heating time for Oxyfuel beam is 22-24 sec. before the surface of the metal starts to melt. This in effect is the ideal time for the start of waterjet impingement to acheive the maximum depth of penetration by the jet.

(iii) Piercing operations by the waterjet beam on red hot surface of steel plates have resulted in an increase in the material removal volume.

(iv) The duration of piercing by the waterjet beam is less than 0.5 - 1.0 sec. Piercing for longer durations results in rapid heat dissipation from the impingement zone and has no further effect on penetration.

(v) Besides the beam heating time and the jet pierce time the accuracy of the jets' focus point and the diameter of the sapphire waterjet are important parameters effecting the volume of material removal. In general, the higher the accuracy of the jet focus points, higher the depth of penetration by the waterjet beam. Similarly, larger the jet diameter greater is the depth of penetration.

(vi) The High Pressure Waterjet induces substantial turbulence in the surrounding air in its path. The turbulence was observed to affect the stability of the oxyfuel beam. Therefore simultaneous jet impingement and heating is not possible with oxyfuel beam as the heat source.

(vii) Plasma cutting beam cannot be used for the heating of the impingement zone. The high temperature (>15,000^{o} C) of the plasma beam results in instantaneous melting of the

material making further impingement by waterjet impractical. In comparison Oxyfuel beam is suitable for the purpose of beam integration.

3. The workcell design with the enclosure suggests that it is feasible to operate the High energy beams such as High Pressure Waterjet and Plasma Beam, etc. within the government approved noise limits. The enclosed workcell recorded noise limits less than 85 dB compared to the 110 dB recorded with an open workcell.

4. The conclusions derived from the surface finishing experiments can be summarized as below:

(i) AWJ can be used as a surface finishing tool to produce precision surfaces with Roughness Average (R_a) value of less than 1 micron.

(ii) Particle size is the most important parameter affecting the surface finish. Garnet abrasive with 220 mesh and mass flow rate of 225g/min resulted in an R_a value of 0.86-0.92 micrometers at a speed of 12.5mmpm.

(iii) Particle sizes above 220 mesh require higher flow rates of 400 gms/min or higher. Further experiments with

suitable designs of nozzle body assemblies that can handle high flow rates are strongly recommended.

(iv) Sapphire nozzle orifices in the range of 0.007"-0.012" and tungsten carbide focussing tube in the range of 0.03"-0.043" give almost similar results on surface finish.

(v) The experiments on surface finish were carried out on stainless steel plates of thickness 12.5mm. and 25mm. Experiments with diverse materials such as glass on the same principle is strongly recommended.

(vi) Dry abrasive feeding by gravity and suction of mesh sizes of 1000 and above was not possible. Investigations using forced slurry feeding of these sizes is strongly recommended.

(vii) The variation of the surface Roughness over depth is affected by the number of passes and the traverse speed of nozzle. Increasing the number of passes reduces the variation of the Roughness values with increasing depth. Similarly reducing the traverse speed improves the surface roughness with increase in depth.

(viii) It was possible to investigate the improvement in Surface roughness wherein the workpiece was held stationary against a traversing jet. It is strongly recommended that

suitable designs of nozzle body assemblies that can handle high flow rates are strongly recommended.

(iv) Sapphire nozzle orifices in the range of 0.007"-0.012" and tungsten carbide focussing tube in the range of 0.03"-0.043" give almost similar results on surface finish.

(v) The experiments on surface finish were carried out on stainless steel plates of thickness 12.5mm. and 25mm. Experiments with diverse materials such as glass on the same principle is strongly recommended.

(vi) Dry abrasive feeding by gravity and suction of mesh sizes of 1000 and above was not possible. Investigations using forced slurry feeding of these sizes is strongly recommended.

(vii) The variation of the surface Roughness over depth is affected by the number of passes and the traverse speed of nozzle. Increasing the number of passes reduces the variation of the Roughness values with increasing depth. Similarly reducing the traverse speed improves the surface roughness with increase in depth.

(viii) It was possible to investigate the improvement in Surface roughness wherein the workpiece was held stationary against a traversing jet. It is strongly recommended that

the alternate method of moving the workpiece surface against a stationary jet also be investigated.

5. The experiments conducted with the cutting of different fiber-composites using AWJ clearly demonstrates feasibility of using AWJ to prevent the composite delamination during cutting. This application of AWJ promises wide practical scope for the composite material industry.

APPENDIX - A

WORKCELL OPERATION

The operation of the three processes is described so as to give the reader a knowledge concerning the technique of beam integration for machining.

A.1 Operation of the Abrasive waterjet:

The operation of the pure water jet is a fairly simple process. A sapphire diamond nozzle is placed in a holder which is fastened to the stem attached to the valve near the end of the high pressure tubing. The diameter of the nozzle varies from 0.003 - 0.014 in. When the nozzle ON is pressed a supersonic high pressure column of jet issues out of the nozzle which can be used for cutting soft materials like plastic, rubber, wood, non-woven products, fish, fabric, etc.

For the operation of the Abrasive waterjet an abrasive nozzle assembly (Fig 7a and 7b) is used. The nozzle assembly is designed by IR and uses a ball orifice and a carbide focussing tube. The alignment of the ball orifice to the carbide focussing tube is made on the Alignment station.

A.1.1 The Alignment Station (Fig 6a)

The alignment station is a stand alone unit for performing the axial alignment of the focussing tube and the sapphire nozzle. It uses ordinary tap water at normal pressure. The alignment process involves the following steps:-

1. The sapphire ball orifice is placed inside the nozzle body and tightened lightly with the set screws. The nozzle body is then tightened to the outlet of the alignment station. Only hand tightening is sufficient.

2. The water is supplied to the system. A thin column of jet issues out of the nozzle. Visually the jet column is centered to the extent possible.

3. The alignment tool is fixed at the bottom of the nozzle body. The column of jet is adjusted to focus through the hole in the alignment tool. The set screws holding the ball orifice are tightened. If the jet column is passing freely through the hole in the alignment tool it indicates that the sapphire and the aligning tube are perfectly aligned. The alignment tool is then removed and replaced by the focussing tube. A thin uninterrupted column of jet issues out of the focussing tube indicating that the sapphire orifice and the focussing tube are aligned.

The advantage is that more useful energy of the jet is available for cutting due to improved alignment.

The nozzle body is then ready for mounting on the machine. The nozzle assembly should be initially tightened with light force and tested at low pressure for any leaks. If there are any leaks through the weep hole further tightening will be necessary. Once all leaks have been stopped the machine is ready to be used for AWJ cutting.

A.1.2 Program Execution

The actual cutting by AWJ on the HS-3000 involves following steps:

1. On power-up the following necessary steps need to be performed to be able to operate the machine:
   a. Press the exit button (Soft key) on the controller.
   b. Enter user Access code. Main Menu comes on the monitor.
   c. Turn the Drives ON by closing and opening the Emergency red switch once.
   d. Press the white soft key for Manual Operation on the menu screen.
   e. Press the soft key for Machine Home. Wait until the Control performs Machine Homing of both the Y as well as the X axes indicated by message "Machine Homed" on the Console.

The machine is now ready for operation.

2. The required NC program to be executed is entered into the controller memory either through the keyboard, or through the PC using a communication package like the PC-Talk.

3. The counter for the abrasive flow provided on the control panel of the machine can be set at any desired value. The flow rate at a particular counter setting is measured by collecting the abrasive for one minute of flow and weighing the same. It is recommended to measure the abrasive flow rate frequently to assure accuracy of the experiments performed. A minor variation in flow rate can be expected due to the disturbances in the system and slight variations in the different batches of the abrasive supplied. The actual effects on the cutting of AWJ due to these minor variations in the abrasive flow rate can be neglected.

If the bulk abrasive transfer system is being used, the air supply valve to this unit is opened and the power switch is pressed ON. Pressure setting on the regulator of this unit is set at 30 psig.

4. The cutting area is ensured to be clean. A supporting material such as Styrofoam may be used to cover the steel grating to prevent the escape of fumes into the cutting environment. The workpiece is placed on the Styrofoam and secured by additional weights placed upon it.

5. The nozzle standoff is adjusted by manually positioning the Z-axis on the slide.

6. The program can be verified by using the graphics and the dry run features of the CNC control. Necessary adjustments in the workpiece positioning or the start point position of the nozzle are made.

7. Press the AUTO-OPERATE soft key on the Controller and enter the desired program number to be executed.

8. Press the intensifier ON and note the pressure reading on the dial.

Wait for the pressure to reach a maximum.

9. Press the cycle start button.

The control will execute the program.

For the purpose of 2 dimensional cutting the workpiece need not have any elaborate clamping fixtures. A simple weight could be placed over the component to prevent its displacement during cutting. Styrofoam may be used as a convenient support material for the workpiece. In case of through cutting abrasive waterjet does not give excessive spillage of water and also operates with minimum noise.

A.2 Operation of the Plasma cutting equipment:

The Plasma arc cutting outfit is supplied by the Linde Gas Co. The unit uses a mechanized torch and the cutting process is fully automated.

Plasma arc cutting can be used to cut any conducting metal. Two sizes of tungsten electrode, 1.6 and 2.0 mm (Fig 12a & 12b) were used for the arc generation. Three sizes of copper nozzles were used for the experiment. The operation involves the following steps.

1. The gas pressure on the Argon and the nitrogen gas cylinders is set at 90 psig.

2. The unit is turned ON by turning the ready-off switch to the ON position.

3. The output current is set to the desired value.

4. The gas flow rate is measured by depressing the buttons under the gas flow meter and adjusted to the desired value.

5. Depending upon the thickness and the material the electrode and the nozzle size are chosen. The setting of the electrode is done using the setting gauge supplied by the manufacturer.

6. The torch is clamped to the special fixture attached to the cutting head of the machine (Fig 3).

The standoff is adjusted to the desired value and is dependent upon the material and its thickness. It is very necessary to maintain the standoff to the correct value in Plasma arc cutting. Too high a standoff will result in the arc being lost and too low a standoff will damage the nozzle.

7. Plasma arc is harmful to the eyes and should not be viewed with naked eye. Protective eye wear should be used to cover the eyes while operating the plasma arc.

8. The task program is entered in the controller. The AUTO OPERATE soft button is pressed.

9. The material is placed underneath the torch. The ground cable is connected to the workpiece by using the clamp provided at its end.

10. The plasma arc START button on the switch board is pressed. Gas flow starts and after a few seconds the pilot arc is initiated. The START button can be released after the pilot arc is initiated.

11. As the START button is released the cutting arc is started. The plasma arc starts to melt the material by piercing. The CYCLE START button on the Allen Bradley controller is pressed.

12. Initially a low traverse speed is used for the nozzle and as the cutting starts 100% recommended speed is used by setting the feed rate override to 100%.

13. Once the program is complete, the STOP button on the switch board is pressed to stop the arc.

A.3 Operation of the Oxyfuel cutting equipment:

The principle of Oxy-acetylene flame cutting is very well known and is already explained in considerable detail in standard books. The oxyfuel cutting equipment uses a type C-58 Oxyfuel cutting torch manufactured by Linde Co.. The torch is equipped with a preheat oxygen port, a cutting oxygen port and a fuel gas port. The gas supply is through the solenoids operated electrically. The fuel gas used is acetylene. Cutting with Oxy-acetylene flame involves the following steps:

1. The cutting nozzle is chosen and assembled on the torch. The table provides a guide for choosing the nozzle diameter. Thicker materials use a larger diameter for increased gas flow as well as increased heat.

2. The task program is entered into the controller. Press the AUTO OPERATE button and enter the program number to be executed.

3. The gas pressures for the preheat and cutting gas as well as the fuel gas are set to the recommended values as given in the table.

4. Close all valves on the torch head initially. Press the PREHEAT Oxygen ON button on the switchboard. Open the fuel gas valve about half revolution on the cutting torch. Light the flame using a lighter. Open the preheat O_2 valve slightly. The flame will burn continuously. Adjust for a neutral flame by appropriately opening both the valves.

5. Move the torch by manual jogging the control to the start point of the cut. Adjust the standoff to position the flame tip to touch the surface of the material.

6. Heat the surface to red hot glow. Open the cutting O_2 valve and press the cutting O_2 button. Also press the CYCLE START button. After the cutting is over press the STOP button to shut the gas supply and kill the flame.

Precautions:

1. Use of eye protection is necessary while cutting with the flame.
2. The workpiece is very hot and care should be taken in handling the workpiece.

APPENDIX - B

Results of AWJ Cutting Experiments on Composites:

In order to enhance the knowledge base of machining by AWJ the application of the AWJ for cutting two different types of Composites was explored at NJIT.

I. The first sample was a anisotropic carbon fibre composite 7/8" thick and useful in Bio-medical engineering Applications. A series of experiments were conducted to determine the operational conditions under which there is no de-lamination of the material. The following experimental conditions were found to give satisfactory results:

(i) Pressure - 40-42 ksi.

(ii) Abrasive - Barton's Garnet #80 HP mesh

(iii) Abrasive flow rate - 0.5lb/min. (225 gm/min)

(iv) nozzle stand-off - 0.1"

(v) orifice/focussing tube diameter - 0.010/0.03 in.

(vi) nozzle traverse speed - 5-6ipm.

It was observed that pressure is the critical factor effecting delamination. Pressures above 45ksi resulted in delamination almost 100% of the time. In about 50 experiments conducted at pressure of 40-42 ksi no delamination was observed in the sample. Reducing the pressure resulted in a increase in the striations near the lower edge of the surface. Abrasive flow-rates below 0.4 lb/min resulted in delamination of the material. Through cuts were not possible beyond a traverse speed of 9 ipm.

II. The second sample consisted of a 1.25 mm thick type G-10* composite sheet. The area of the sheet is 20"x20". The requirement was to cut 10 grids on the sheet at specific locations without delamination of the material (Fig 25). Each grid consists of 10x10 rectangular holes. The tolerance of the wire thickness between each rectangular plate is 1.25mm +/- (0.25mm). The following procedure was adopted to produce the required shape on the HS-3000 hydro-abrasive workcell.

The job was finished in two stages. Precisely two programs were written in order to complete the job. In the first stage piercing operations were carried out at the center of each of the 1000 rectangular holes. The following parameters were used for the operation:

Sapphire diameter - 0.007 in.
Tungsten carbide tube - 0.030 in.
Abrasive mesh - 80 mesh garnet.
Intensifier Pressure - 14-16 ksi.
Abrasive flow rate - 0.2 lb/min.
nozzle stand off - 0.1 in.
Jet pierce time - 1 sec.

In the second stage the actual cutting of the grid was performed. The nozzle started at the center of the pierced hole of the first rectangular hole in the first grid of the sheet. The rectangular hole was cut and the nozzle moved to the center of the second rectangular

hole and so on. After all the 100 rectangular holes in the first grid were finished the nozzle moved to the center of the first rectangular hole in the second grid. The following parameters were used in the second operation:

sapphire diameter - 0.007"

Carbide diameter - 0.03"

Intensifier Pressure - 26-28 ksi

Abrasive flow rate - 0.2 lb/min.

Abrasive mesh - #80 garnet.

nozzle traverse rate - 75 ipm.

nozzle standoff- 0.1 in.

The cycle time for the entire operation was 180 min.

In all 4 nos were produced by this operation. In all the pieces no delamination was observed at any place in the whole sheet.

From the obtained results it may be concluded that AwJ is ideally suited for the machining of fiber composites. But the precise operating conditions to avoid the delamination needs to be determined experimentally in each case. The conditions of machining depends upon the properties of the fiber composite material under study.

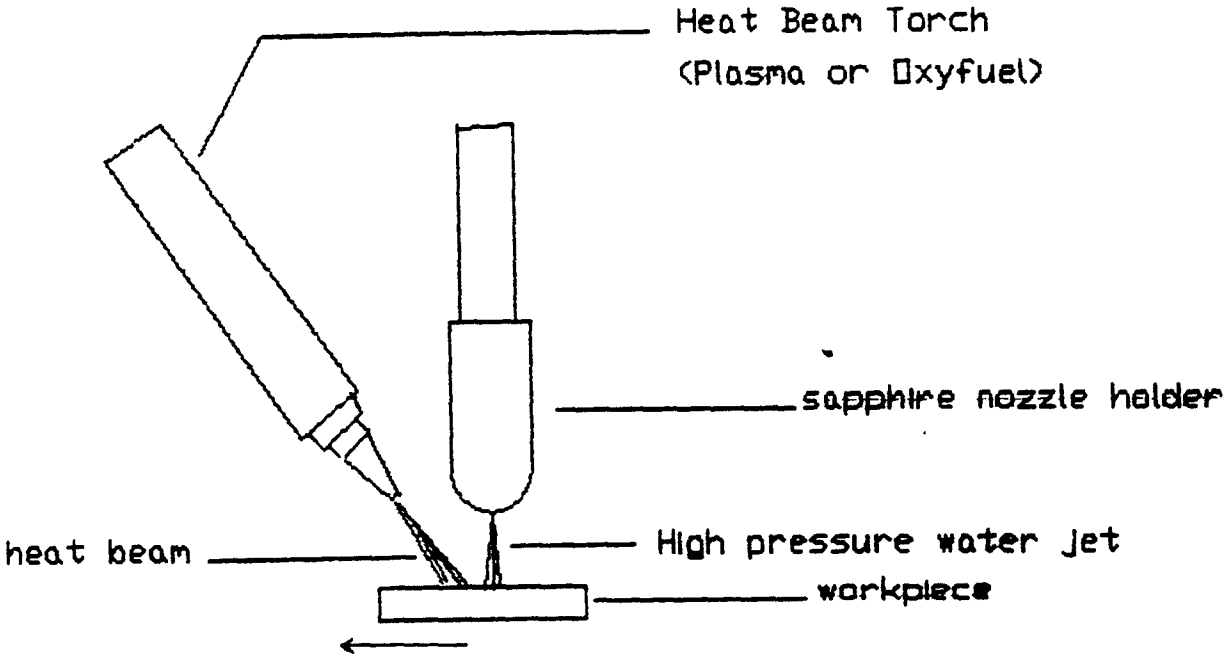

Fig 1 Schematic of beam Integration method

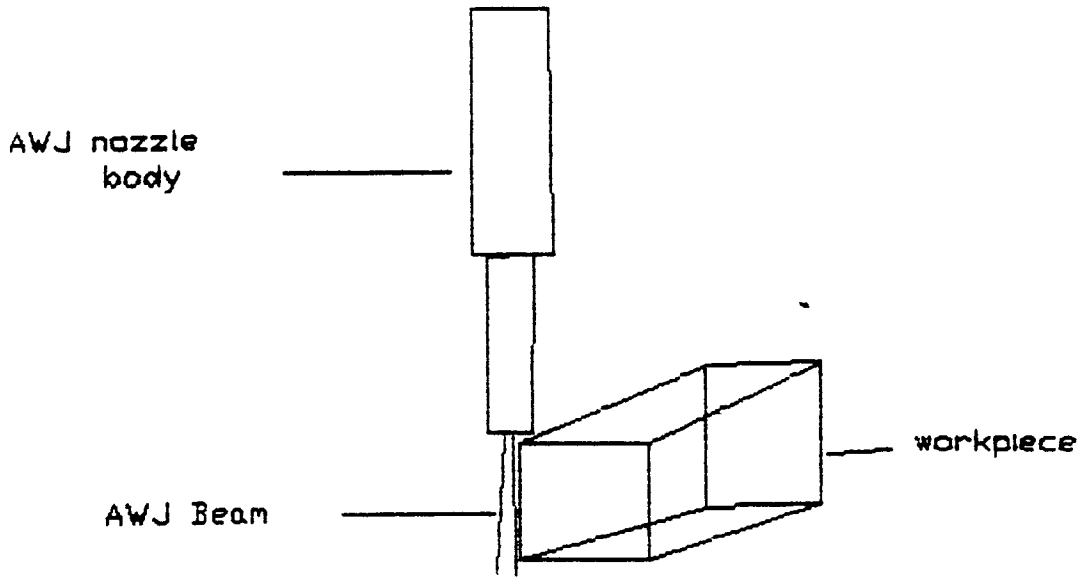

Fig 2. Schematic of Surface Finishing Operation

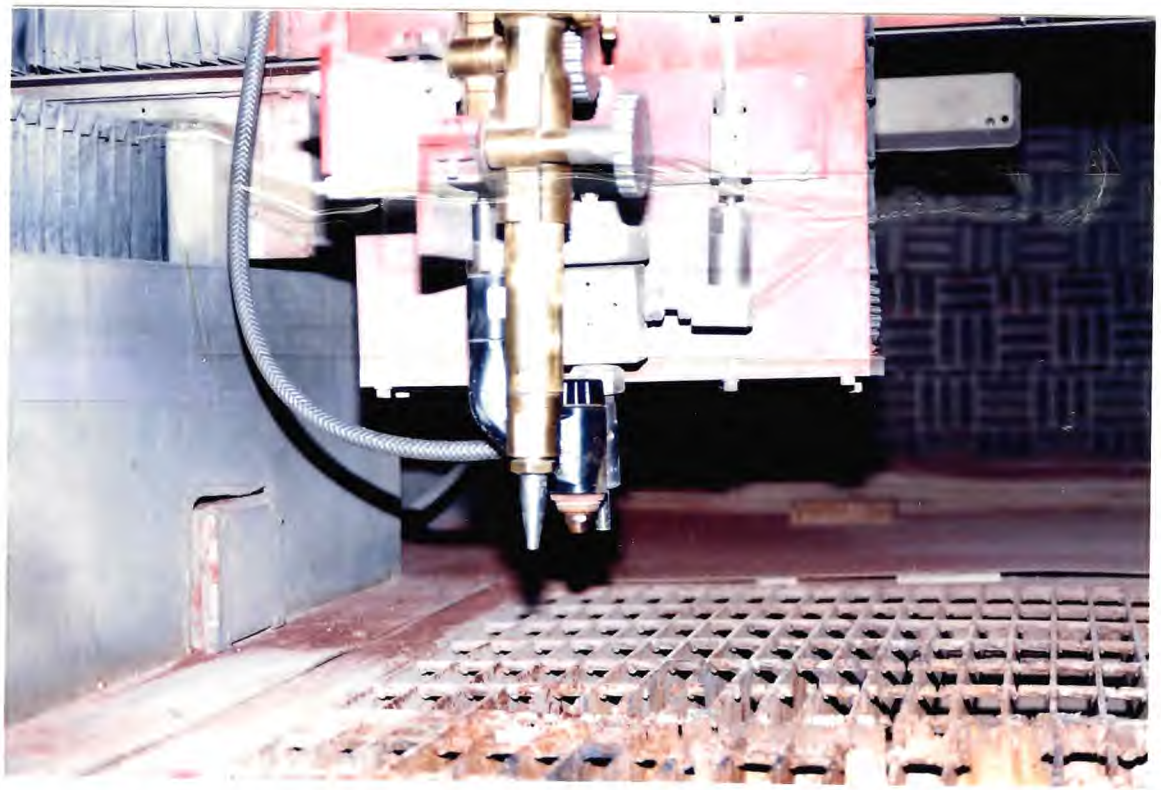

Fig 3. Figure showing construction of the Integrated workcell with all the three cutting tools mounted.

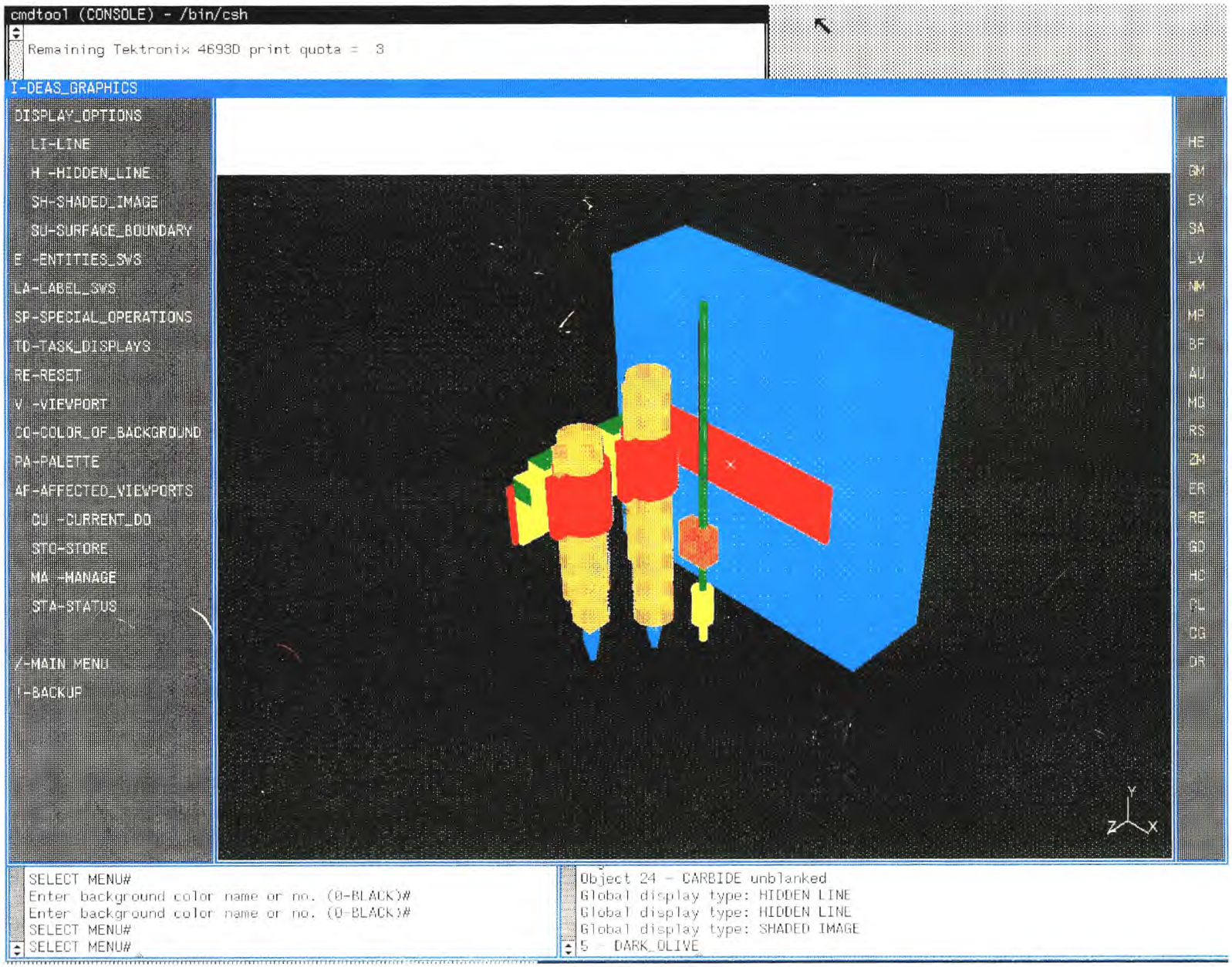

Fig 3a. 3D Model of the torches arrangement for the Integrated Workcell.

Fig 4. Picture showing the workcell view with enclosure.

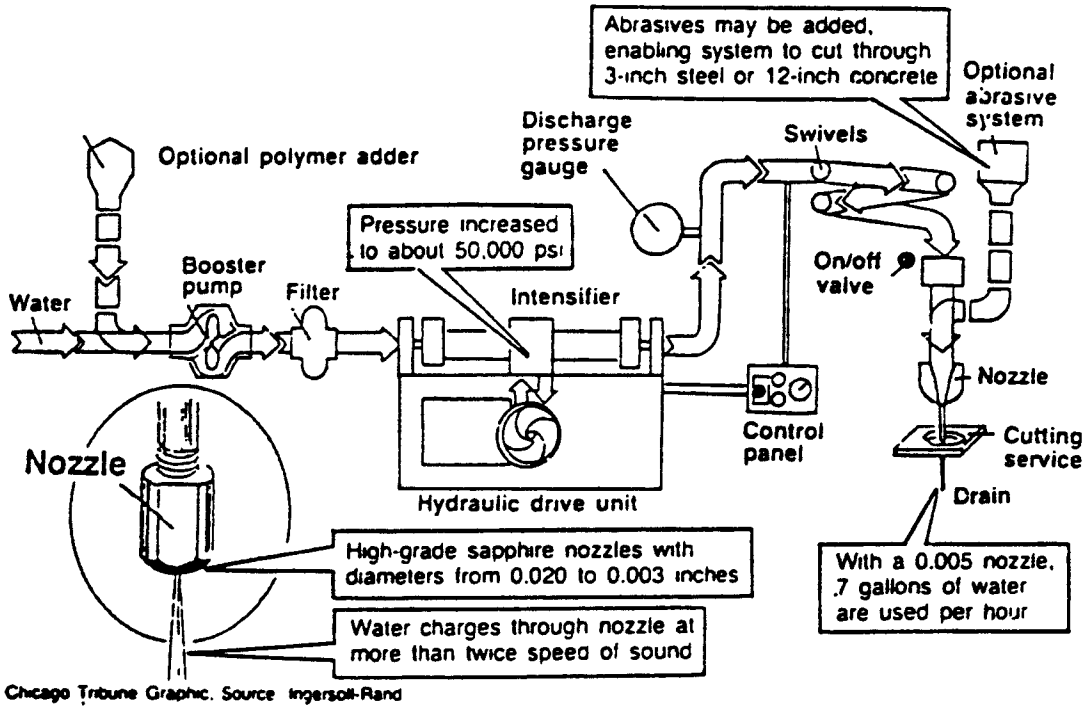

Fig 5a. Basic Components of the Waterjet System.

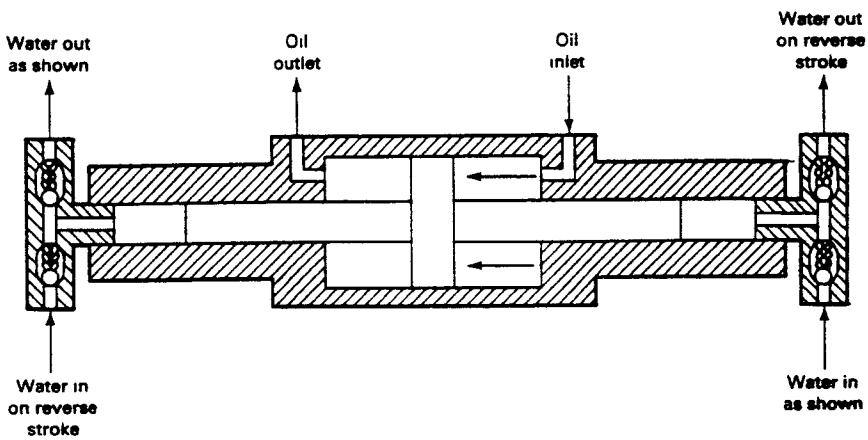

Fig 5b. Schematic of the Hydraulic Intensifier.

Fig 6a. The nozzle alignment station.

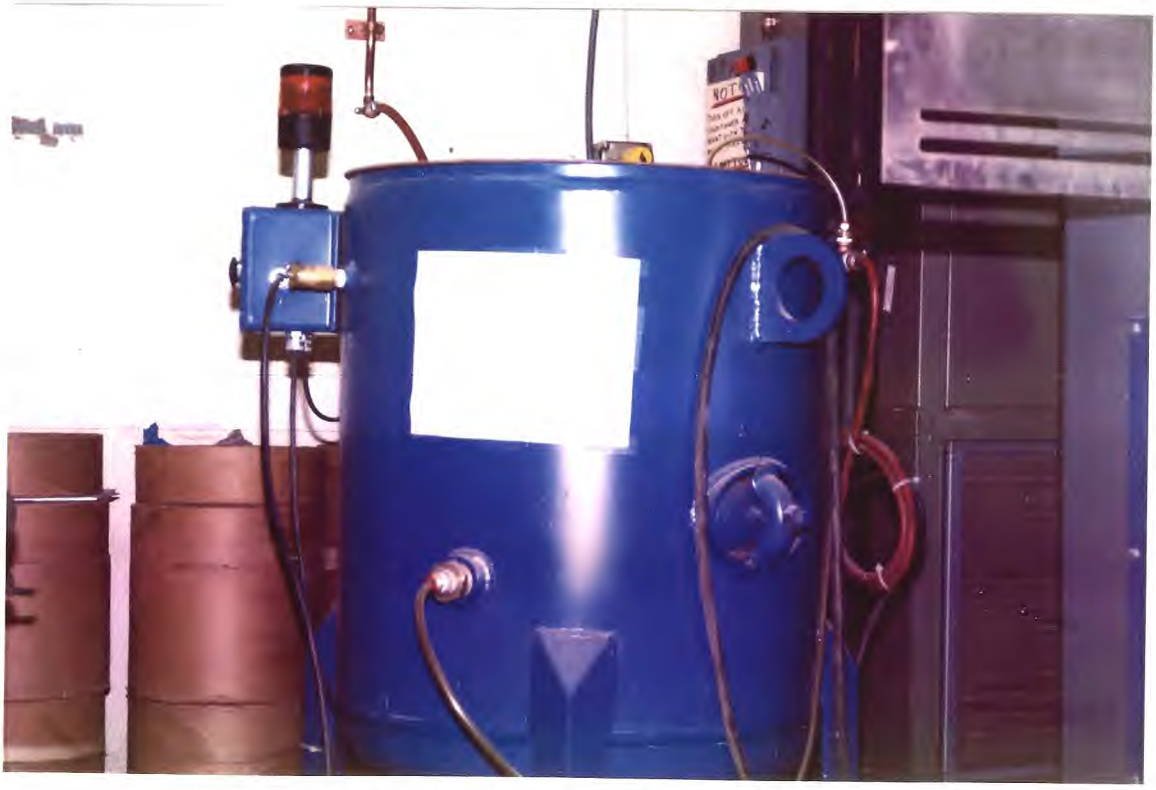

Fig 6b. The bulk abrasive transfer System

Fig 7a. Components of the hydro-abrasive cutting nozzle body.

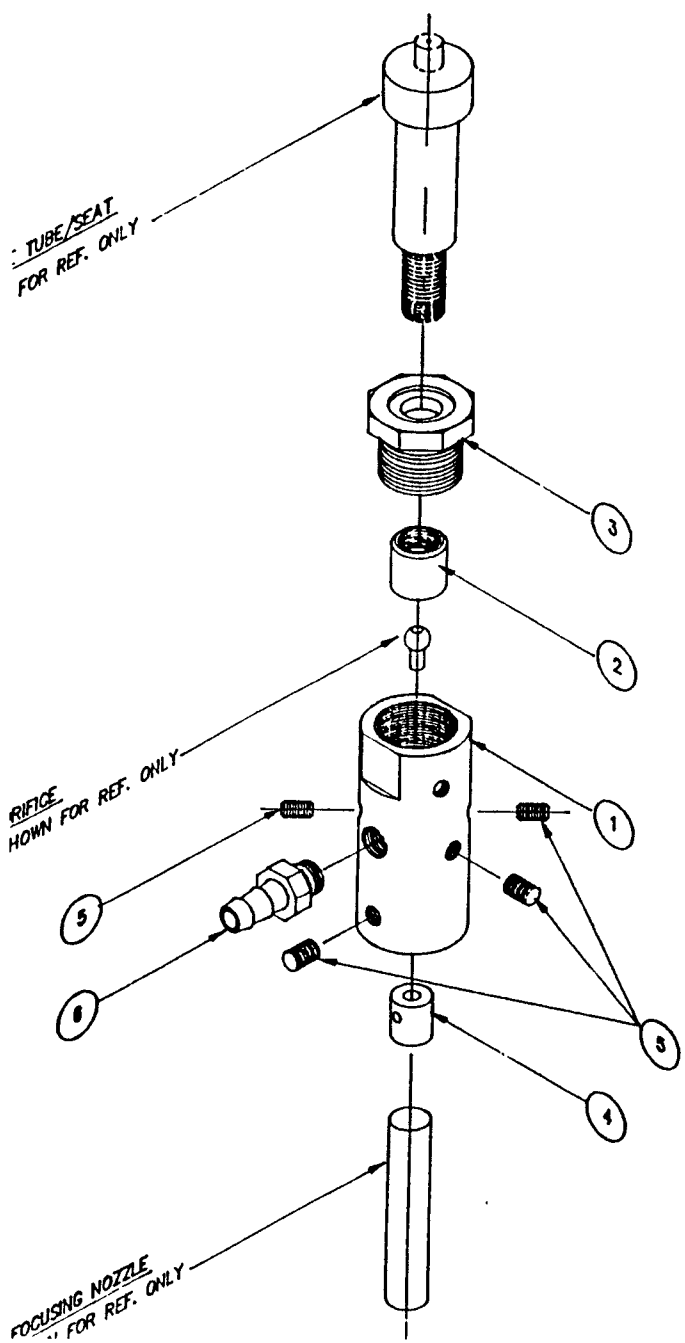

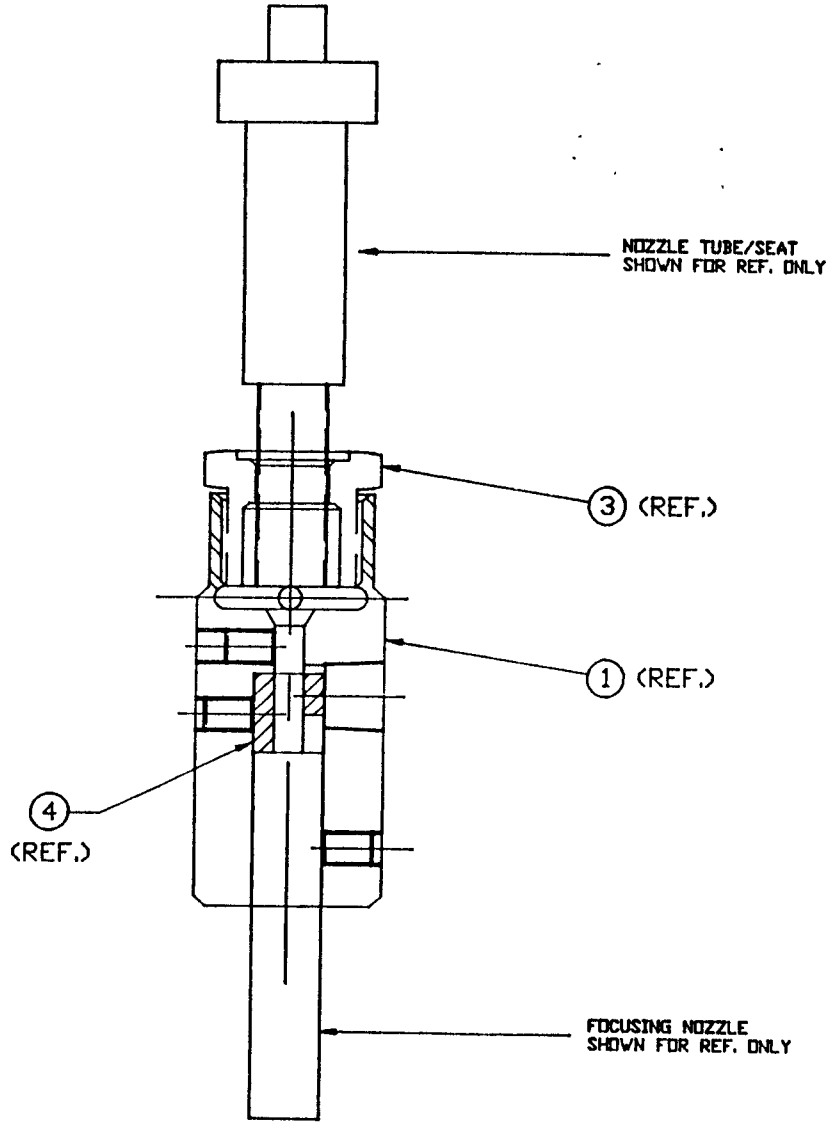

Fig 7b. Schematic of the hydroabrasive nozzle construction.

Fig 8. The Allen Bradley CNC Controller and the Control for the PAC and the OFC torches.

Fig 9. The Plasma Arc Cutting system

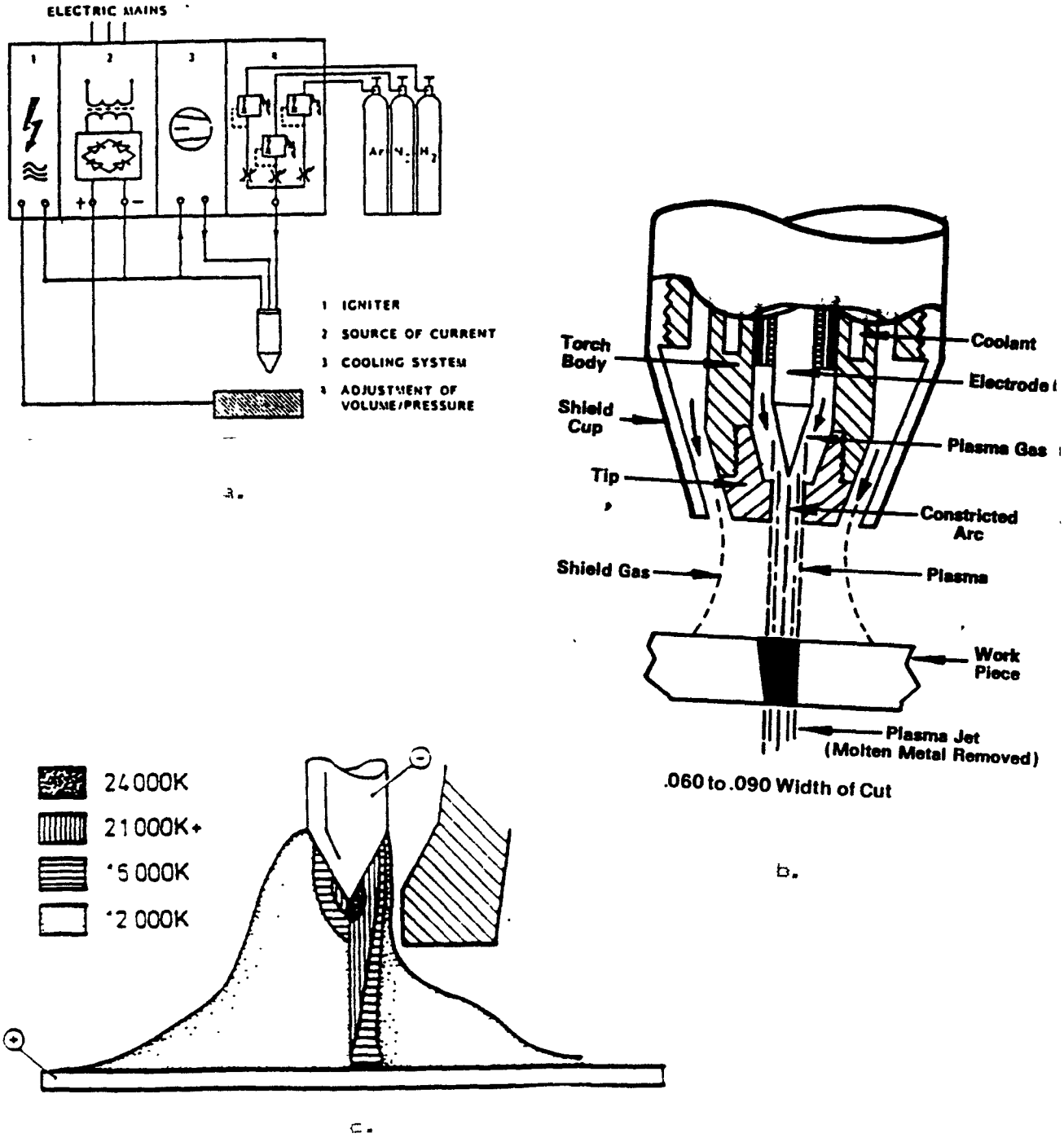

Fig 10. a. Plasma Arc cutting Schematic

b. Schematic for the torch Operation

c.Temperature zones for the plasma beam

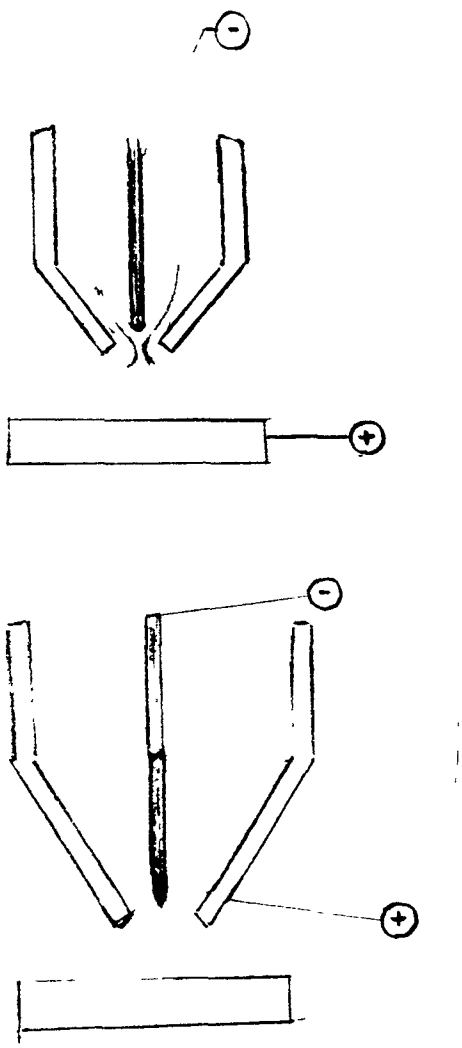

Fig 11. Different modes of Plasma Arc cutting process

a. Transferred arc mode

b. Non-transferred arc mode.

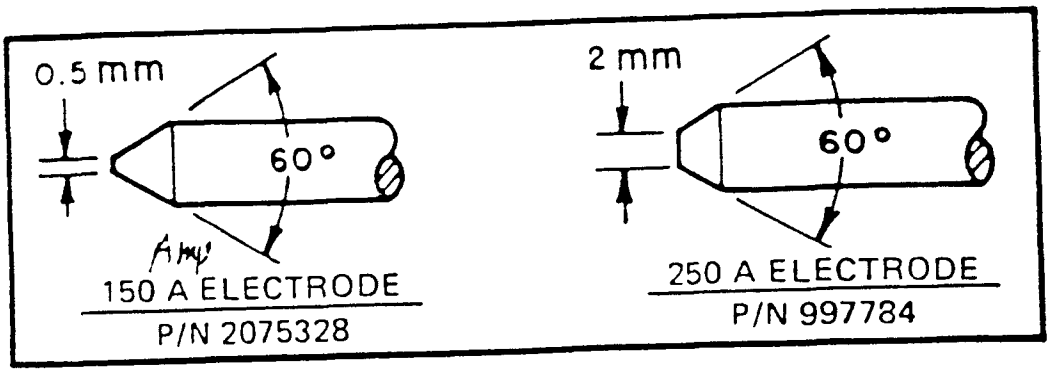

a.

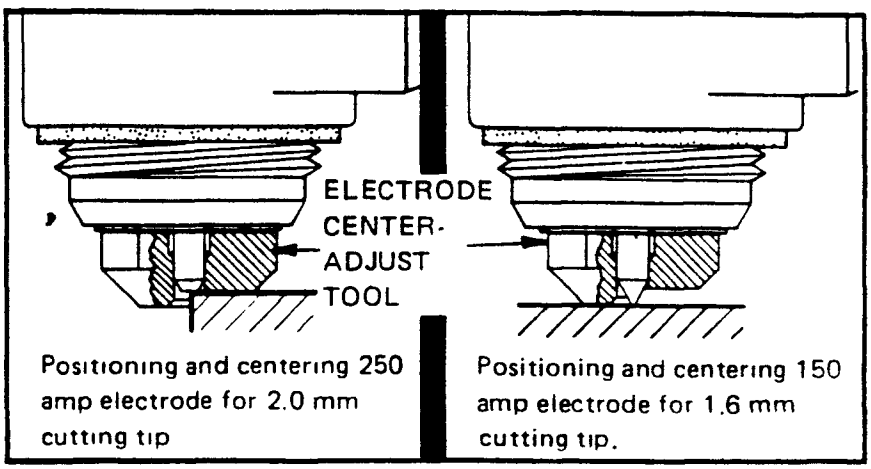

b.

Fig 12. a. Types of Electrodes in Plasma arc cutting

b. Procedure for electrode adjustment.

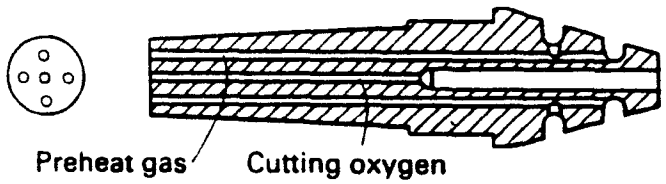

Fig 13. The cutting nozzle for Oxy-acetylene torch.

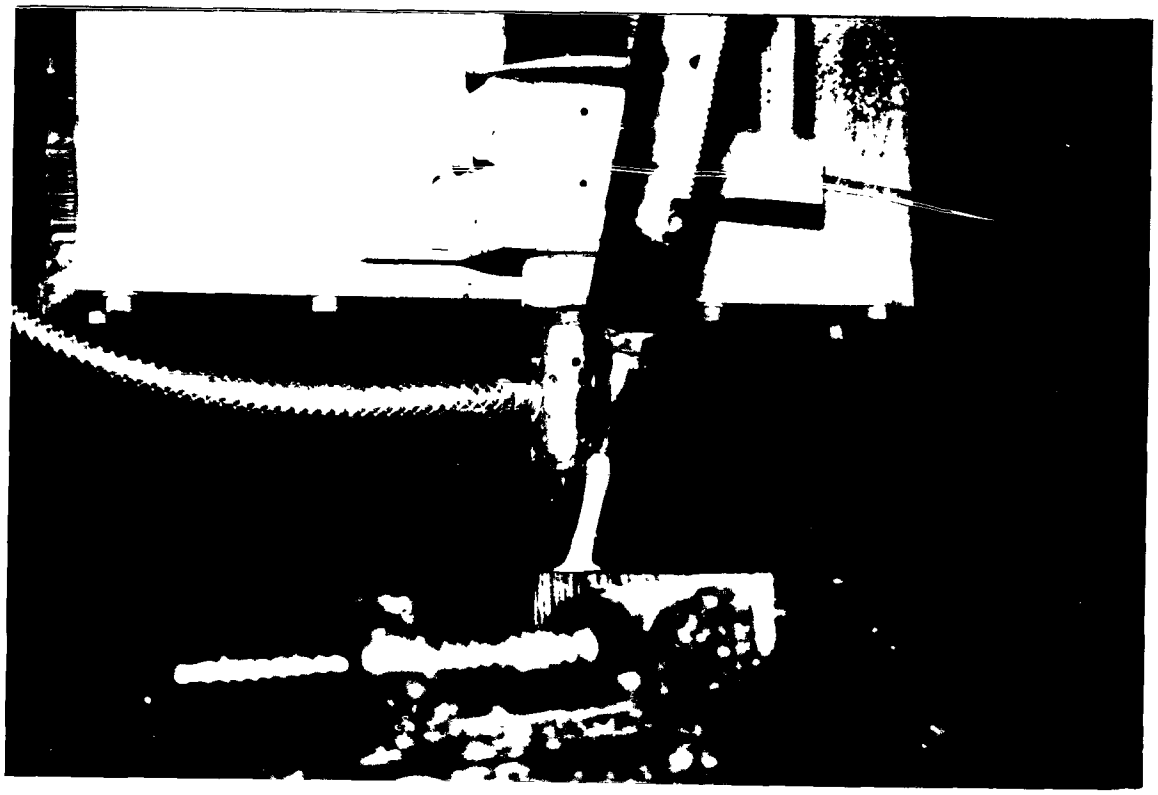

Fig 14. Experimental Setup for Integrated Cutting.

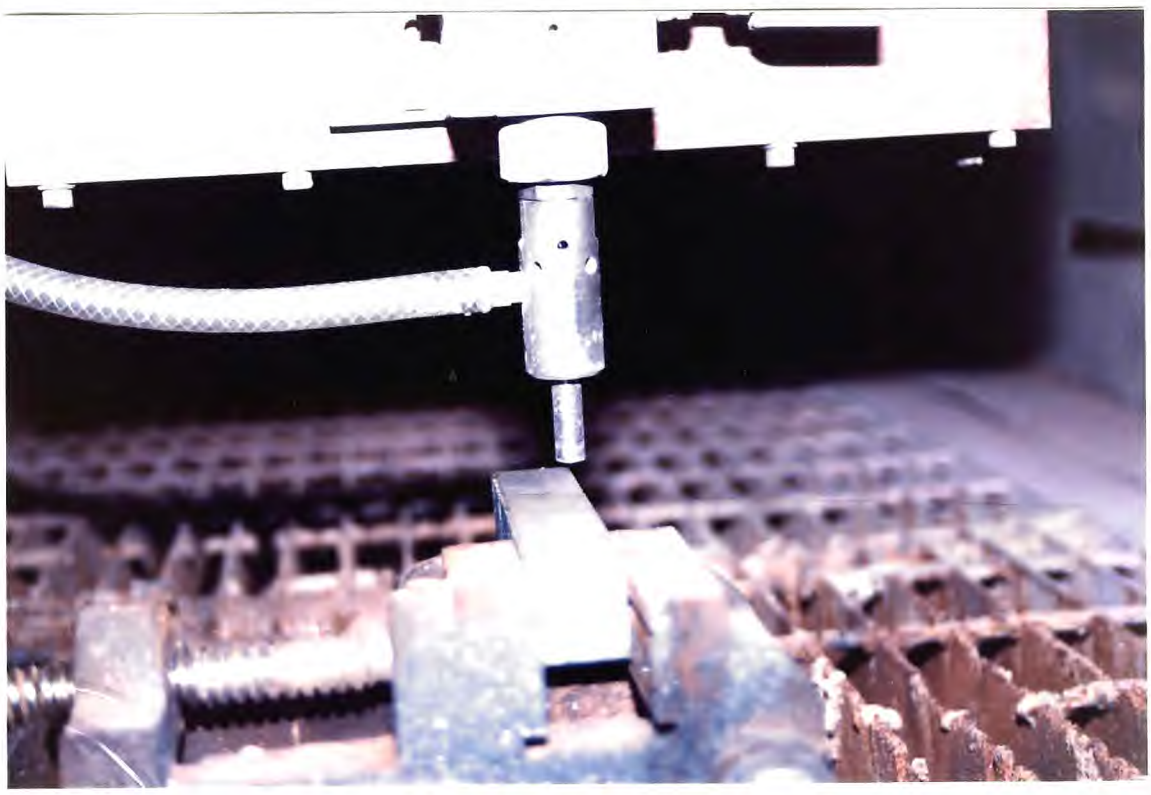

Fig. 15. Experimental Setup for Surface finishing Operation

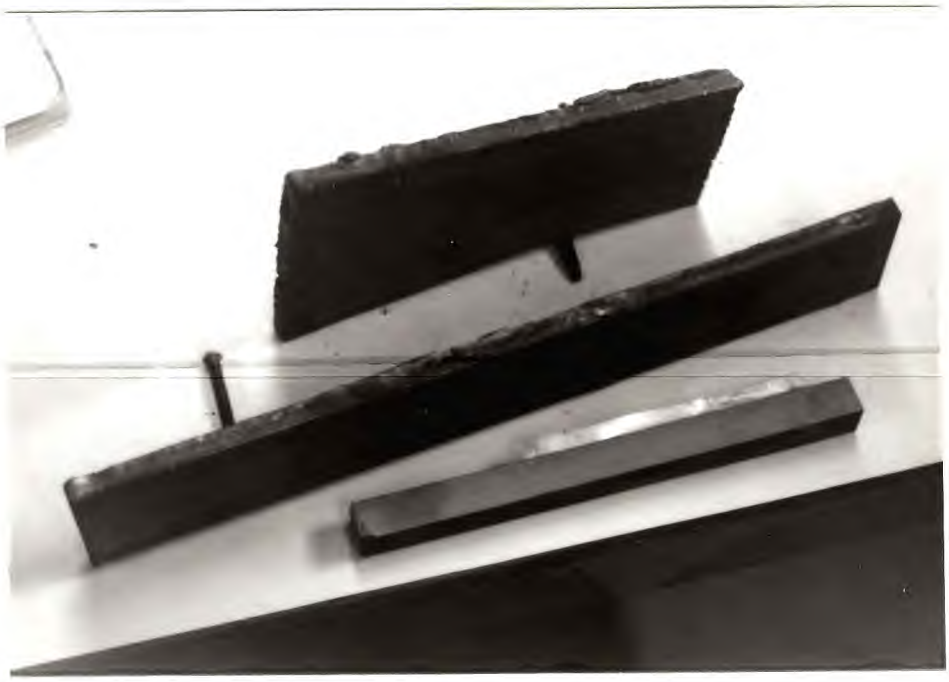

Fig 16 Samples of Individual cutting processes

Top - Plasma Cutting (carbon steel 0.25" thickness)

middle - Oxyfuel cutting (carbon steel 0.25" thickness)

bottom - Waterjet (0.5" thickness)

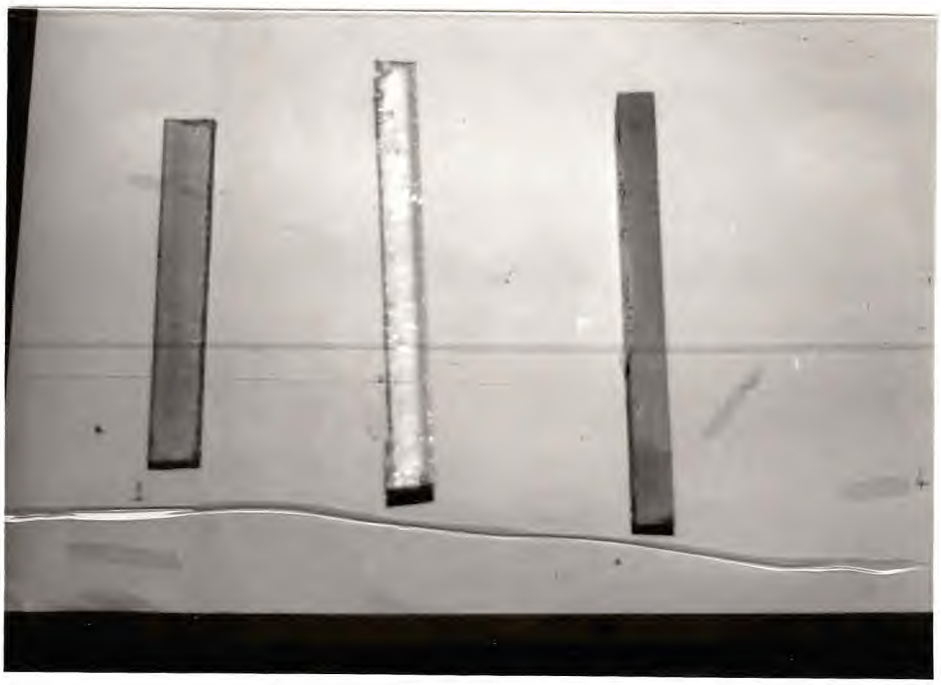

Fig 17. Figure showing Plasma cutting 0f different Samples

a. left - Titanium (0.5" thick)

b. middle - Aluminium (0.5" thick)

c. right - stainless steel (0.5" thick)

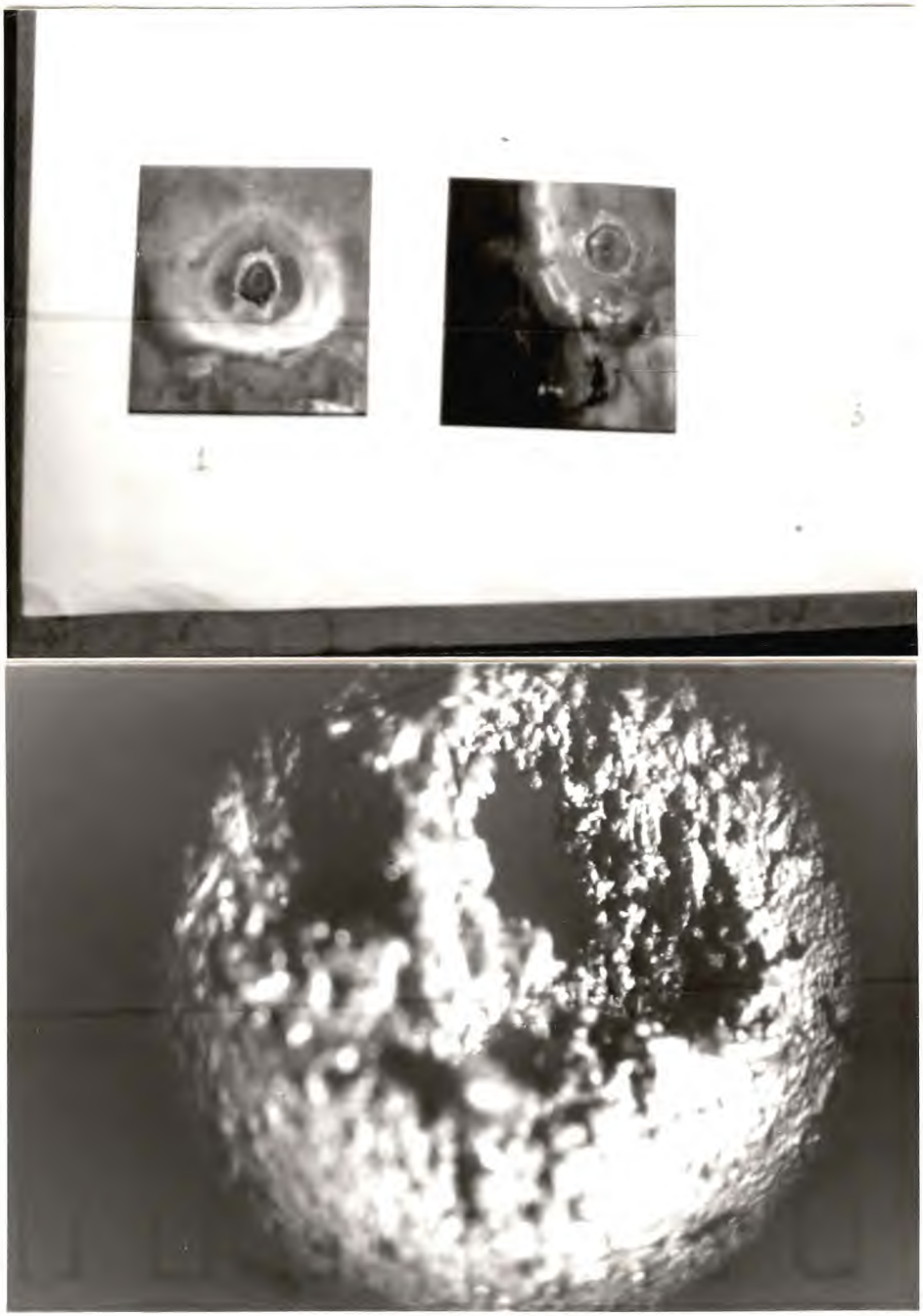

Fig 18. a. Piercing Samples with Integrated Cutting.

b. Enlarged view of a piercing sample.

Parameters: heat beam - Oxyfuel beam.
thickness 3.125 mm.
material - carbon steel.
sapphire - 0.254mm.
jet pierce time - 0.5 sec.

Fig 19 a. Effect of Oxyfuel beam heating time on the material.

left - 10 sec. right - 30 sec
material - plain carbon steel.
thickness - 3.125 mm.

Fig 19b. Effect of Oxyfuel beam heating with time.

from left: 1. 7 secs. 2. 15 secs
3. 20 secs. 4. 28 secs.

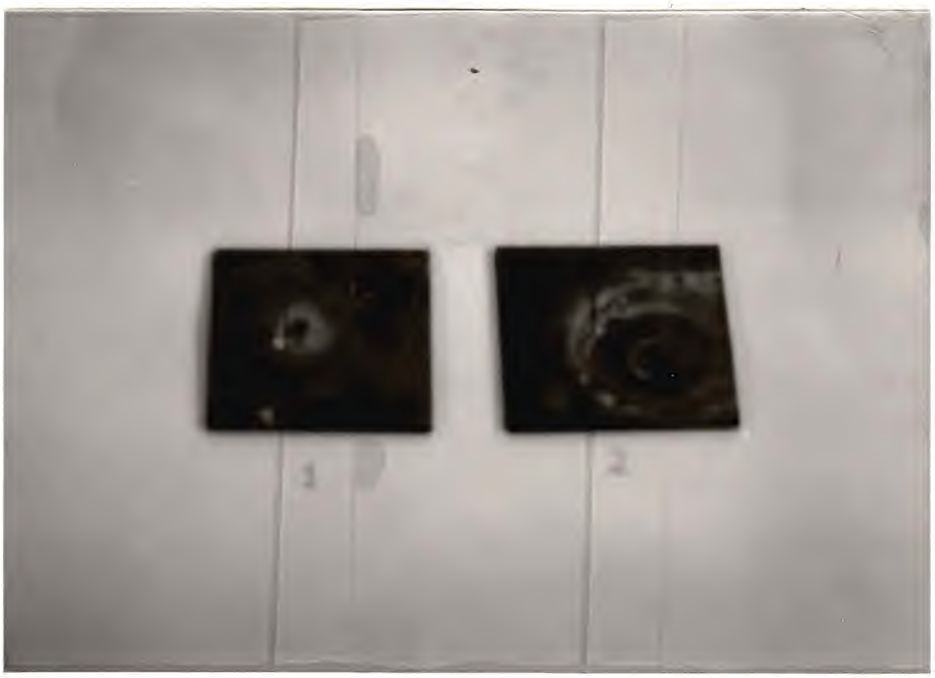

Fig 20 Effect of heating time on Waterjet piercing.

a. left - 10 secs. right - 22 secs.

b. left - 10 secs. right - 22 secs.

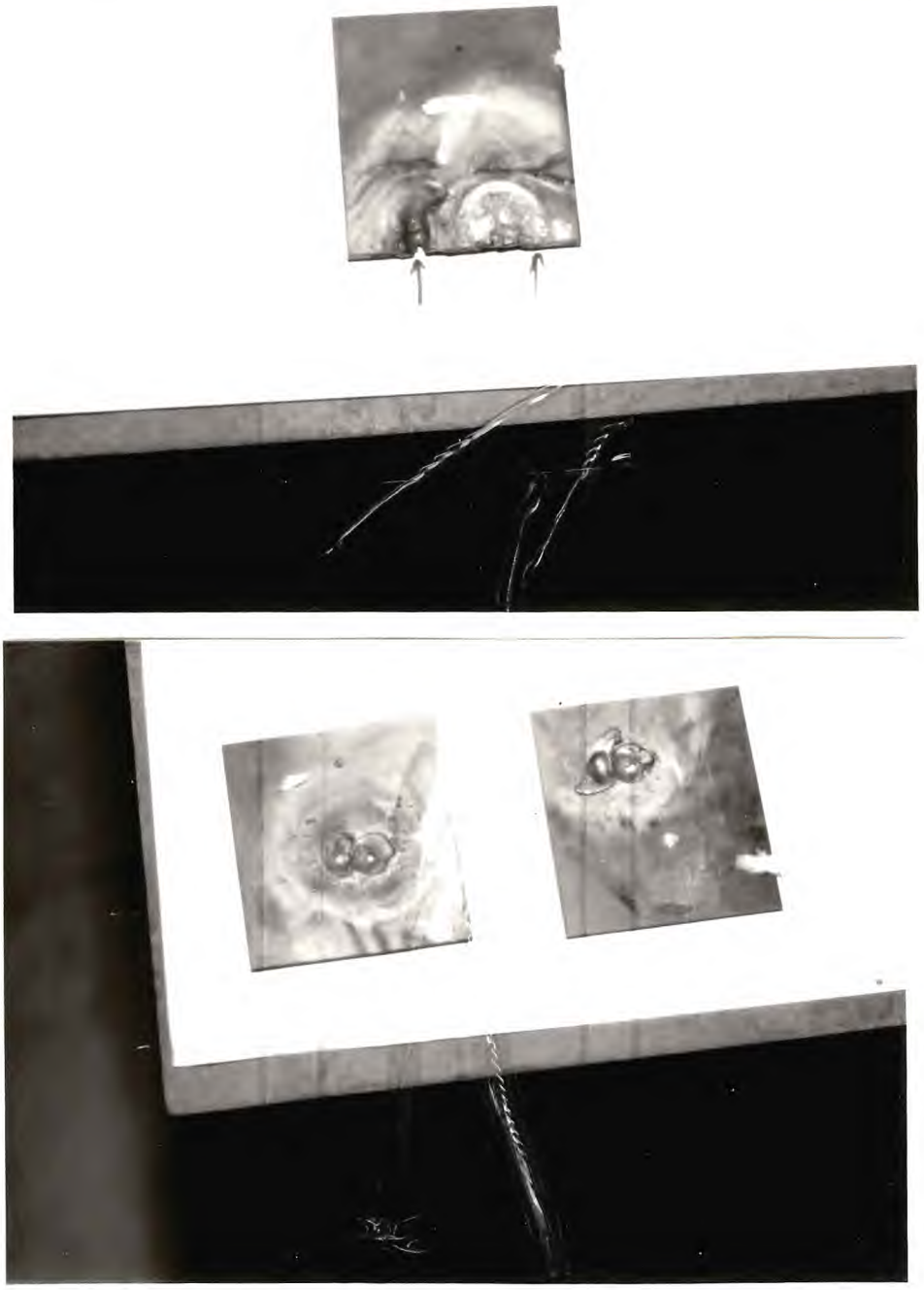

Fig 21. Samples of linear cutting using Integrated beam.

a. Cutting started at the edge.

b. Cutting started at the center.

material - 3.125mm thickness, plain carbon steel

Fig 22. Sample workpiece used for surface finishing operation.

material - stainless steel.

thickness - 25.4 mm.

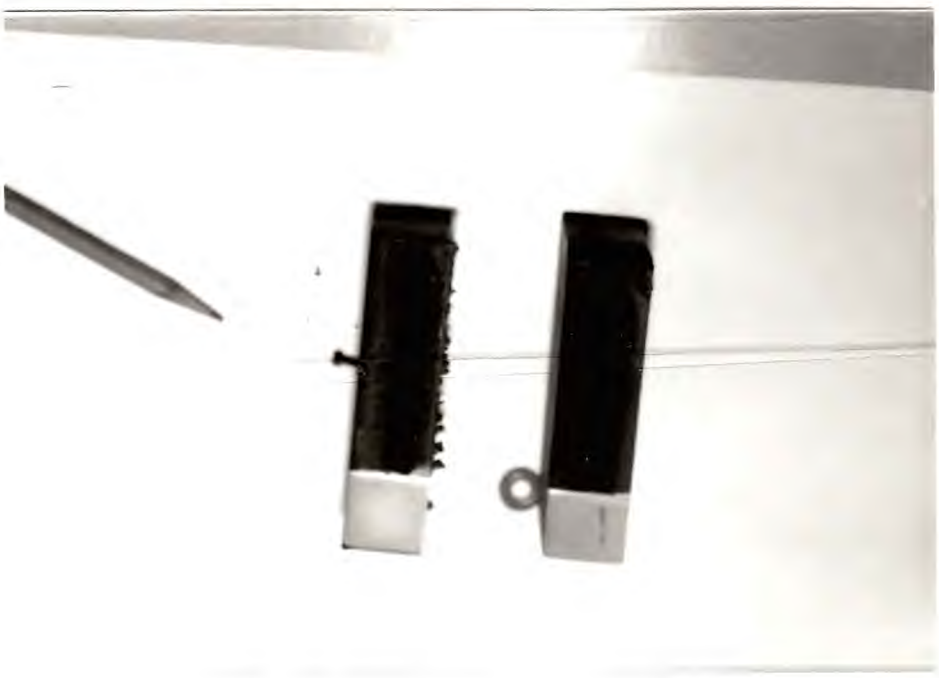

Fig 23. Samples of surface finishing operation by AWJ

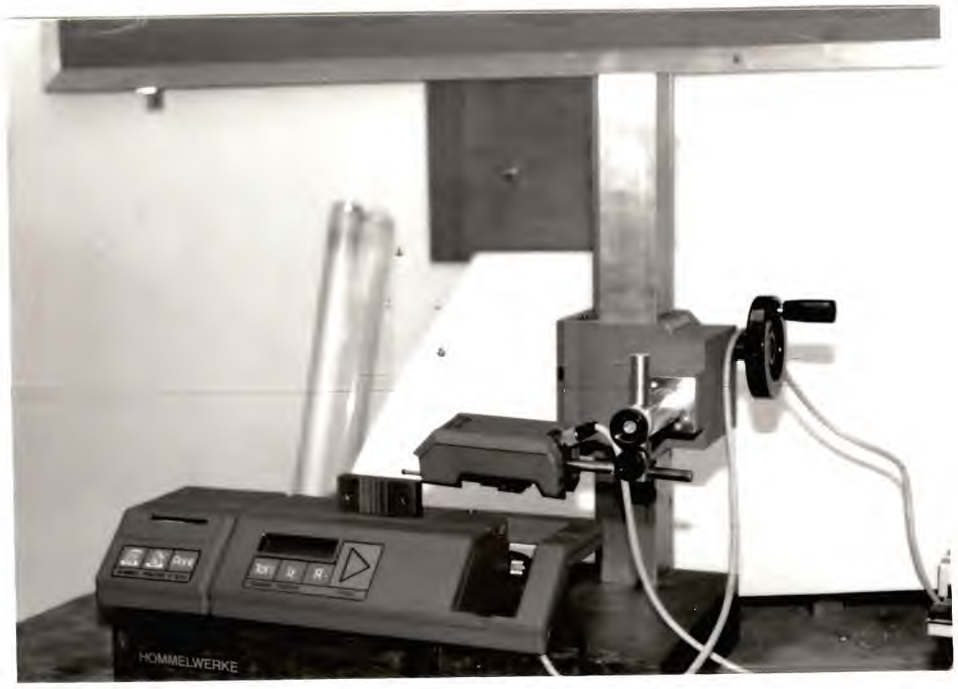

Fig 24. Experimental setup for the measurement of surface roughness

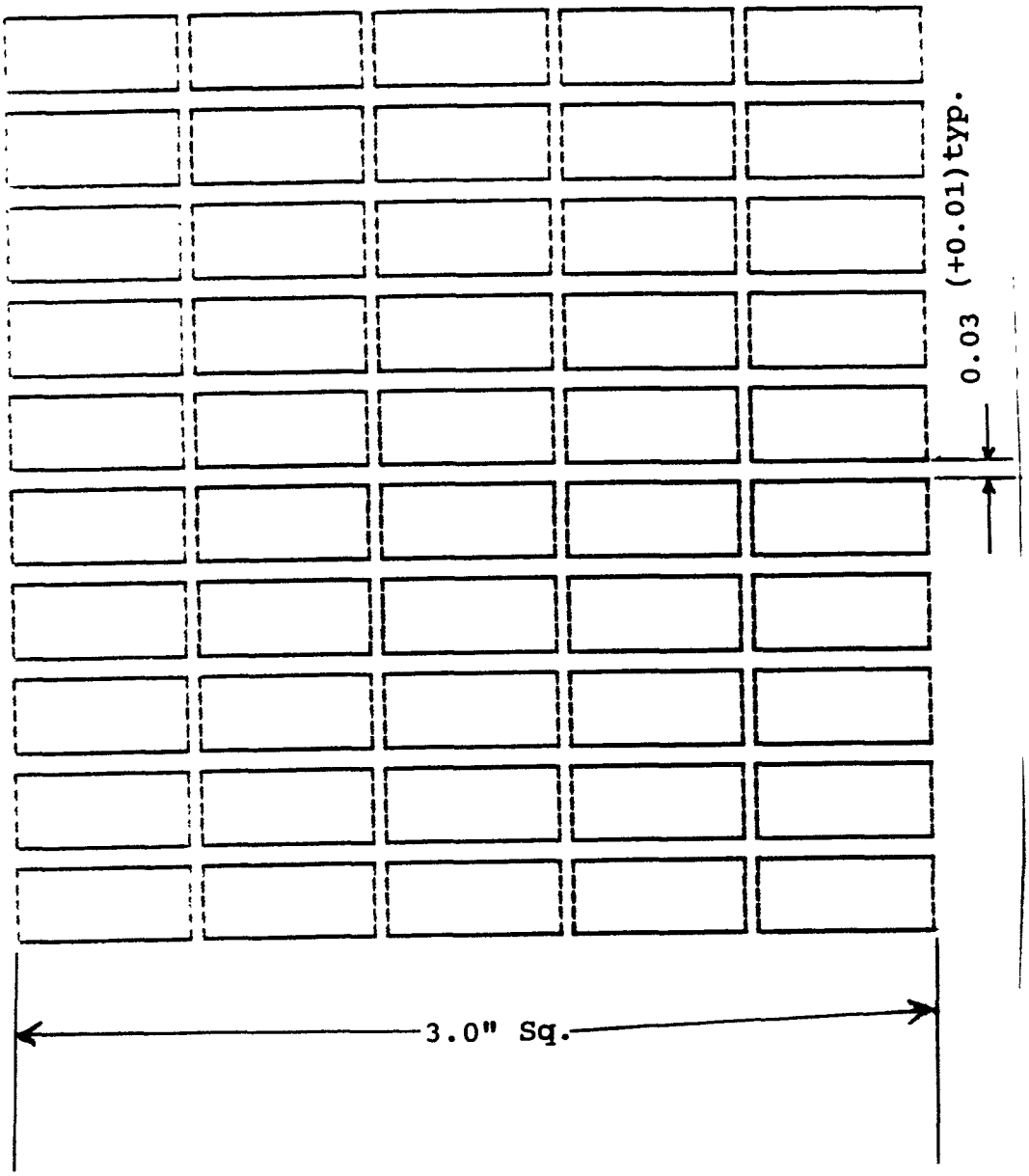

Fig 25. Sketch showing the details of dimensions for cutting of grid pattern on composite sheet described in Appendix-B. Each sheet contains 10 such grids located at specific co-ordinates.

TABLE I

Parameters affecting the AWJ performance [1]:

1. Hydraulic Parameters:-

   * Waterjet pressure
   * Waterjet orifice diameter

2. Abrasive parameters :-

   * Abrasive flow rate
   * Abrasive particle size
   * Abrasive material

3. Mixing parameters :-

   * Mixing tube length
   * Mixing tube Diameter

4. Cutting Parameters :-

   * Traverse speed
   * Number of passes
   * Stand-off distance
   * Jet angle
   * Material properties

TABLE II

Parameters Affecting Plasma Arc Cutting Performance :

* Output Current, Amps.
* Type of Cutting process, Transferred Arc or Non Transferred Arc
* Type of gas, Argon, air, etc.
* Gas Pressure, psig.
* Gas Flow Rates
* Nozzle Diameter, mm or In.
* Nozzle stand-off
* Electrode Tip Geometry, flat or pointed.
* Material properties
* Cutting speed ipm
* Material thickness
* Type of torch design, Water-injection, Dual gas flow, water -cooled, etc.

TABLE III

Parameters affecting performance of Oxyfuel Cutting:

* Fuel gas type
* Gas pressures
* Nozzle Diameter
* Cutting Speed
* Nozzle Stand-off
* Material properties
* Material Thickness

Table IV [35]

RECOMMENDED CUTTING SPEED FOR PCM-250

Plate Thickness in. (mm)	Cutting Tip (orifice Dia)	Current Amps.	Gas Flow @ 90psig Using Argon-H_2 cfh.	Using Argon-N_2 cfh	Cutting Speeed in/min. Ar-H_2	Ar-N_2	stand-off (Tip-to-work) in.
Stainless Steel							
1/16 (2)	1.4mm	80	---	Ar:15 H_2:25	-	180	1/4
1/8 (3)						90	
3/16 (5)						56	
1/4 (6)						38	
1/8 (3)	1.6mm	100	---	Ar:15 N_2:30	-	105	1/4
3/16 (5)						75	
1/4 (6)						60	
1/2 (13)	2.8mm	250	Ar:62 H_2:32	Ar:62 N_2:15	40	35	3/8
3/4 (19)					35	31	
1 (25)					31	27	
1.5 (38)					16	14	
2 (51)					9	8	
2.5 (64)					8	5	
Steel							
1/16 (2)	1.4mm	80	—	Ar:15 H_2:25	-	170	1/4
1/8 (3)						85	
3/16 (5)						52	
1/4 (6)						34	
1/8 (3)	1.6 mm	100	—	Ar:15 N_2:30	—	100	1/4
3/16 (5)					—	75	
1/4 (6)					—	60	
1/2 (13)	2.8 mm	250	Ar:75 H_2:32	Ar:62 cfh N_2:15 cfh		35	3/8
3/4 (19)						32	
1 (25)						25	
1.5 (38)						12	
2 (51)						8	
2.5 (64)						4	
3.8 (76)						3.5	
Aluminium							
3/16 (5)	1.4mm	80	—	Ar:62 cfh N_2:15 cfh	—	120	1/4
1/4 (6)						75	
3/8 (10)						45	
3/16 (5)	1.6mm	100	Ar:52 H_2:21	Ar:62 N_2:31	100	88	1/4
3/8 (10)		150			85	75	
3/8 (10)	2.8	250	Ar:62 H_2:21	Ar:62 N_2:15	150	92	3/8
1/2 (13)					95	84	
3/4 (19)					80	78	
1 (25)					53	47	
1.5 (36)					40	35	
2 (51)					30	26	
2.5 (64)					14	12	

TABLE V [36]

Cutting Speeds for Oxy-Acetylene Cutting:

Nozzle Size in.	Steel Thickness in.	Gas Pressure, psig Cutting oxygen	Preheat oxygen	Acetylene	Cutting Speed ipm
1/2	1/2	90	20-25	5-7	21-30
3/4	3/4	↓	↓	↓	20-28
1	1				19-25
1.5	1.5				14-23
2.0	2.0				13-20
2.5	2.5				12-19
4.0	3-4				8-17
6.0	6				7-10

TABLE VI [1]

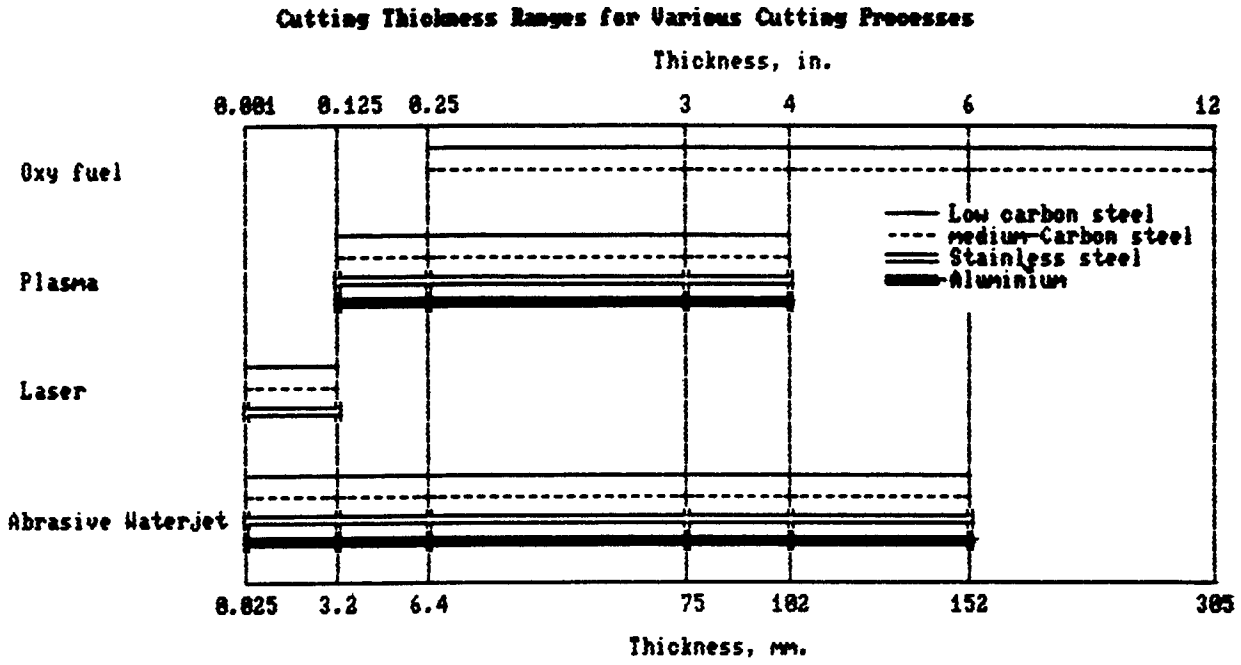
Cutting Thickness Ranges for Various Cutting Processes
Thickness, in.
0.001
0.125
0.25
3
4
6
12
Oxy fuel
Plasma
Laser
Abrasive Waterjet
Low carbon steel
medium-Carbon steel
Stainless steel
Aluminium
0.025
3.2
6.4
75
102
152
305
Thickness, mm.

TABLE VII

Comparison of OFC and PAC processes [1]:

	Oxyfuel	Plasma
Flame Temp.	3040°C	28,000°C
Action	Oxidation, melting expulsion	Melting, expulsion
Preheat	Yes	No
Kerf	Narrow	Wide
Cut	Both sides square	One side Square
Speed	Moderate	High
Heat-Affected zone	Moderate	Narrow
Cutting ability :		
Carbon steel	Yes	Yes
Stainless steel ..	No	Yes
Aluminium	No	Yes
Copper	No	Yes
Special alloys ...	Some	Yes
Non-metallics	No	Yes

TABLE VIII - A

Experiment Matrix for study of improvement of the surface finish

Batch I

De = 0.228 mm (0.009 in.)
Dt = 0.762 mm (0.03 in.)

mesh # → / Traverse speed ↓	Coarse 80 mesh	Fine 220 mesh
	Thickness	
12.7) (0.5)	12.7 (0.5) 25.4 (1.0)	12.7 (0.5) 25.4 (1.0)
63.5 (2.5)	12.7 (0.5) 25.4 (1.0)	12.7 (0.5) 25.4 (1.0)
127.0 (5.0)	12.7 (0.5) 25.4 (1.0)	12.7 (0.5) 25.4 (1.0)
177.8 (7.5)	12.7 (0.5) 25.4 (1.0)	12.7 (0.5) 25.4 (1.0)
254.0 (10.0)	12.7 (0.5) 25.4 (1.0)	12.7 (0.5) 25.4 (1.0)

Initial pressure = 345 Mpa (50 ksi);

Operating pressure = 331.2 Mpa (48 ksi)

Abrasive flow rate = 225 gm/min (.5 lb/min)

Material : SS 403

TABLE VIII - B

Experimental matrix to determine the surface finish by AWJ

Batch II

Do = 0.228 mm (0.009 in.)
Dt = 1.092 mm (0.043 in)

mesh # → / Traverse speed ↓ mm. (ipm)	Coarse 80 mesh	Fine 220 mesh
	Thickness	
63.5 (2.5)	12.7 (0.5) 25.4 (1.0)	12.7 (0.5) 25.4 (1.0)
127.0 (5.0)	12.7 (0.5) 25.4 (1.0)	12.7 (0.5) 25.4 (1.0)
177.8 (7.5)	12.7 (0.5) 25.4 (1.0)	12.7 (0.5) 25.4 (1.0)
254.0 (10.0)	12.7 (0.5) 25.4 (1.0)	12.7 (0.5) 25.4 (1.0)

Initial Pressure - 345 Mpa (50 ksi)

Operating pressure - 331.2 Mpa (48 ksi)

Abrasive Flow Rate - 225 g/min. (0.5 lb/min)

Material : SS 304

TABLE VIII - C

Experimental Matrix to determine Surface Finish by AWJ

Batch III

Do = 0.305 mm (0.012 in)
Dt = 1.092 mm (0.043 in)

mesh # → / Traverse speed ↓	Coarse 80 mesh	Fine 220 mesh
	Thickness	
63.5 (2.5)	12.7 (0.5) 25.4 (1.0)	12.7 (0.5) 25.4 (1.0)
127.0 (5.0)	12.7 (0.5) 25.4 (1.0)	12.7 (0.5) 25.4 (1.0)
177.8 (7.5)	12.7 (0.5) 25.4 (1.0)	12.7 (0.5) 25.4 (1.0)
254.0 (10.0)	12.7 (0.5) 25.4 (1.0)	12.7 (0.5) 25.4 (1.0)

Initial pressure - 345 Mpa (50 ksi)

Operating pressure - 331.2 Mpa (48 ksi)

Abrasive flow rate - 225 g/min. (0.5 lb/min)

Material : SS 304

Table IX

Approximate depth of HAZ in gas cut Carbon steels:
[source: Ref(1)]

Plate thickness mm.	Plate thickness in.	HAZ Depth mm	HAZ Depth in.
Low carbon steels			
<13	<1/2	<0.8	<1/32
13	1/2	0.8	1/32
150	6	1.4	1/18
High Carbon steels			
<13	<1/2	<0.8	<1/32
13	1/2	0.8-1.6	1/32-1/16
150	6	1.4-6.0	1/18-1/4

Table X

Piercing Experiments with pure waterjet :

Material : Aluminium

No.	Sapphire Dia. (mm)	Intensifier Pressure ksi.	Material Thickness (mm)	Pierce Time sec.
1.	0.0106	48.0	2.28	92
2.	0.1778	48.0	2.28	14.0
3.	0.254	47.0	2.28	10.0
4.	0.3048	46.0	2.28	6.0
5.	.3556	45.0	2.28	3.0

Note.

1. Drop in intensifier pressure is due to increased sapphire diameter.

Table XI

Abrasive Particle properties
(ref: source [36])

	Material	Mesh	Roundness*	Sphericity*	Specific Gravity
1.	Garnet	50 80 150	0.42	0.78	3.4 to 4.3
2.	Aluminium oxide	40 - 100	0.35	0.78	3.95 to 4.0
3.	Silicon carbide	40 - 100	0.31	0.75	3.2
4.	Silica Sand	40 - 100	0.57	0.78	2.2 to 2.6
5.	Steel grit	40 -100	0.55	0.82	8.7
6.	Glass	40 - 100	0.50	0.78	2.0

*Roundness and sphericity based on comparison with magnified particle pictures to the chart below [36].

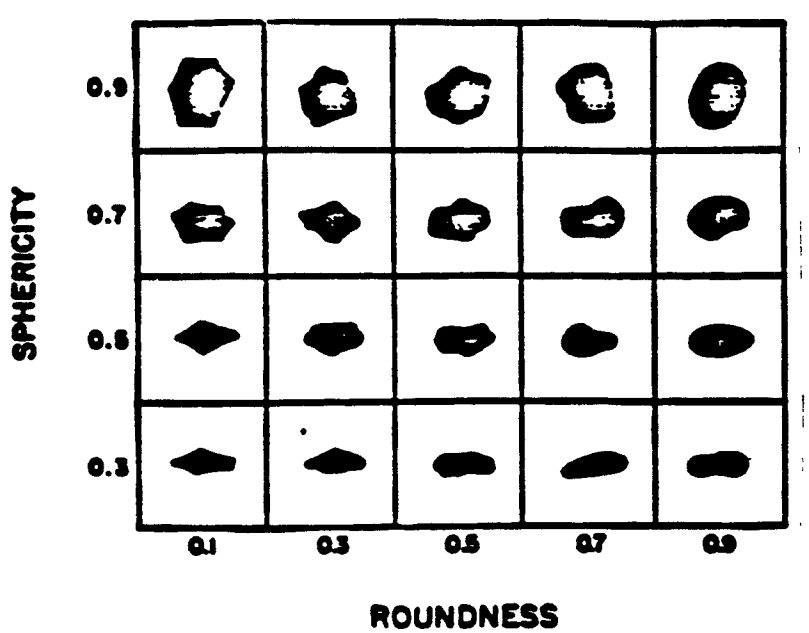

Table XII

USA Sieve series and Tyler Equivalents

A.S.T.M.—E-11-70

Sieve Designation		Sieve Opening		Nominal Wire Diameter		Tyler Screen
Standard (a)	Alternate	mm	in (approx equivalents)	mm	in (approx equivalents)	Scale Equivalent Designation
125 mm	5 in.	125	5	8	.3150	
106 mm	4.24 in	106	4.24	6.40	.2520	
100 mm	4 in. (b)	100	4.00	6.30	.2480	
90 mm	3½ in.	90	3.50	6.08	.2394	
75 mm	3 in.	75	3.00	5.80	.2283	
63 mm	2½ in	63	2.50	5.50	.2165	
53 mm	2.12 in	53	2.12	5.15	.2028	
50 mm	2 in. (b)	50	2.00	5.05	.1988	
45 mm	1¾ in	45	1.75	4.85	.1909	
37.5 mm	1½ in	37.5	1.50	4.59	.1807	
31.5 mm	1¼ in	31.5	1.25	4.23	.1665	
26.5 mm	1.06 in	26.5	1.06	3.90	.1535	1.050 in
25.0 mm	1 in (b)	25.0	1.00	3.80	.1496	
22.4 mm	⅞ in	22.4	0.875	3.50	.1378	.883 in
19.0 mm	¾ in.	19.0	0.750	3.30	.1299	.742 in
16.0 mm	⅝ in	16.0	0.625	3.00	.1181	.624 in
13.2 mm	.530 in	13.2	0.530	2.75	.1083	.525 in
12.5 mm	½ in (b)	12.5	0.500	2.67	.1051	
11.2 mm	7/16 in	11.2	0.438	2.45	.0965	.441 in
9.5 mm	⅜ in	9.5	0.375	2.27	.0894	.371 in
8.0 mm	5/16 in	8.0	0.312	2.07	.0815	2½ mesh
6.7 mm	.265 in	6.7	0.265	1.87	.0736	3 mesh
6.3 mm	¼ in (b)	6.3	0.250	1.82	.0717	
5.6 mm	No 3½ (c)	5.6	0.223	1.68	.0661	3½ mesh
4.75 mm	No 4	4.75	0.187	1.54	.0606	4 mesh
4.00 mm	No. 5	4.00	0.157	1.37	.0539	5 mesh
3.35 mm	No 6	3.35	0.132	1.23	.0484	6 mesh
2.80 mm	No. 7	2.80	0.11	1.10	.0430	7 mesh
2.36 mm	No. 8	2.36	0.0937	1.00	.0394	8 mesh
2.00 mm	No. 10	2.00	0.0787	.900	.0345	9 mesh
1.70 mm	No 12	1.70	0.0661	.810	.0319	10 mesh
1.40 mm	No. 14	1.40	0.0555	.725	.0285	12 mesh
1.18 mm	No 16	1.18	0.0469	.650	.0256	14 mesh
1.00 mm	No 18	1.00	0.0394	.580	.0228	16 mesh
850 µm	No. 20	0.850	0.0331	.510	.0201	20 mesh
710 µm	No. 25	0.710	0.0278	.450	.0177	24 mesh
600 µm	No. 30	0.600	0.0234	.390	.0154	28 mesh
500 µm	No. 35	0.500	0.0197	.340	.0134	32 mesh
425 µm	No. 40	0.425	0.0165	.290	.0114	35 mesh
355 µm	No. 45	0.355	0.0139	.247	.0097	42 mesh
300 µm	No. 50	0.300	0.0117	.215	.0085	48 mesh
250 µm	No. 60	0.250	0.0098	.180	.0071	60 mesh
212 µm	No. 70	0.212	0.0083	.152	.0060	65 mesh
180 µm	No. 80	0.180	0.0070	.131	.0052	80 mesh
150 µm	No. 100	0.150	0.0059	.110	.0043	100 mesh
125 µm	No. 120	0.125	0.0049	.091	.0036	115 mesh
106 µm	No. 140	0.106	0.0041	.076	.0030	150 mesh
90 µm	No. 170	0.090	0.0035	.064	.0025	170 mesh
75 µm	No 200	0.075	0.0029	.053	.0021	200 mesh
63 µm	No. 230	0.063	0.0025	.044	.0017	250 mesh
53 µm	No. 270	0.053	0.0021	.037	.0015	270 mesh
45 µm	No. 325	0.045	0.0017	.030	.0012	325 mesh
38 µm	No. 400	0.038	0.0015	.025	.0010	400 mesh

most commonly used range in abrasive-waterjet cutting

(a) These standard designations correspond to the values for test sieves apertures recommended by the International Standards Organization Geneva, Switzerland

(b) These sieves are not in the fourth root of 2 Series, but they have been included because they are in common usage

(c) These numbers (3½ to 400) are the approximate number of openings per linear inch but it is preferred that the sieve be identified by the standard designation in millimeters or µm

1000 µm = 1 mm

Table XIII

Piercing Experiments with Integrated beam:

Variation of Piercing depth with heating time:

Time of Heating	Sapphire Dia. (in) 0.01	0.007	0.004
	Depth (mm)		
5	0.1	0.1	0.005
10	0.15	0.12	0.03
15	0.25	0.2	0.1
20	1.1	1.0	0.4
22	3.2	3.2	1.2

Pressure - 48 ksi.
Material: Plain carbon steel
Thickness - 3.2mm.
Waterjet Pierce time - 0.5sec.

Table XIV

Piercing Experiments with Integrated beam:

Variation of Piercing depth with heating time:

Time of Heating	Sapphire Dia. (in)		
	0.01	0.007	0.004
	Depth (mm)		
5	0.12	0.1	0.005
10	0.25	0.22	0.03
15	0.25	0.24	0.1
20	1.3	1.0	0.4
22	3.2	3.2	1.2

Pressure - 48 ksi.
Material: Plain carbon steel
Thickness - 3.2mm.
Waterjet Pierce time - 1.0sec.

Table XV

Piercing Experiments with Integrated beam:

Variation of Piercing depth with heating time:

Time of Heating	Depth (mm)
5	0.1
10	0.17
15	0.75
20	1.4
25	2.6

Pressure - 48 ksi.
Material: Plain carbon steel
Thickness - 6.35mm
Waterjet Pierce time - 0.5sec.

Table XVI

Piercing Experiments with Integrated beam:

Variation of Piercing depth with heating time:

Time of Heating	Depth (mm)
5	0.1
10	0.17
15	1.15
20	1.3
25	2.75

Pressure - 48 ksi.
Material: Plain carbon steel
Thickness - 6.35mm
Waterjet Pierce time - 1.0sec.

Table XVII

Piercing Expt with Integrated Beam:

Variation of beam penetration depth with Distance from Beam Focus:

Distance from Beam focus X mm	Beam Penetration d mm.
-4.5	0.0
-3.5	1.03
-2.5	1.75
-1.5	2.5
-0.5	2.9
0.0	3.2
0.5	2.86
1.5	2.3
2.5	1.67
3.5	1.04
4.5	0.0

Sapphire Dia - 0.254mm.
Intensifier Pressure - 345 MPa (50ksi.)
material - carbonsteel
thickness - 3.2 mm.
Waterjet pierce time - 1.0sec.
Material Heating time - 22 secs.

Table XVIII

Piercing Expt with Integrated Beam:

Variation of beam penetration depth with Distance from Beam Focus:

Distance from Beam focus X mm	Beam Penetration d mm.
-2.6	0.0
-1.5	1.3
-0.5	2.1
0.0	2.76
0.5	1.86
1.5	1.42
2.5	0.4
2.6	0.1

Sapphire Dia - 0.254mm.
Intensifier Pressure - 345 MPa (50ksi.)
material - carbonsteel
thickness - 6.3mm.
Waterjet pierce time - 1.0sec.
Material Heating time - 22 secs.

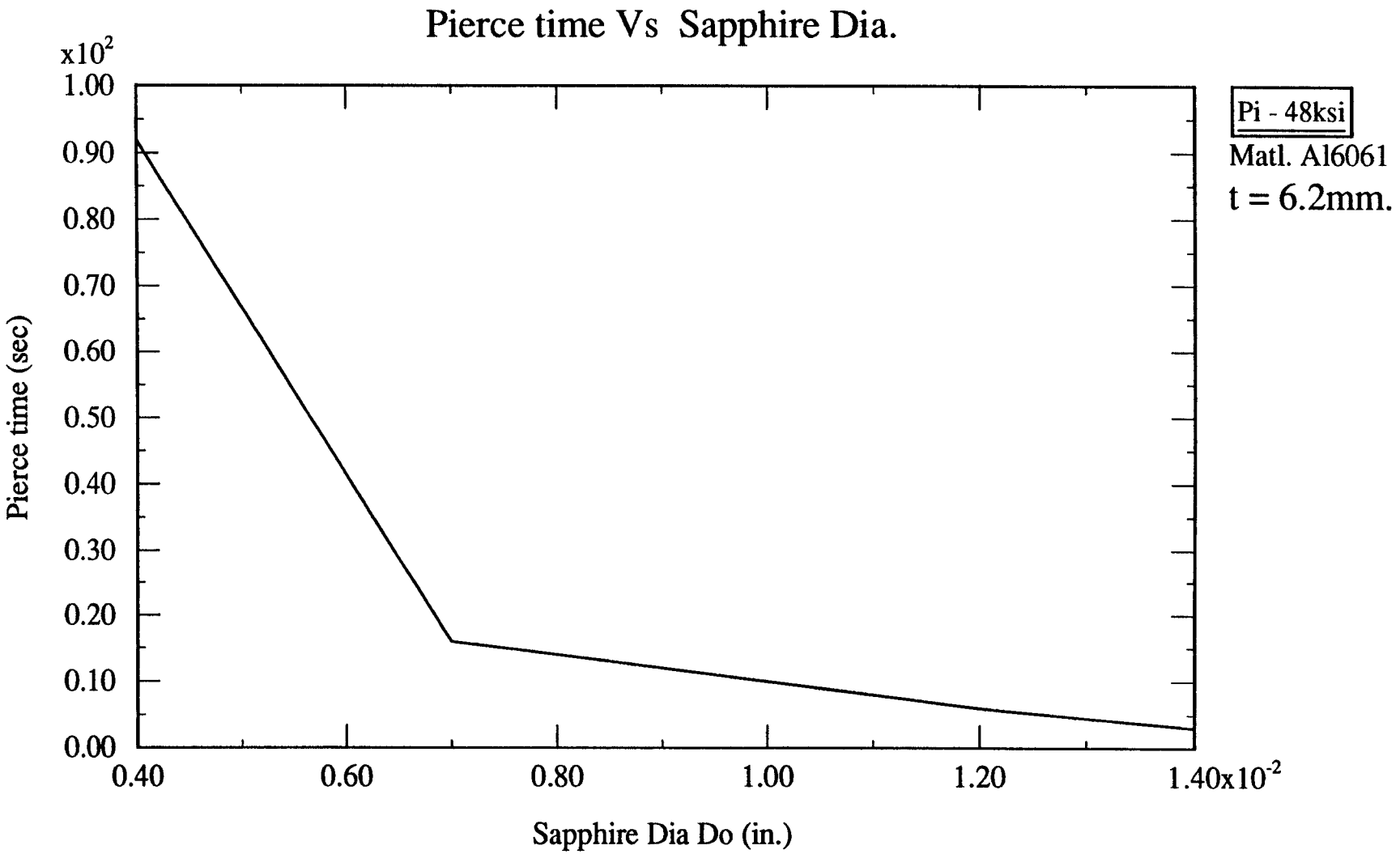

Fig. 26 Variation of pierce time with Sapphire diameter for a pure waterjet. Operation performed is through piercing of Aluminium of 6.2mm thickness.

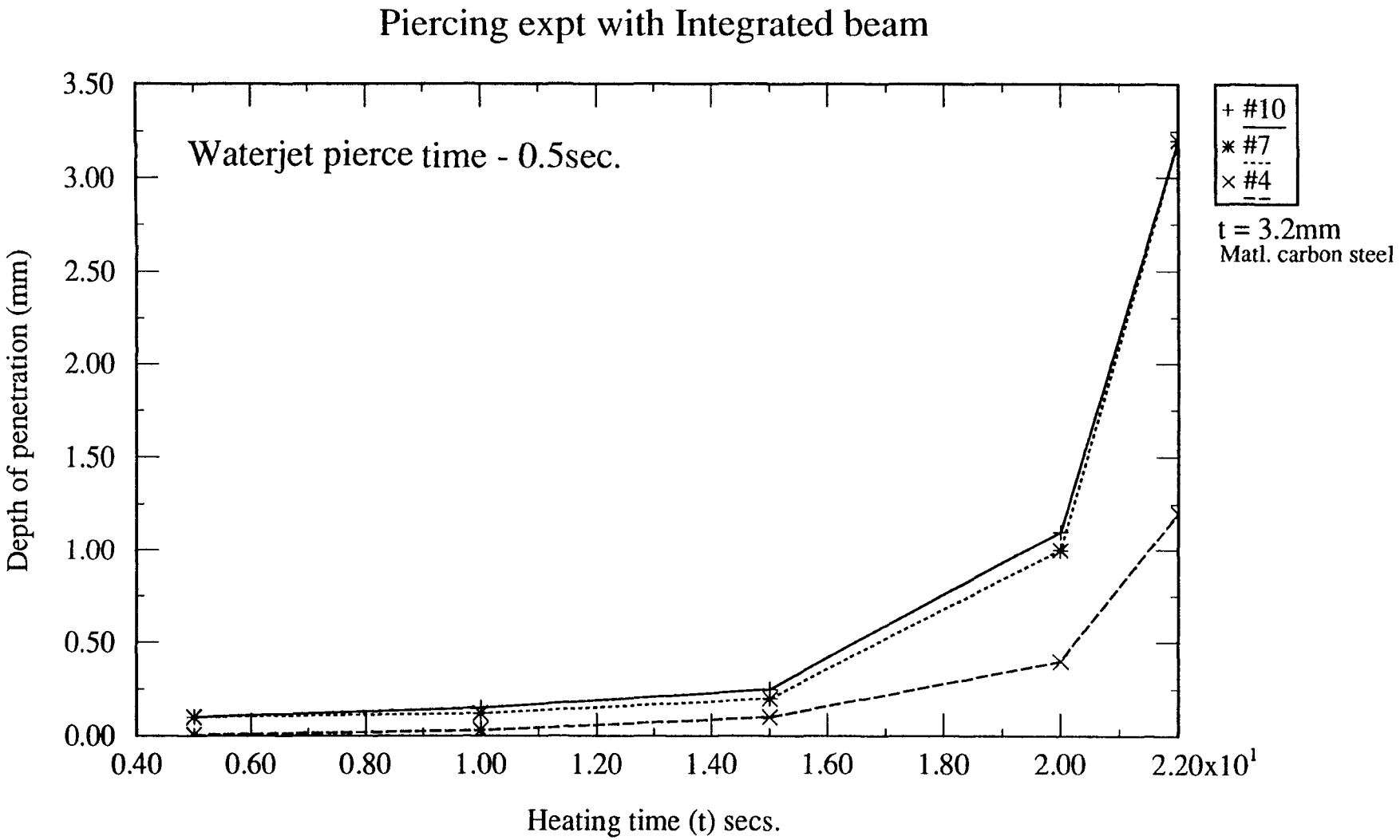

Fig 27. Variation of piercing depth with heating time using an integrated beam. Pressure Pi - 50 ksi.

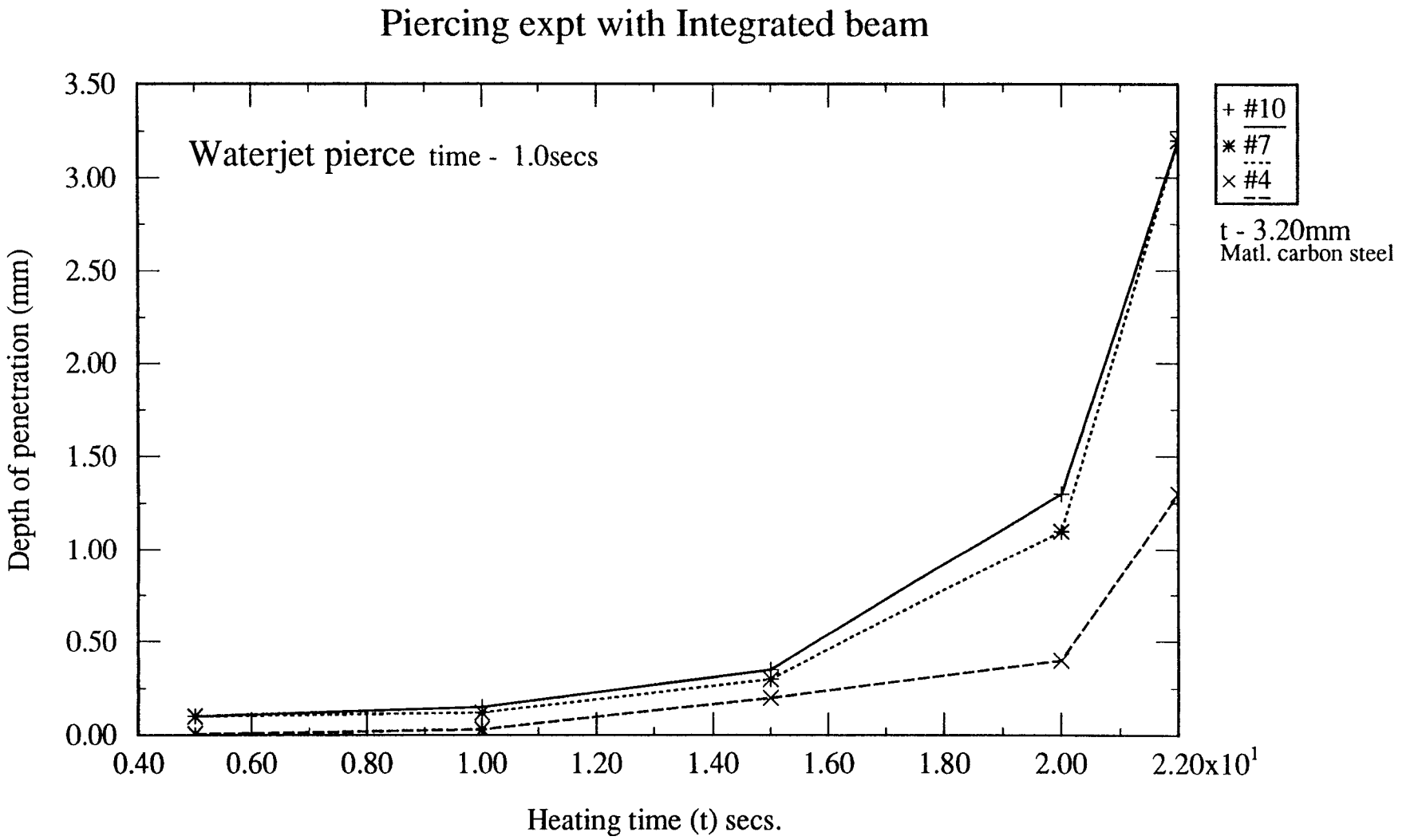

Fig 28. Variation of piercing depth with heating time using an integrated beam. Pressure Pi - 50 ksi., metal - carbon steel, waterjet pierce time - 1.0 sec.

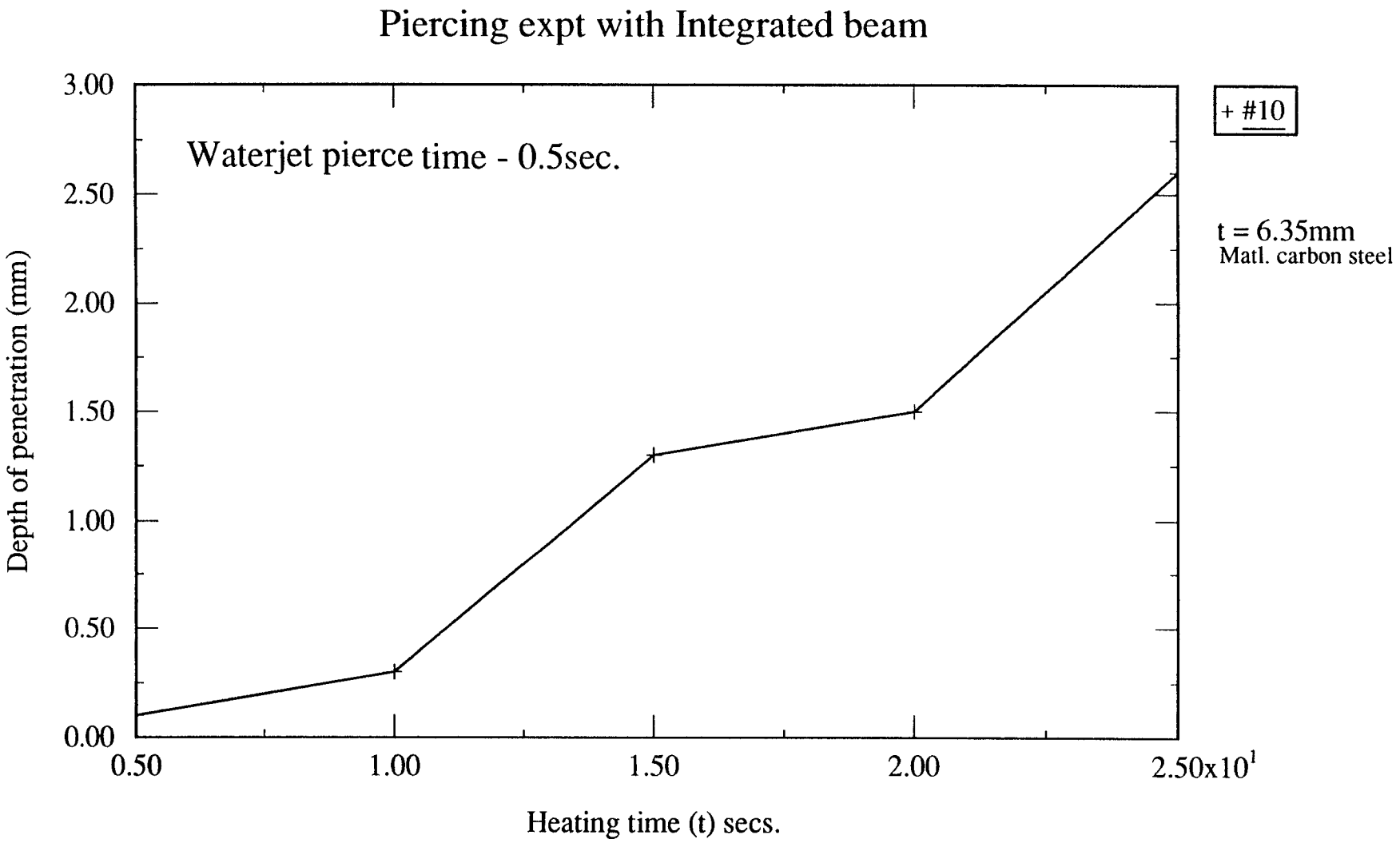

Fig 29. Variation of piercing depth with heating time using an integrated beam. Pressure Pi - 50 ksi., metal - carbon steel, waterjet pierce time - 0.5 sec. thickness - 6.35mm.

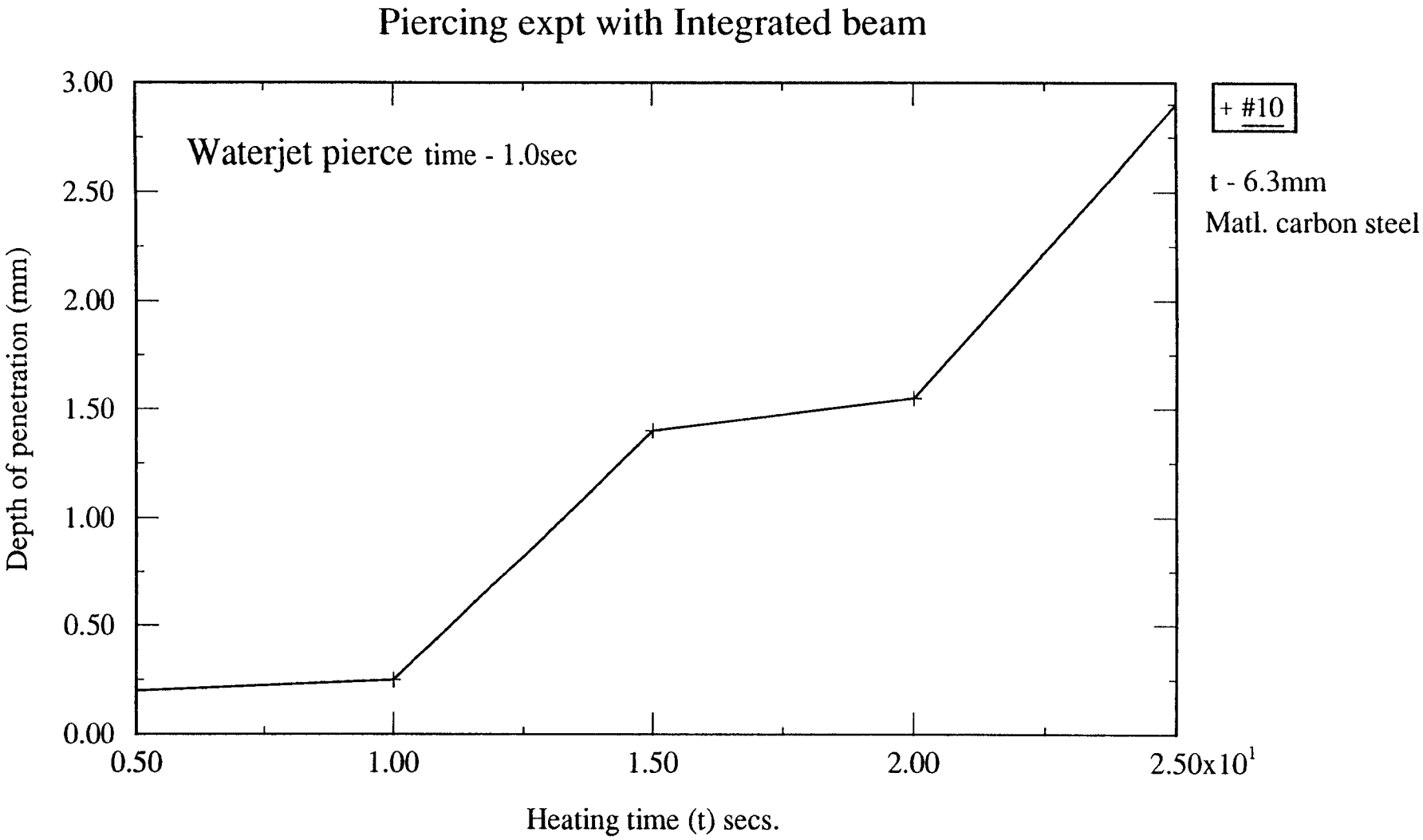

Fig 30.. Variation of piercing depth with heating time using an integrated beam. Pressure Pi - 50 ksi., metal - carbon steel, waterjet pierce time - 1.0 sec. thickness - 6.35mm.

TempleGraph 2.4, Origin: /afs/cad/usr/class/vvs1472@mesunw4 - Thu Aug 22 20:31 49 1991 (data file was int61.dat)

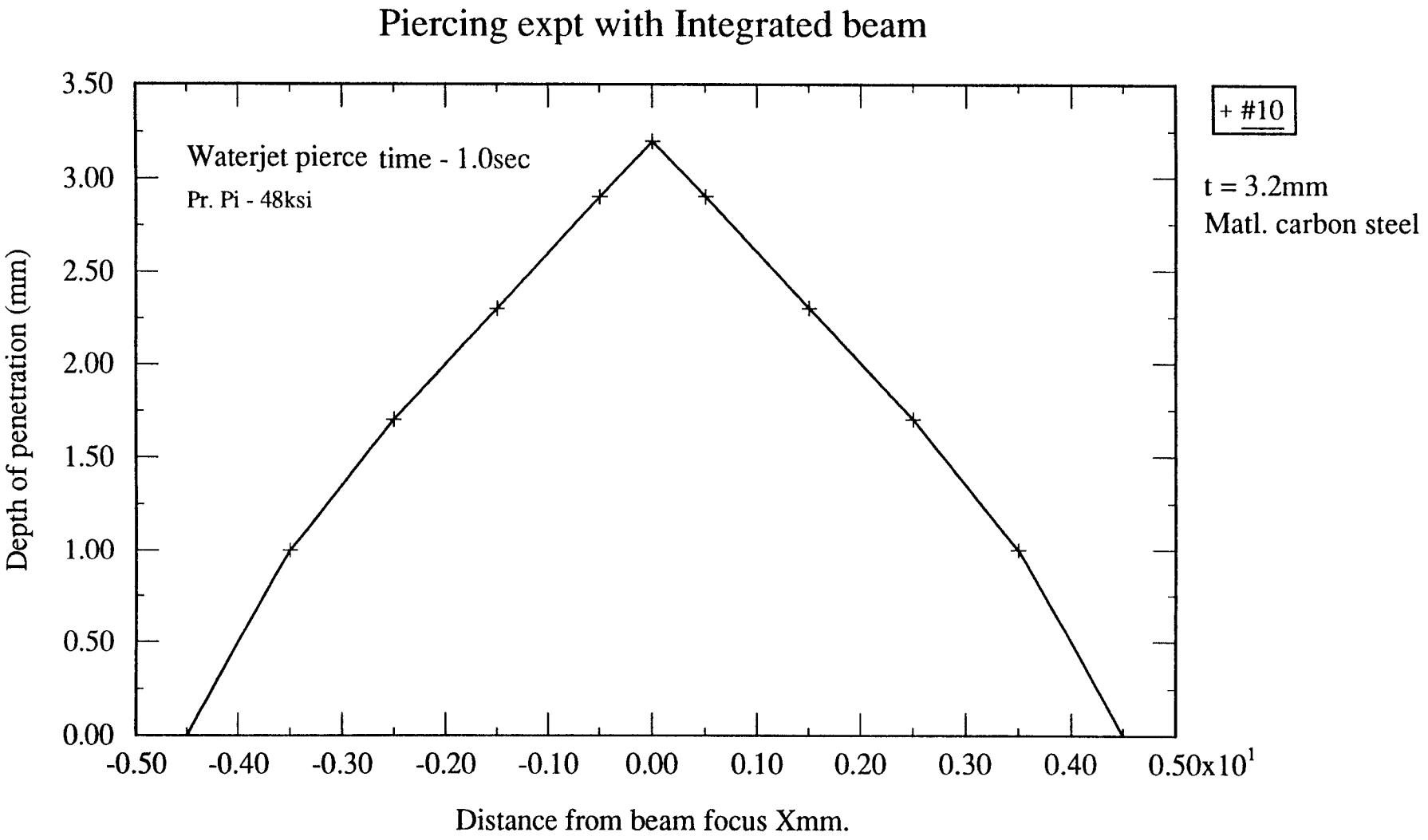

Fig 31. Variation of Beam penetration depth with Distance.

TempleGraph 2 4, Origin /afs/cad/usr/class/vvs1472@mesunw4 - Thu Aug 22 20 51·26 1991 (data file was deep3 dat)

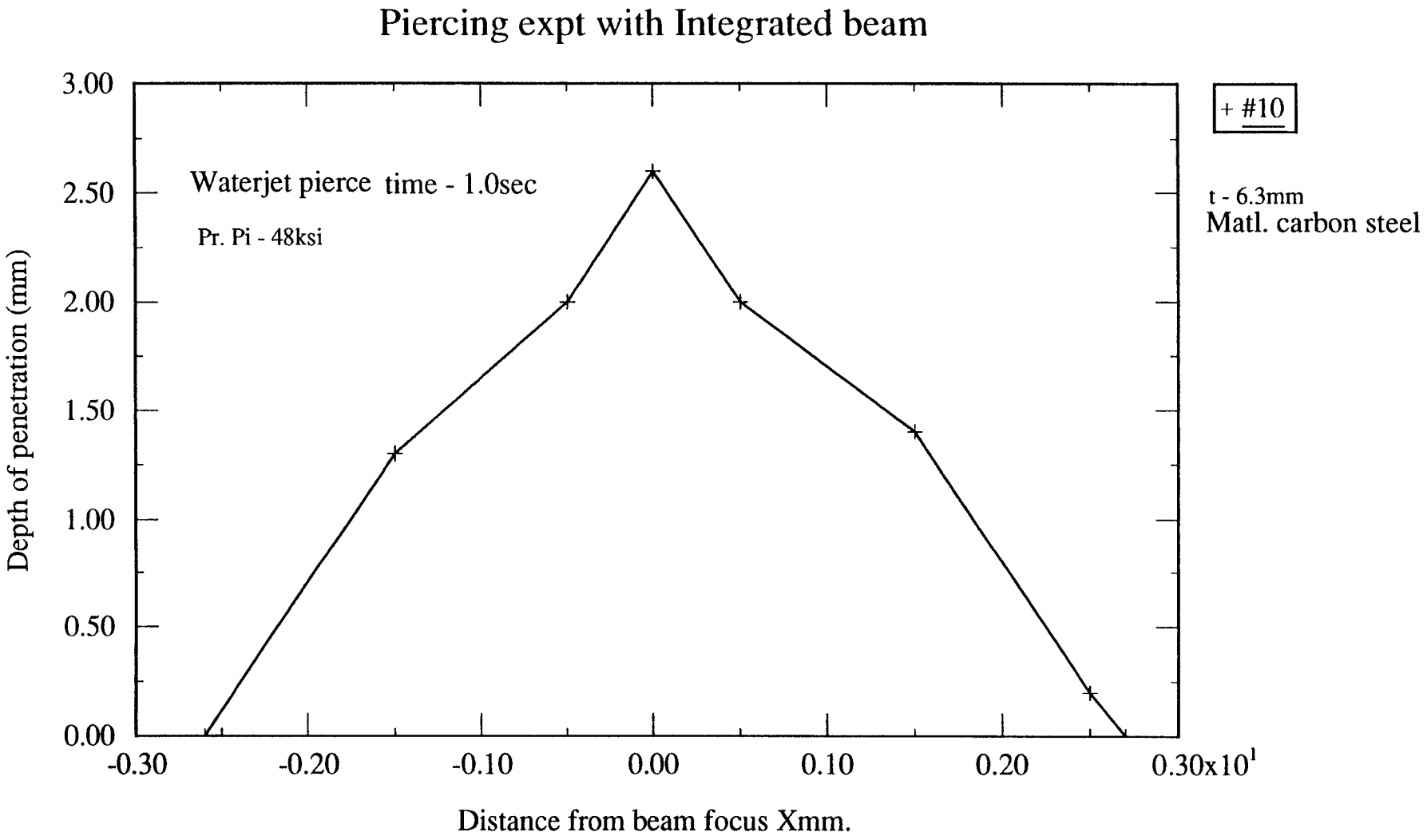

Fig 32. Variation of Beam penetration depth with Distance.

TempleGraph 2 4, Origin: /afs/cad/usr/class/vvs1472@mesunw4 - Thu Aug 22 21 32:15 1991 (data file was deep6 dat)

Table XIX - A

Effect of particle size on surface finish :

Material : Stainless steel SS 304

Thickness = 12.5 mm

Sapphire Dia. = 0.228 mm.

Carbide Dia. = 0.762 mm.

Abrasive type = garnet

Abrasive flow rate = 225 gms/min.

# of passes = 3

Measurement Depth = 6.0mm

I. Cutting speed = 12.5 mmpm.

No.	grit #	Roughness (Ra)
1.	80	1.35
2.	220	0.92

II. Cutting Speed = 62.5 mmpm.

No.	grit #	Roughness (Ra)
1.	80	1.85
2.	220	1.35

III. Cutting Speed = 125.0 mmpm.

No.	grit #	Roughness (Ra)
1.	80	2.35
2.	220	1.63

IV. Cutting Speed = 250.0 mmpm.

No.	grit #	Roughness (Ra)
1.	80	3.5
2.	220	2.4

Table XIX - B

Effect of particle size on surface finish :

Material : Stainless steel SS 304

Thickness = 25.4 mm

Sapphire Dia. = 0.228 mm.

Carbide Dia. = 0.762 mm.

Abrasive type = garnet

Abrasive flow rate = 225 gms/min.

# of passes = 3

Measurement Depth = 12.5 mm.

I. Cutting speed = 12.5 mmpm.

No.	grit #	Roughness (Ra)
1.	80	1.32
2.	220	0.90

II. Cutting Speed = 62.5 mmpm.

No.	grit #	Roughness (Ra)
1.	80	1.72
2.	220	1.26

IV. Cutting Speed = 250.0 mmpm.

No.	grit #	Roughness (Ra)
1.	80	3.5
2.	220	1.93

III. Cutting Speed = 125.0 mmpm.

No.	grit #	Roughness (Ra)
1.	80	2.35
2.	220	1.60

IV. Cutting Speed = 190.5 mmpm.

No.	grit #	Roughness (Ra)
1.	80	2.62
2.	220	1.75

Table XX - A

Effect of Focussing tube diameter on Roughness :

Material : Stainless steel SS 304.

Material thickness = 12.5 mm.

Sapphire Dia = 0.228 mm.

Abrasive type = garnet

Abrasive grit = # 220.

Abrasive flow rate = 225 gm/min.

# of passes = 3

I. Cutting speed = 12.5 mmpm.

No.	Focussing tube Dia. mm.	Roughness (Ra)
1.	0.762	0.93
2.	1.0922	0.94

III. Cutting speed = 125.0 mmpm.

No.	Focussing tube Dia. mm.	Roughness (Ra)
1.	0.762	1.85
2.	1.0922	1.74

II. Cutting speed = 62.5 mmpm.

No.	Focussing tube Dia. mm.	Roughness (Ra)
1.	0.762	1.45
2.	1.0922	1.49

IV. Cutting speed = 190.5 mmpm.

No.	Focussing tube Dia. mm.	Roughness (Ra) s
1.	0.762	2.06
2.	1.0922	2.14

V. Cutting speed = 254.0 mmpm

No.	Focussing tube Dia. mm.	Roughness (Ra)
1.	0.762	2.25
2.	1.0922	2.35

Table XX - B

Effect of Focussing tube diameter on Roughness :

Material : Stainless steel SS 304.

Material thickness = 25.4 mm.

Sapphire Dia = 0.228 mm.

Abrasive type = garnet

Abrasive grit = # 220.

Abrasive flow rate = 225 gm/min.

# of passes = 3

I. Cutting speed = 12.5 mmpm.

No.	Focussing tube Dia. mm.	Roughness (Ra)
1.	0.762	1.02
2.	1.0922	0.98

III. Cutting speed = 125.0 mmpm.

No.	Focussing tube Dia. mm.	Roughness (Ra)
1.	0.762	1.60
2.	1.0922	1.74

II. Cutting speed = 62.5 mmpm.

No.	Focussing tube Dia. mm.	Roughness (Ra)
1.	0.762	1.28
2.	1.0922	1.34

IV. Cutting speed = 190.5 mmpm.

No.	Focussing tube Dia. mm.	Roughness (Ra) s
1.	0.762	2.20
2.	1.0922	2.31

II. Cutting speed = 254.0 mmpm.

No.	Focussing tube Dia. mm.	Roughness (Ra)
1.	0.762	2.43
2.	1.0922	2.38

Table XXI - A

Effect of Cutting Speed on Roughness (Ra) :

Material : Stainless steel SS 304

Sapphire Dia : 0.228 mm

Focussing tube Dia: = 0.762 mm.

Abrasive type : Garnet

Abrasive size = 220 mesh.

Abrasive flow rate = 225 gms/min.

# of passes = 3

I. thickness = 12.5 mm.

No.	Cutting Speed mmpm.	Roughness Ra
1.	12.5	0.86
2.	62.5	1.35
3.	125.0	1.75
4.	190.5	1.94
5.	254.5	2.45

II. thickness = 25.4 mm.

No.	Cutting Speed mmpm.	Roughness Ra
1.	12.5	0.86
2.	62.5	1.35
3.	125.0	1.95
4.	190.5	2.45
5.	254.5	3.07

Table XXI - B

Effect of Cutting Speed on Roughness (Ra) :

Material : Stainless steel SS 304

Sapphire Dia : 0.228 mm

Focussing tube Dia: = 0.762 mm.

Abrasive type : Garnet

Abrasive size = 80 mesh.

Abrasive flow rate = 225 gms/min.

# of passes = 3

I. thickness = 12.5 mm.

No.	Cutting Speed mmpm.	Roughness Ra
1.	12.5	1.38
2.	62.5	1.80
3.	125.0	2.15
4.	190.5	2.90
5.	254.5	3.25

II. thickness = 25.4 mm.

No.	Cutting Speed mmpm.	Roughness Ra
1.	12.5	1.42
2.	62.5	1.90
3.	125.0	2.10
4.	190.5	2.95
5.	254.5	3.27

Table XXII

Effect of Pressure on Roughness Average (R_A)

Abrasive - Garnet

Sapphire/nozzle Diameter - 0.228/0.762 (mm) (#9/30)

Abrasive flow rate - 225gms/min.

Material - stainless steel (SS 304) 1.0" thick

Measurement depth from top surface - 12.5mm

(i) Pass number - 1

Pressure (ksi)	R_A #220 mesh	R_A # 80 mesh
30	1.6	3.3
40	1.45	2.6
50	1.01	1.52

(ii) pass number = 2

Pressure (ksi)	R_A #220 mesh	R_A # 80 mesh
30	1.34	2.88
40	1.19	2.12
50	0.95	1.62

(iii) pass number = 3

Pressure (ksi)	R_A #220 mesh	R_A # 80 mesh
30	1.17	2.46
40	1.04	1.93
50	0.95	1.43

(iv) pass number = 4

Pressure (ksi)	R_A #220 mesh	R_A # 80 mesh
30	1.1	2.38
40	1.03	1.64
50	0.92	1.43

maximum lateral depth of cut in all cases = .25mm (0.01in)

Table XXIII

Effect of Sapphire nozzle on Roughness value:

Material : Stainless steel (SS 304)
Thickness: 1.0"
Abrasive : Garnet (# 220mesh)
Nozzle Traverse Speed : 12.5 mmpm. (0.5 ipm.)
Pressure = 50 ksi

1. No. of passes = 1.

Sapphire/ Carbide Combination	Roughness (R_A) at D = 5mm	Roughness (R_A) D = 15 mm.
# 9/43	1.01	1.26
# 12/43	1.01	1.17

(ii) No. of passes = 2

Sapphire/ Carbide Combination	Roughness (R_A) at D = 5mm	Roughness (R_A) D = 15 mm.
# 9/43	0.96	1.06
# 12/43	0.91	1.03

(iii) No. of passes = 3

Sapphire/ Carbide Combination	Roughness (R_A) at D = 5mm	Roughness (R_A) D = 15 mm.
# 9/43	0.90	1.0
# 12/43	0.90	0.95

(iv) No. of passes = 4

Sapphire/ Carbide Combination	Roughness (R_A) at D = 5mm	Roughness (R_A) D = 15 mm.
# 9/43	0.90	1.0
# 12/43	0.90	0.95

D - Measurement depth from beam incident surface.

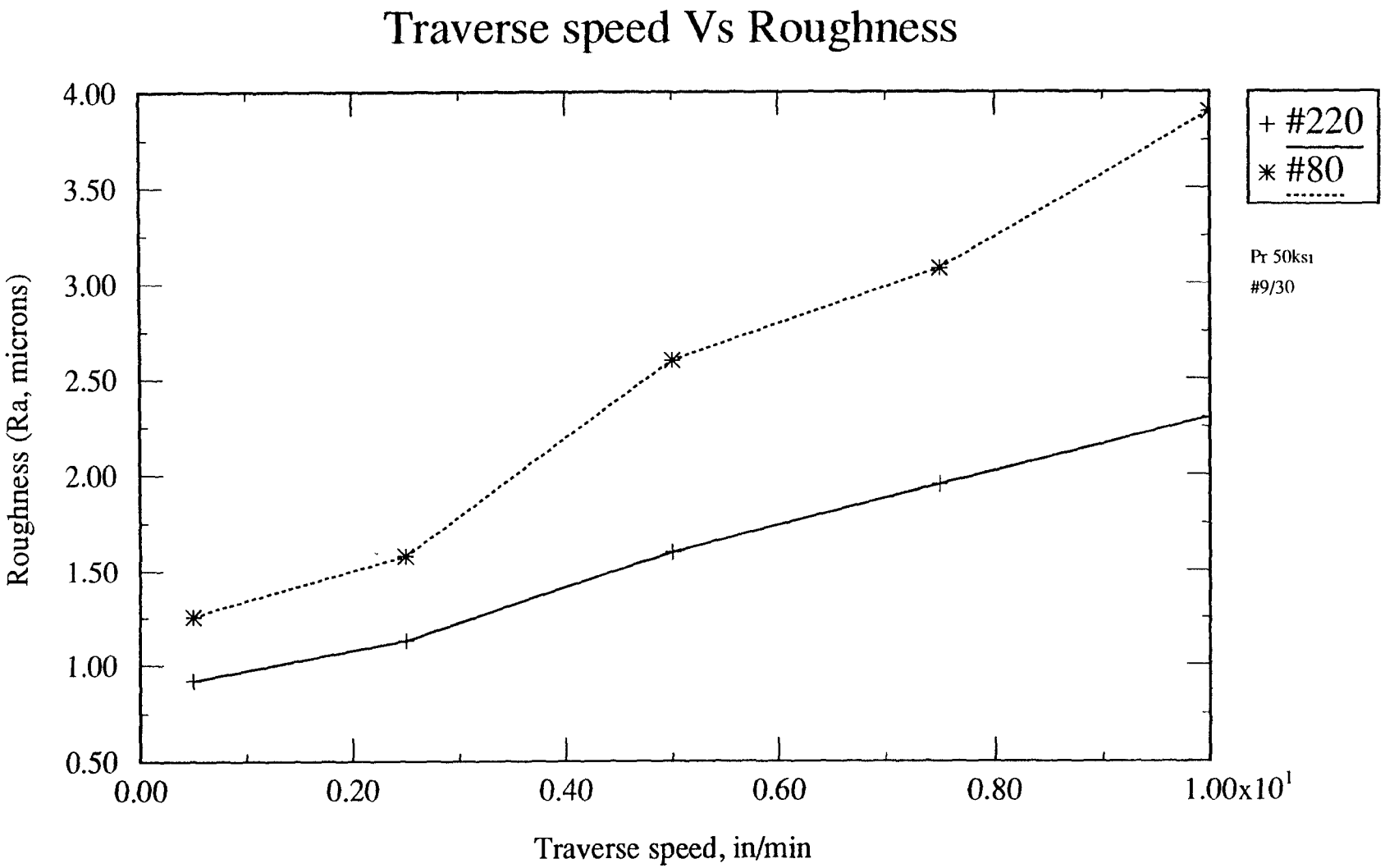

Variation of Roughness (Ra) with traverse Speed.

Fig 33. Experiments to improve surface finish using AWJ as a surface finishing tool Material - SS304, Thickness - 25mm., Measurements were taken at 12.5mm depth from the top surface. Roughness results after 3 passes of the AWJ beam.

TempleGraph 2 4, Origin /afs/cad/usr/class/vvs1472@mesunw5 - Tue Aug 20 16:24:39 1991 (data file was /afs/cad mit edu/usr/class/vvs1472/speed mif data)

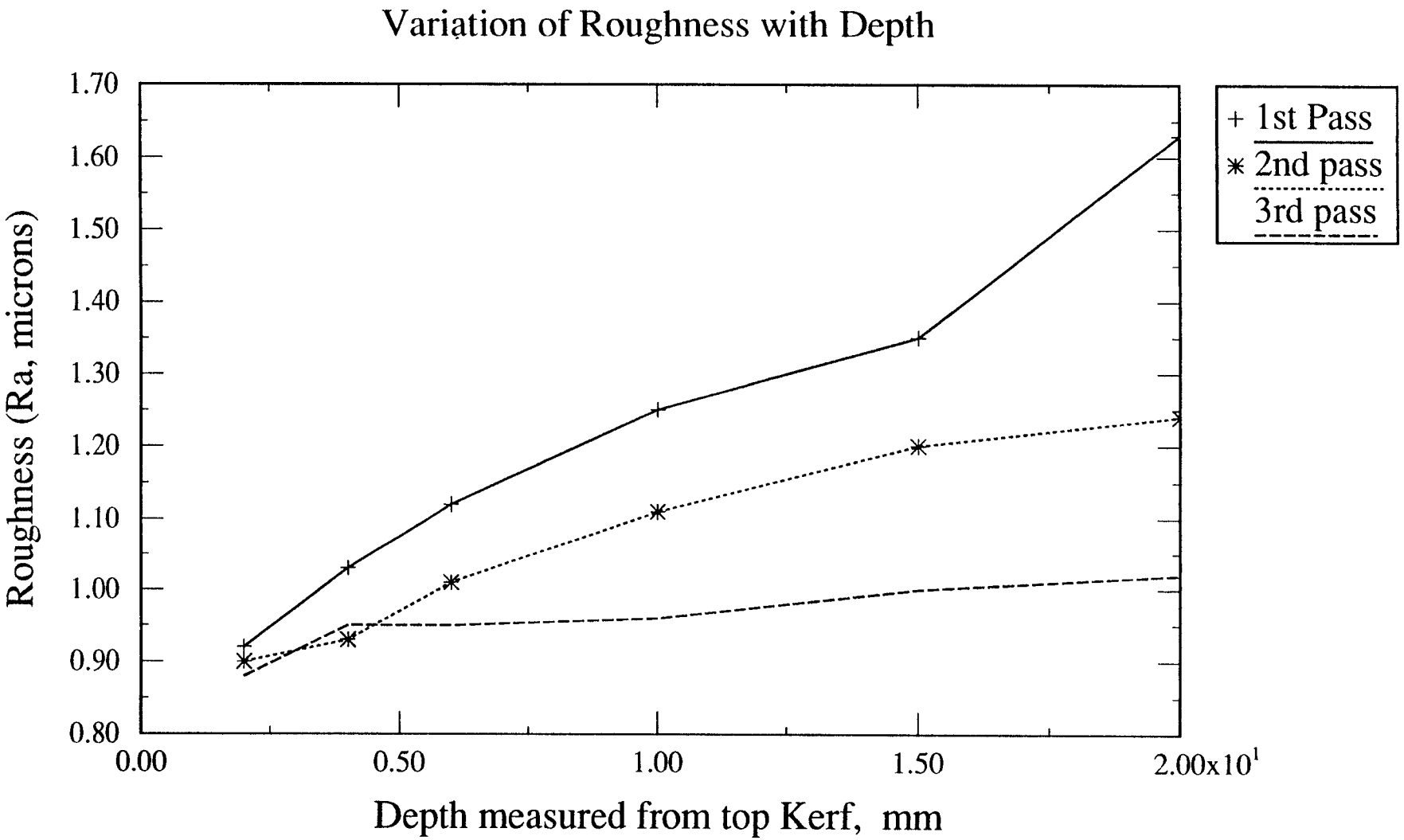

Sapphire-0.228mm., Carbide-0.762mm, P1-345Mpa traverse speed, 0.5in/min

Fig 34. Experiments to improve surface finish using AWJ as a surface finishing tool.

TempleGraph 2.4, Origin: /afs/cad/usr/class/vvs1472@mesunw5 - Tue Aug 20 16.43:22 1991 (data file was /afs/cad.nit.edu/usr/class/vvs1472/Depth.mif data)

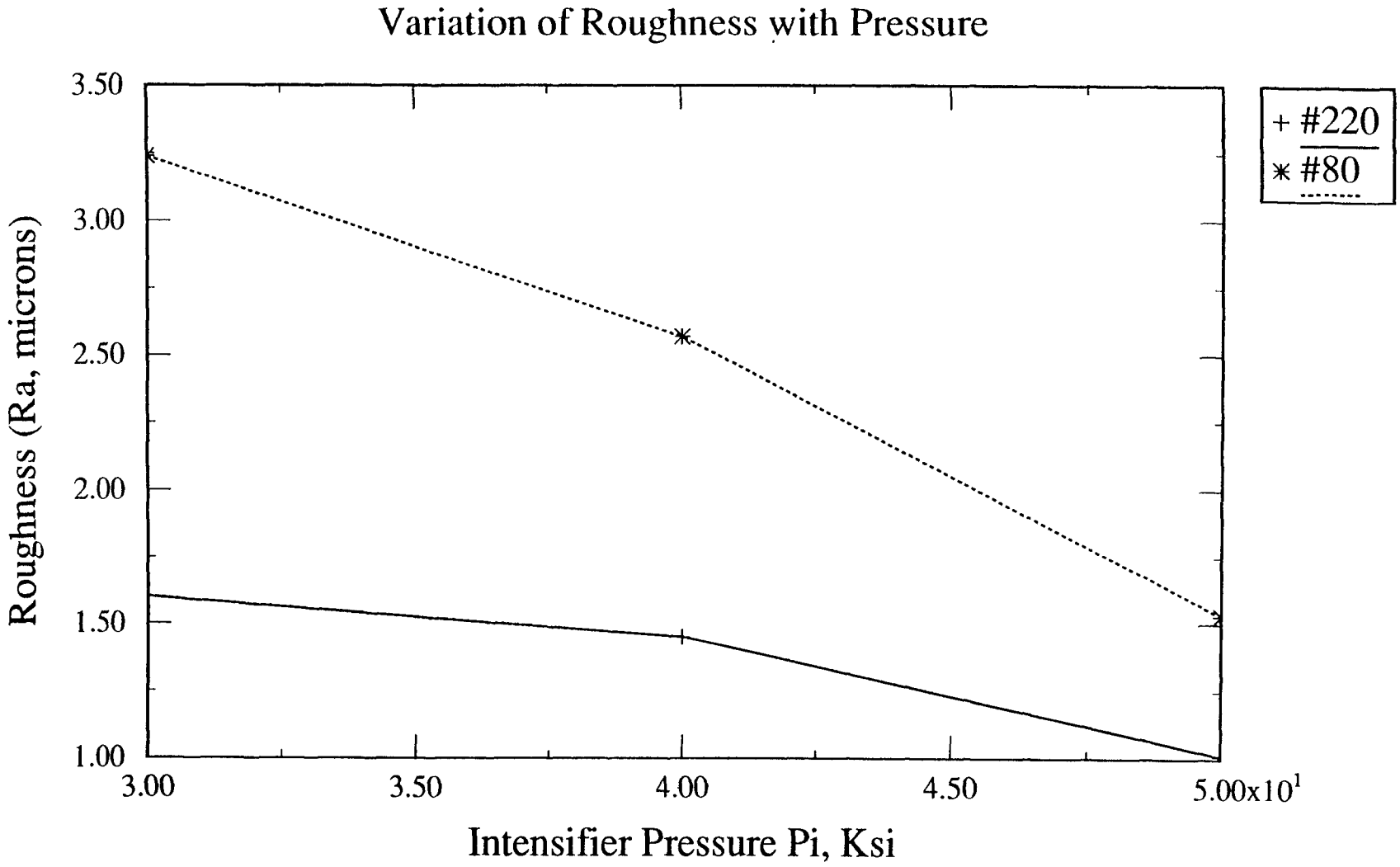

Sapphire-0.228mm, Carbide-0.762mm, 1st Pass

Fig 35. Experiments to improve surface finish using AWJ as a surface finishing tool.
Material SS304, Thickness - 25mm, Roughness measured at a depth of 12.5mm from the top edge of the surface.

TempleGraph 2 4, Origin· /afs/cad/us

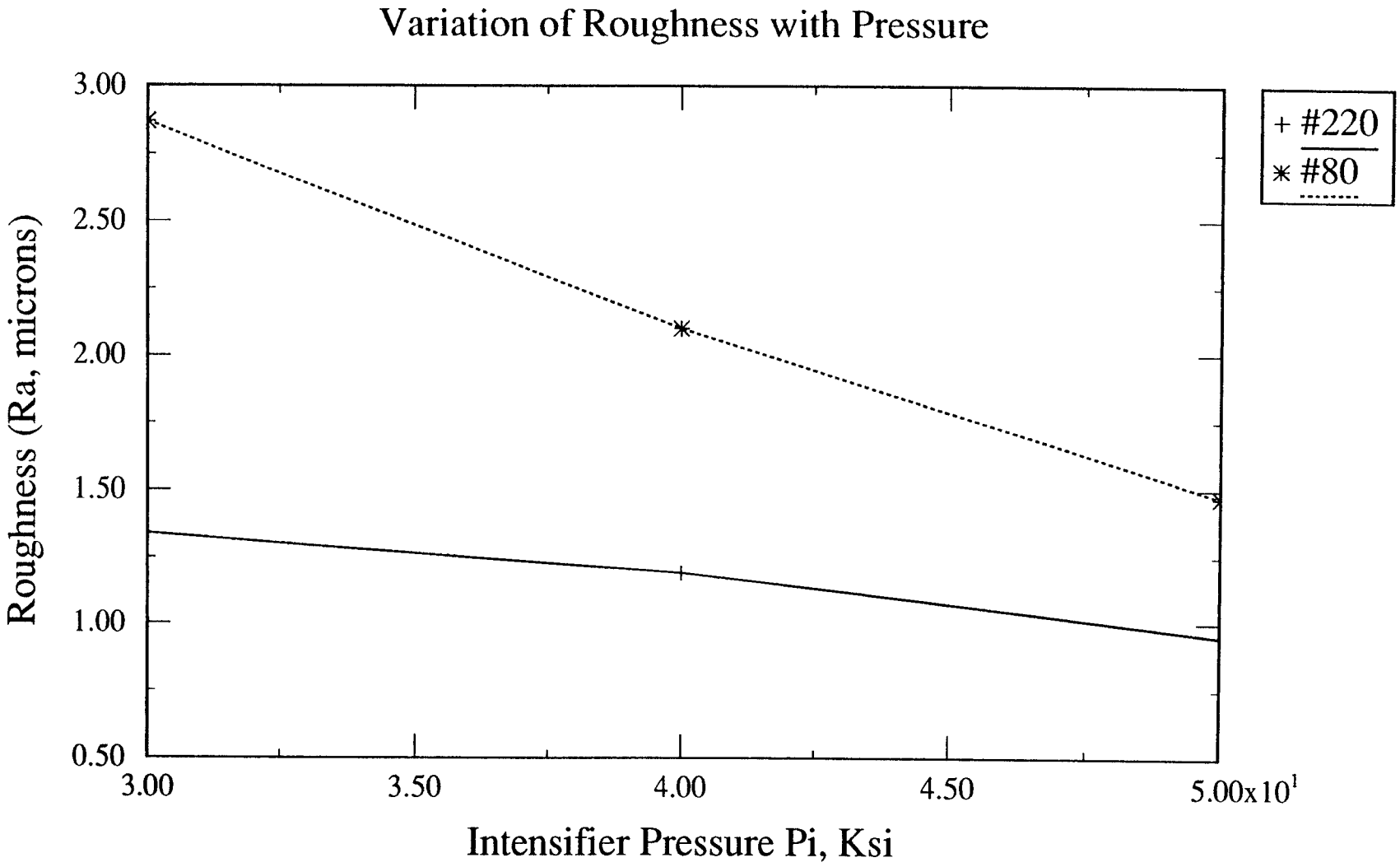

sapphire-0.228mm,Carbide-0.762mm,2nd Pass

Fig 36. Experiments to improve surface finish using AWJ as a surface finishing tool.
Material SS304, Thickness - 25mm, Roughness measured at a depth of 12.5mm from the top edge of the surface.

TempleGraph 2.4, Origin: /afs/cad/usr/class/vvs1472@mesunw5 - Tue Aug 20 10 35 01 1991 (data file was pressure2 dat)

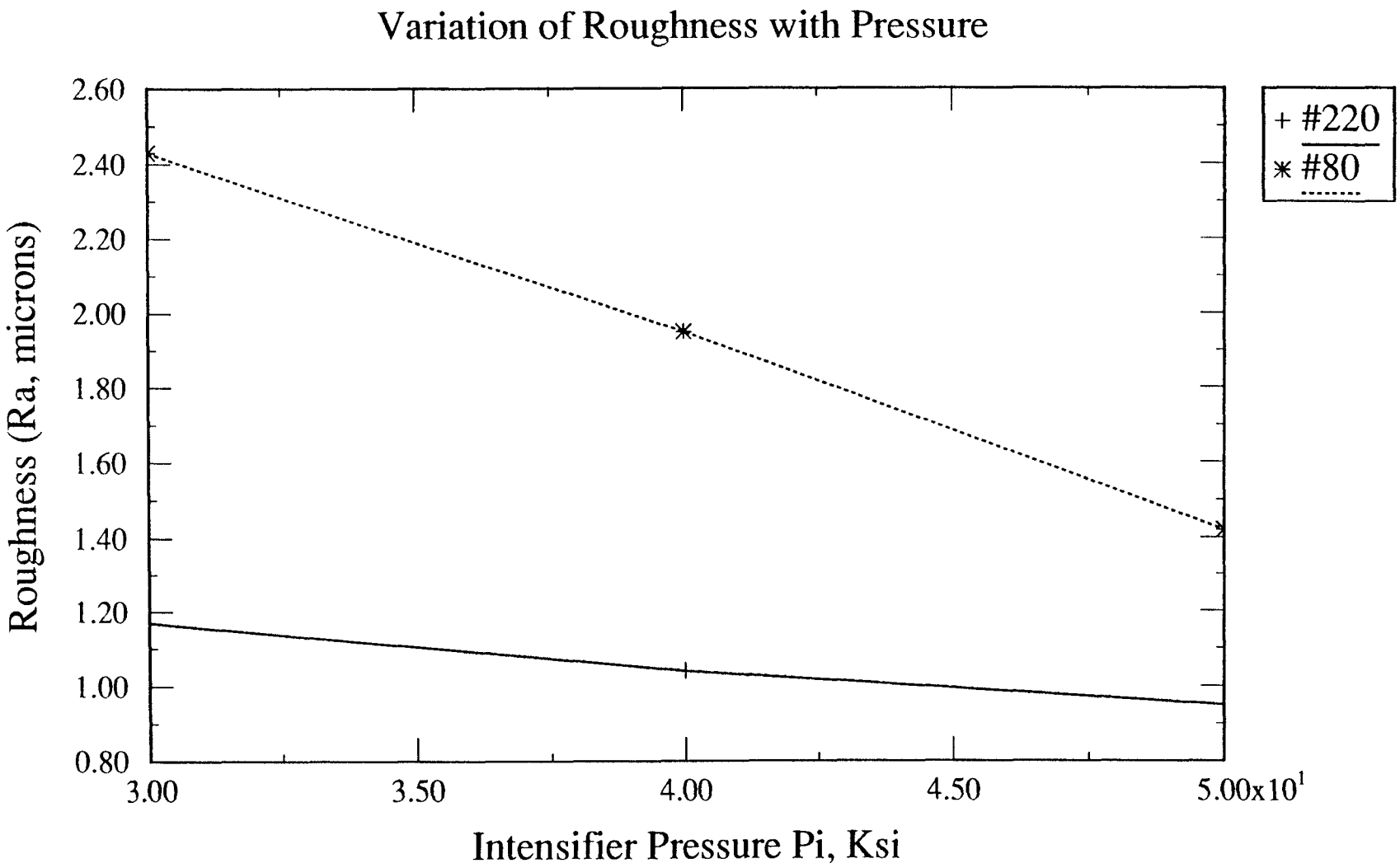

Sapphire-0.228mm,Carbide-0.762mm, 3rdpass

Fig 37. Experiments to improve surface finish using AWJ as a surface finishing tool.
Material SS304, Thickness - 25mm, Roughness measured at a depth of 12.5mm from the top edge of the surface.

TempleGraph 2.4, Origin: /afs/cad/usr/class/vvs1472@mesunw5 - Tue Aug 20 10:53:56 1991 (data file was pr3 dat)

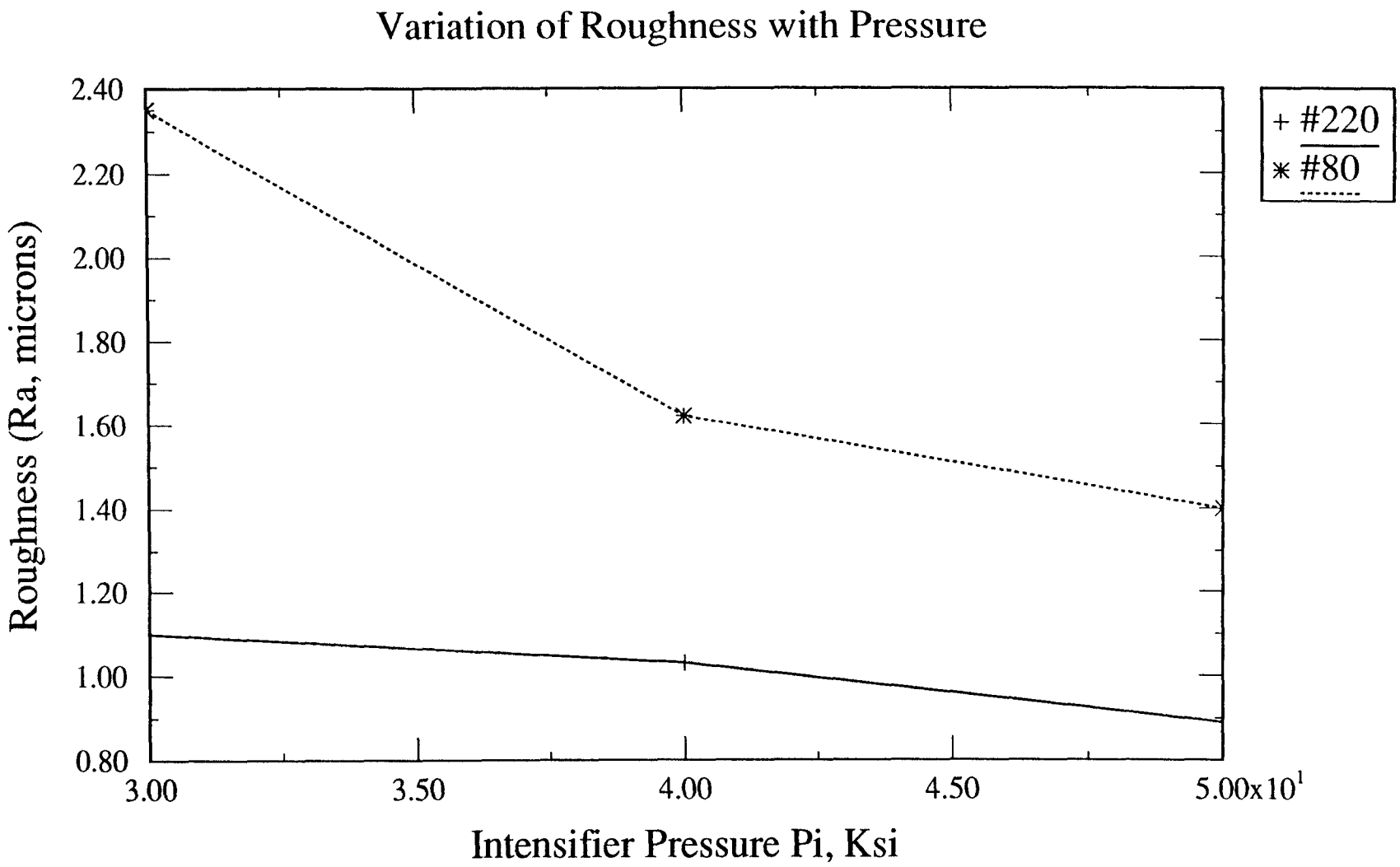

sapphire-0.228mm, Carbid-0.762mm, 4th pass

Fig 38. Experiments to improve surface finish using AWJ as a surface finishing tool.
Material SS304, Thickness - 25mm, Roughness measured at a depth of 12.5mm from the top edge of the surface.

TempleGraph 2.4, Origin: /afs/cad/usr/class/vvs1472@mesunw5 - Tue Aug 20 11:13:56 1991 (data file was pr4 dat)

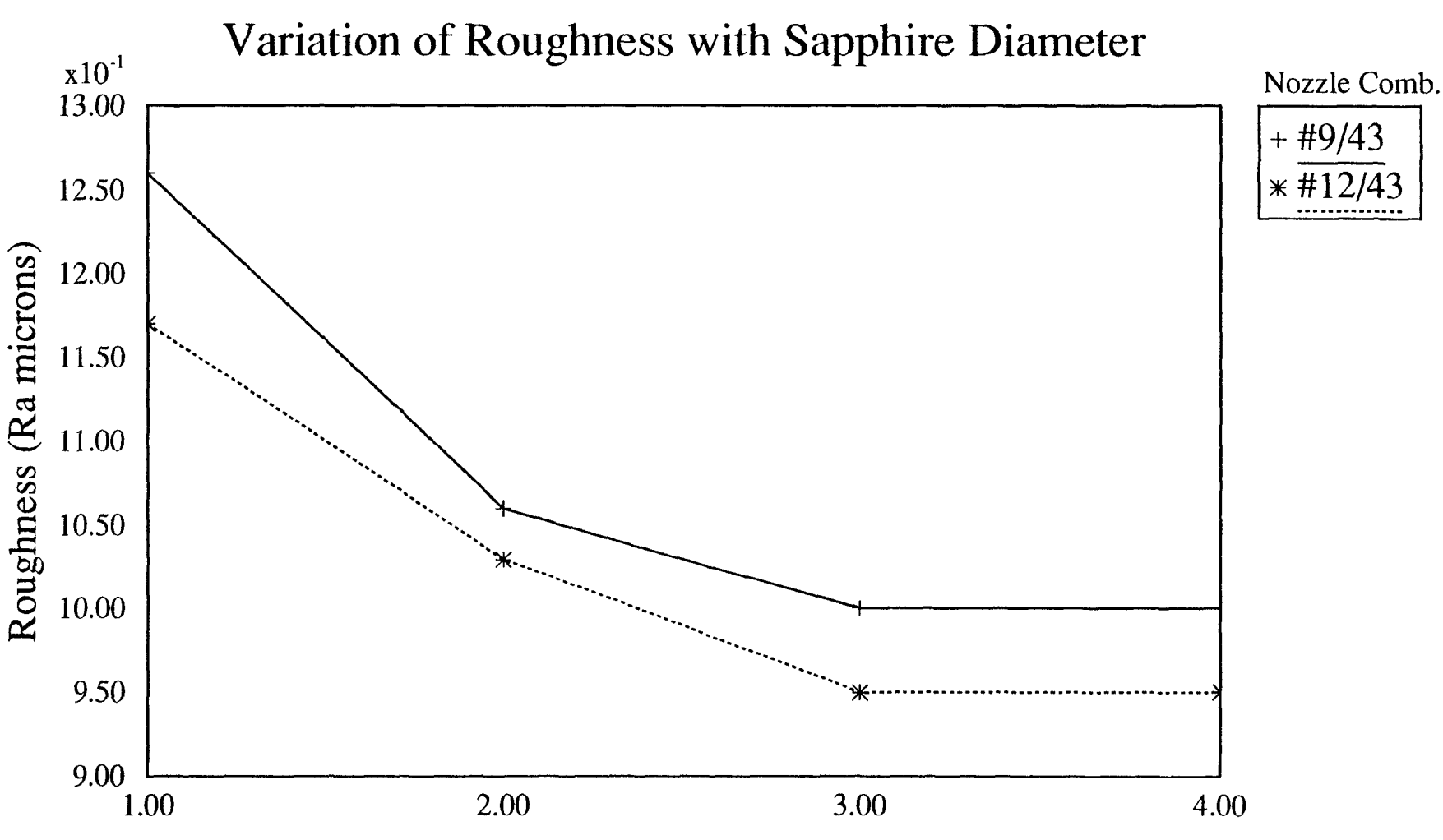

Pressure Pi - 50 ksi, Abrasive 220mesh ,traverse speed - 0.5in/min

Fig 35. Experiments to improve surface finish using AWJ as a surface finishing tool Material - SS304, Thickness - 25mm., Measurements were taken at 12.5mm depth from the top surface. Roughness results after 3 passes of the AWJ beam.

TempleGraph 2.4, Origin: /afs/cad/usr/class/vvs1472@mesunw5 - Tue Aug 20 17:28:40 1991 (data file was /scratch/sapvar.muf data)

REFERENCES

[1] Shearing, Slitting and Cutting, **METALS HANDBOOK**, 9th Edition, vol 14, Forming and Forging, 1988, pp. 701-740.

[2] Geskin, E.S., Chen, W.L., and Lee, W.T., "Glass Shaping by the Use Of Abrasive Waterjet", **Glass Digest**, Nov.1988, pp. 60 -64.

[3] M. Hashish," Machining of Advanced Composites with Abrasive-Waterjets", **MANUFACTURING REVIEW**, vol 2, No. 2, Jun 1989, pp. 142-150.

[4] T.J. Labus, "Automated Waterjet Cutting - a Flexible Manufacturing Method", **Proceedings, 1st International Symposium On Jet Cutting Technology**, 1978, pp. 95-108.

[5] M. Hashish, M.P. duPlessis, "Theoretical and Experimental Investigation of Continuous Jet Penetration of Solids", **Transactions ASME, Journal of Engineering for Industry**, 1978, vol 100, pp. 88-94.

[6] M. Hashish, "A Modeling Study of Metal Cutting With Abrasive Waterjets", **Transactions ASME, Journal of Engineering Materials and Technology**, 1984, vol 106, pp. 88-100.

[7] M. Hashish, "Visualization of the Abrasive-Waterjet Cutting Process", **Journal of Experimental Mechanics,** 1990, vol 75, pp. 103-116.

[8] R. Kobayashi, T. Arai, Y. Masuki, "Water Jet Nozzle Geometry and Its Effect on Erosion Process of Metallic Material", **Proceedings of the 5th American Waterjet Conference**, 1989, pp. 59-68.

[9] H.Y.Li, E.S. Geskin, W.L. Chen, "Investigation of Forces Exerted by an Abrasive Water Jet on a Workpiece", **Proceedings of the 5th American Waterjet Conference**, 1989, pp. 69-78.

[10] Weilong Chen, "Study of Particle Velocities and Conditions of Abrasive Waterjet Formation", **DOCTORAL DISSERTATION**, New Jersey Institute of Technology, Dec, 1989.

[11] H. Louis, H. Haferkamp, and W. Schikorr, "Jet Cleaning Investigations on polymeric Model Layers", **7th International Symposium on Jet Cutting Technology**, Jun 1984, pp. 119-132.

[12] R. Paseman and L. Griffith, " Cleaning the Tube side of Heat Exchangers", **Proceedings of the Fourth U.S. Water jet Conference**, Aug 1987, pp.147-154.

[13] C.D. Burnham, T.J. Kim,"Statistical Characterization of Surface finish produced by a High pressure Abrasive Waterjet", **Proc. of the 5th American Waterjet Conference, 1989**, pp. 165-176.

[14] S Matsui.,H Matsumara, Y Ikemoto, K Tsukita, H Shimizu, "High Precision Cutting Methods For Metallic Materials by Hydroabrasive Waterjet Systems", **Proceedings of 10th International Symposium on Jet Cutting Technology,** Nov., 1990.

[15] M. Hashish, "Milling with Abrasive Waterjets: A Preliminary Investigation", **Proceedings of the Fourth U.S. Waterjet Conference**, Aug. 1987. pp. 1-10.

[16] H. Blickwedel, N. S. Guo, H. Haferkamp, H. Louis, "Prediction of the Abrasive Jet Cutting Performance and Quality", **10th International Symposium on Jet Cutting Technology**, Nov 1990.

[17] M. Hashish, "Aspects of Abrasive-Waterjet Performance Optimization", **Proc. of the 8th International Symposium on Jet Cutting Technology**, 1986, pp. 297-308.

[18] M. Hashish, "Optimization Factors in Abrasive-Waterjet Machining", **Proc. of the ASME Winter Annual Meeting**, vol 34, pp. 163-180.

[19] M. Hashish, "Effect of Pressure on the Performance of Abrasive-Waterjet (AWJ) Machining", **Proc. of the Manufacturing International,** vol 1, Apr. 1988, pp. 255-263.

[20] Hamatani G.,"Machinability of High Temperature Composites by Abrasive Waterjet", **Proc. of the ASME Winter Annual Meeting**, vol 35, pp. 49-62.

[21] Tan, D.K.M.,"A Model for the Surface Finish in Abrasive Waterjet Cutting", **Proc. of the 8th International Symposium on Jet Cutting Technology**, 1986, paper 31.

[22] **Operation Manual for the HS-3000 Hydroabrasive Workcell**, Ingersoll Rand Co., 1990.

[23] D. Chio,"Technological and Economic Analysis and Comparison between Laser and Waterjet Cutting with Robot", **Proc. of 9th International Conf. on Robotics**, 1989, pp. 907-918.

[24] D.C. Schroter, "Motion Equipment Design for Hydroabrasive Waterjet Systems", **Proc. of the 10th**

International Symposium on Jet Cutting Technology, Nov 1990, paper H1.

[25] K. Zaring, "Advanced Abrasive-Waterjet Hardware and Cutting Performance", **Proc. of the 5th American Water Jet Conference**, Aug 1989, pp. 473-482.

[26] H. J. Warnecke, W. Sturz, M. Hopf, Jong-oh Park, "Plasma Arc Cutting with Industrial Robots", **Proc. of the 9th International Conference on Robotics**, Nov. 1990, pp. 917-925.

[27] N-J Ho, F.V. Lawrence Jr., C.J. Altstetter, "The Fatigue Resistance of Plasma and Oxygen Cut Steel", **The Welding Journal**, Nov 1981, pp. 231-236.

[28] Ed Bohlen, "30 Years of Plasma Cutting Process", **Company Report**, Linde Gas Co.

[29] M. Mawson, "Thermal Cutting in Fabrication", **Metal Construction**, vol 15, 1983, pp. 444-447.

[30] I.S. Shapiro, " An Evaluation of the Performance of A Plasma Torch for the Cutting of Metal", **Welding Production**, vol 28, 1981, pp. 37-40.

[31] Laschenko, Lysenko, Bogdano, "Plasma Arc Cutting of Metal Above a Water Pool Surface", **Welding Production**, Apr 1985, pp. 13-17.

[32] S.A. Maguire, "Planning the Total Plasma Arc Cutting System", **Welding Journal**, Dec 1982, pp. 33-36.

[33] B. Rolland and H. Conn, "Some Results from Combining Plasma Arc Cutting with a 40-Ton Press", **Welding Journal**, Feb 1978, pp. 26-29.

[34] M. Hashish, "A Modelling Study of Metal Cutting with Abrasive Waterjets", Transactions ASME, Journal Of Engineering and Materials Technology, vol 106, pp. 88-99.

[35] **PCM-250 Plasma Arc Cutting Manual**, Linde gas Co.

[36] **Oxy-Acetylene Welding and Cutting Manual**, Linde Gas Co., 12th Edition, 1989.